A STUDY OF ULTRASONIC EFFECTS ON THE MARINE BIOFOULING ORGANISM OF BARNACLE, *AMPHIBALANUS AMPHITRITE*

GUO SHIFENG

NATIONAL UNIVERSITY OF SINGAPORE

2012

A STUDY OF ULTRASONIC EFFECTS ON THE MARINE BIOFOULING ORGANISM OF BARNACLE, *AMPHIBALANUS AMPHITRITE*

GUO SHIFENG

(***B. ENG. CQUT, M. ENG. CQU***)

A THESIS SUBMITTED FOR

THE DEGREE OF DOCTOR OF PHILOSOPHY

DEPARTMENT OF MECHANICAL ENGINEERING

NATIONAL UNIVERSITY OF SINGAPORE

2012

Declaration

I hereby declare that this thesis is my original work and it has been written by me in its entirety. I have duly acknowledged all the sources of information which have been used in the thesis. This thesis has also not been submitted for any degree in any university previously.

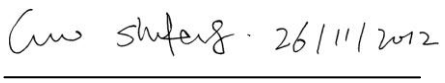

Guo Shifeng
21 November 2012

Acknowledgements

First of all, I would like to express my sincere gratitude to my supervisors, Associate Prof. Lee Heow Pueh and Prof. Khoo Boo Cheong, for providing me the precious opportunity to study under their supervision. In the past four years, I indeed have learnt and benefitted from their profound knowledge and strict academic attitude, which will benefit my whole life. It is impossible for me to finish my thesis without their invaluable guidance, sincere support, and continuous encouragement. Special thanks to Associate Prof. Lim Siak Piang and Lim Kian Meng for their help and suggestions in my research.

I would also like to express my appreciation to Dr. Serena Lay Ming Teo for her sincere guidance and invaluable suggestions on my project. I would like to thank her for providing me all the convenience and facilities for the barnacle experiments.

I gratefully acknowledge the financial support from National University of Singapore through the Research Scholarship, without which it would have not been possible for me to pursue my degree in NUS.

I would like to thank Ms. Serina Siew Chen Lee from TMSI (Tropical Marine Science Institute) on the barnacle cyprids culture. I would also express my sincere thanks to my fellow lab mates and friends Zhuang Han, Liu Yang, Tse Kwong Ming,

Zhu Jianhua, Chen Xiaobin, Thein Min Htike, Arpan Gupta, Wu Liqun, Liu Yilin, and Sun Qiang for their help in the past four years.

I would like to thank the lab officers of dynamic lab for providing me the convenience and help for my experiments.

Finally, I would express my deepest gratitude and love to my families for their continuous support and sincere encouragement.

Table of Contents

Summary

Marine biofouling is the undesirable accumulation of microorganisms, plants, and animals on man-made structures immersed in the sea. It generates serious impact on the marine industries, in particular in the shipping industries where fouling increases significant friction resistance and corrosion issues. It is estimated that billions of dollars per year for excess oil consumption and maintenance costs. The impact of biofouling also generates environmental issues such as an increase of green house gas emission due to higher fuel consumption, production of large quantities of organic waste during the cleaning and repainting process, and introduction of organisms into new environments. Among the marine fouling organisms, barnacles are a major problem due to their sizes and gregarious nature. In this thesis, a systematic study of ultrasound on the marine fouling organism of barnacle, *Amphibalanus amphitrite* is investigated.

The effect of ultrasound on barnacle cyprid settlement, mortality, and exploration behavior was firstly explored using frequencies of 23, 63 and 102 kHz. Ultrasound effectively reduced cyprid settlement and changed cyprid exploration behavior. Low frequency of 23 kHz achieved more inhibition than the other two frequencies with the same acoustic intensity. The inhibitory mechanism was then explored using spectrum analysis method and ultrasonic cavitation was verified to be the mechanism.

To reduce the possible cavitation effects on other marine organisms, low intensity ultrasound was further explored. The results revealed that with low intensity of 5 kPa, only frequency within 20-25 kHz inhibited settlement but did not increase the mortality. Also, the application of ultrasound treatment in an intermittent mode of “5

min on and 20 min off" at 23 kHz with a pressure of 5 kPa produced the same effect as with the continuous ultrasound application.

Furthermore, the effect of ultrasound on barnacle cyprid footprints (protein adhesives secreted when cyprids explore surfaces) and juvenile barnacle's adhesion strength was explored using atomic force microscopy (AFM) and Nano-tensile tester, respectively. Ultrasound changed the morphology of cyprid footprints and reduced the amount of temporary adhesive secretion. Ultrasound also reduced the adhesion strength of the newly metamorphosed barnacles. The evidence from this study suggests that ultrasound treatment results in a reduced cyprid footprint secretion and affects the subsequent recruitment of barnacles onto a substrate by reducing the ability of larval and early settlement stages of barnacles from firmly adhering to the substrate.

Finally, other than the effect of ultrasound on barnacle cyprid, the interaction of ultrasonic cavitation bubbles and juvenile barnacles was investigated using high speed photography. Ultrasonic cavitation generated liquid jet damaged the shells of newly metamorphosed barnacles. The mechanism was explored with spark generated bubbles and the pressure threshold that damaged the juvenile barnacles was able to be estimated by single bubble-barnacle interaction analysis.

List of Tables

List of Figures

Nomenclature

p	Acoustic pressure
p_i	Pressure of incident wave
p_r	Pressure of reflective wave
u	Particle velocity of liquid
k	Wave number
ω	Ultrasound frequency
c_0	Sound velocity in the seawater
ρ_0	Density of seawater
s	Cross sectional area of cyprid
F_i	Inertia force
m	Mass of cyprid
R_m	Maximum bubble radius
H	Distance between bubble formation point and boundary
H'	Dimensionless distance
P_{jet}	Liquid jet pressure
R_0	Initial bubble radius
ρ	Density of water
v	Velocity of water jet
c	Sound velocity in water

Acronyms

TBT	Tributyltin
FRC	Fouling release coating
AF	Antifouling
TMSI	Tropical Marine Science Institute
ANOVA	Analysis of variance
SE	Standard error
FSW	Filtered seawater
PDFSW	Partially degassed filtered seawater
PZT	Piezoelectric transducer
AFM	Atomic force microscopy
FP	Footprint
V	Volt
FFT	Fast Fourier Transformation
CA	Contact angle
SIPC	Settlement-inducing protein complex
FPS	Frames per second
SPC	Self polishing copolymer
H’	Dimensionless distance
DC	Direct current
APTES	3-aminopropyl trithoxysilane
PMMA	Polymethyl methacrylate
PDMS	Polydimethylsiloxane

Chapter 1. Introduction

1.1. Marine biofouling

Marine biofouling, the accumulation of submerged surfaces by undesired organisms, causes serious problems on man-made surfaces and structures such as ships, marine platforms, heat exchangers, offshore rigs and oceanographic sensors. It induces most detrimental effects on the shipping industry as the biological colony on the ship hull results in higher frictional resistance and substantially reduces speed and maneuverability. For example, the heavy calcareous fouling results in the power penalties of up to 86% at cruising speed, and even relatively light fouling by diatom 'slimes' generates a 10-16% penalty (Callow and Callow 2011).

According to the recent study on the economic impact of biofouling, the approximate cost of fouling to the US Navy fleets is between $180 and 260 million per annum (Callow and Callow 2011). The impact of biofouling also induces environmental issues such as an increase of green house gas emission due to higher fuel consumption, production of large quantities of organic waste during the cleaning and repainting process, and introduction of organisms into new environments. Figure 1.1 shows examples of vessels fouled by marine organisms.

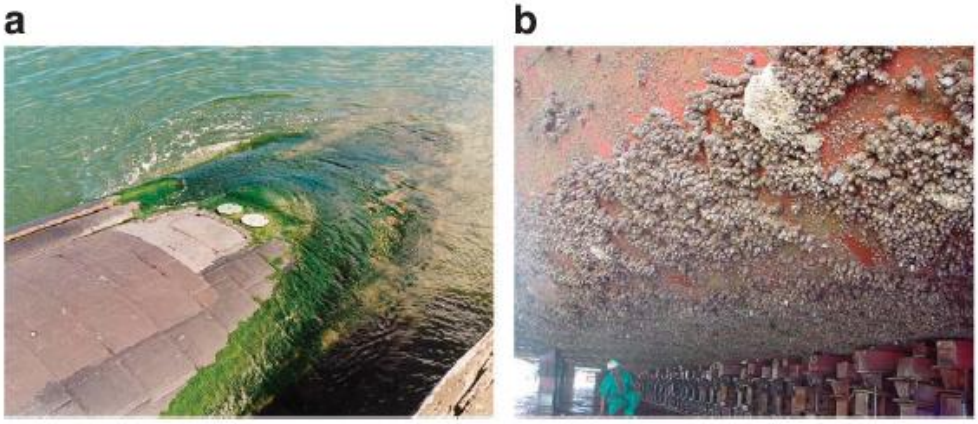

Figure 1.1. Vessels fouled by marine organisms. Images show (a) fouling by the green alga (seaweed) *Ulva*) and (b) barnacles (Callow and Callow 2011).

Fouling is not only limited to vessels, but is also commonly found in offshore structures, oil rigs and water-cooling pipes in power plants (Qian et al. 2000; Whomersley and Picken 2003). The heavily fouled structures increase the wave generated force and reduce the stability of the offshore platforms. The fouling to the seawater intake structures in vessels or cooling water systems of power plant reduces the effective diameter of the pipe and therefore reduces the cooling capacity. Fouling organisms also desensitize sensors or sonar devices monitoring the coastal environment, and corrode the surfaces of harbor installations (Delauney et al. 2010; Laurent et al. 2011).

1.2. Development of fouling

When a clean surface is submerged in seawater, it begins to adsorb a molecular film mainly comprised of dissolved organic material immediately. Accumulation of organisms on the conditioned surface depends on the availability of the colonizing stages, and their relative rates of attachment and surface exploitation. The organisms generate a fouling community, depending on the surface property, temperature,

geographical location, season and other factors such as competition and predation among marine creatures (Callow and Callow 2011).

Marine biofouling can be mainly classified into two categories: micro and macro-fouling, both lead to corrosion of surfaces (Callow and Callow 2002). Micro-fouling refers to the formation of initial biofilm consisting of unicellular microorganisms such as bacteria, algae, and diatom, whereas macro-fouling refers to the development of fouling on the substrata due to the accumulation of bryozoans, mussels, barnacles, polychaetes, and others (Callow and Callow 2002). In the process of fouling formation, the microfouling usually occurs first, and is followed by macrofouling. The fouling process has been generally stated by a linear 'successional' model (Chambers et al. 2006; Yebra et al. 2004). The model describes the colonization of the first layer of fouling by the formation of the bacterial biofilm, which is followed by spores of macroalgae, fungi and protozoa within a week, and the larvae of invertebrates, such as barnacles are developed in weeks. However, this classical view may be challenged as motile spores of seaweeds are capable of settling within minutes of presenting a clean surface and larvae of some species of barnacles, bryozoans and hydroids can settle within a few hours of immersion (Callow 1997; Roberts 1991). Also, it is questionable to assume the causal relation between one stage and the next and even more misleading to assume that controlling or blocking initial stages of colonization, such as biofilm formation, will reduce or eliminate macrofouling (Callow and Callow 2011). On the other hand, it is certain that the attachment of the larvae will be affected by the presence of bacterial biofilms, and positive, negative and neutral effects have been verified when biofilms of specific bacteria have been tested against algal spores and larvae of invertebrates (Dobretsov et al. 2006; Huggett et al. 2006).

1.3. Marine fouling organisms

The variety of marine biofouling organisms is highly diverse. It is estimated that 1700 species comprising more than 4000 organisms are responsible for biofouling (Almeida 2007). In this section, some typical marine fouling organisms were introduced. These organisms are bacteria, diatom, alga, mussel, and barnacles.

1.3.1. Bacteria

Bacteria are the typical microorganisms to populate a surface placed in the marine environment that create the initial biofilm (Marhaeni et al. 2009). Early biofilms composed of bacteria and organic matter on immersed surfaces are the key drivers for the subsequent attachment of fouling organisms (Figure 1.2A). Bacterial adhesion to a substratum is a multi-stage process comprising the transport of cells to the material surface, initial adhesion of cells, followed by irreversible attachment and surface colonization of cells. The formation of an initial bacterial film lags behind the formation of organic conditioning layer as the transport of molecules to surface is faster than bacteria. Also, the colonization of bacteria is strongly influenced by the conditioning films (Salerno et al. 2004; Scheider 1997).

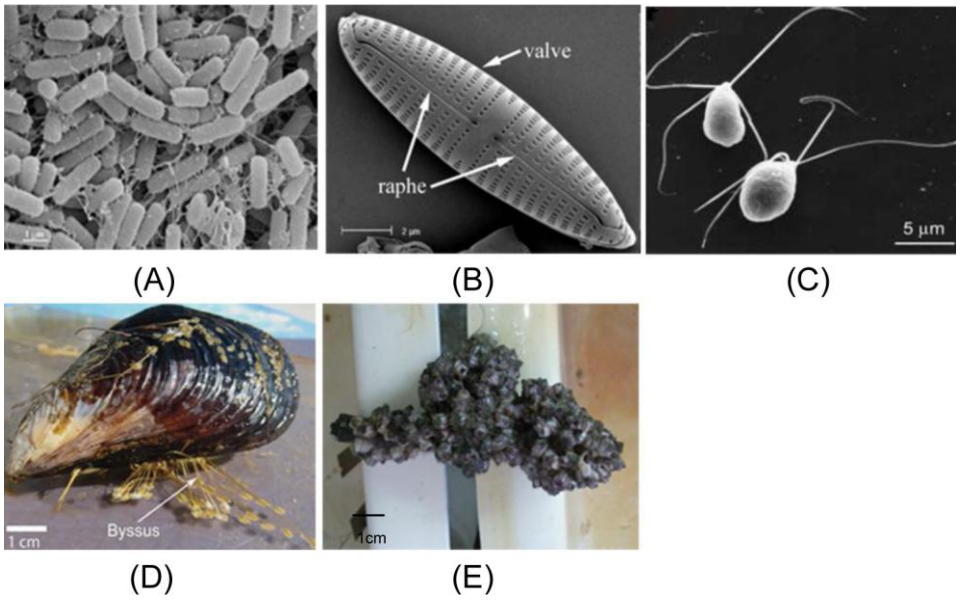

Figure 1.2. Diversity of a range of representative fouling organisms. (A) bacteria (scanning electron micrograph (SEM);(Gu 2003)), (B) SEM of diatom (Navicula) (Callow and Callow 2011), (C) alga (Callow and Callow 2002), (D) mussel (Image Courtesy of Matthew Harrington), and (E) adult barnacles.

1.3.2. Diatom

Diatoms are a significant component of marine biofilm that form on artificial surfaces in the marine environment (Figure 1.2B). They exhibit the nature of both planktonic (free-floating) and benthic (organisms that attach to the submerged surfaces) life strategies, and occupy a diverse habitats (Hoagland et al. 1993; Molino et al. 2009). The benthic diatoms present a serious problem for the man-made structures immersed in the sea as they are a major component of the microbial slim layers that develop on the submerged surfaces, which increase costs associated with extra fuel consumption, corrosion and maintenance (Molino et al. 2009).

1.3.3. Green alga

The green alga, a kind of slippery grass-like plant that is often found in the intertidal zones and is considered as a major macrofouling alga (Figure 1.2C). Enteromorpha

colonizes new surfaces through the production of vast quantities of microscopic motile spores. The swimming spores attach rapidly once a suitable settlement site is detected, resulting in firm attachment to the substratum (Callow and Callow 2002). This is followed by an irreversible commitment to adhesion involving withdrawal of flagella and the secretion of a strong adhesive. The settlement of spores is affected by many factors, such as, light, bacteria, and presence of chemical clues.

1.3.4. Mussel

Mussels (Mytilus, Dreissena and Perna), are the significant fouling organisms because of their large size and accessibility of the attachment apparatus that cause a serious and persistent fouling problems particular aquaculture nets, off-shore rigs and industrial coolant outflows (Aldred et al. 2006; Nishida et al. 2003). The mussels form many threads by secreting an adhesive protein from the foot, and attach with byssal threads, which makes them clump together (Figure 1.2D). Individual adhesive proteins are produced by the foot of mussels and are utilized to form a strong underwater attachment.

1.3.5. Barnacle

Barnacles are crustacean arthropods, which are distantly related to crabs, lobsters, shrimp, etc (Figure 1.2E). They are found on hard substrates in virtually all marine habitats, in vast numbers. Barnacles are considered among the most problematic macrofoulers, due to their size and their gregarious colonization of solid surfaces (Crisp and Meadows 1962). This incurs significant hydrodynamic drag and can potentially damage the protective coatings on steel hulls (Schultz 2007). Prior to attachment on surface, the cyprid larvae of barnacles explore surfaces and select a settling location, where the adult barnacles grow. Once a suitable place is found,

cyprids settle and metamorphose into barnacles. *Amphibalanus amphitrite* (= *Balanus amphitrite*: Pitombo 2004) is considered to be a serious pest because it rapidly colonizes immersed man-made structures and is widely found throughout the sub-tropics (Aldred and Clare 2008). In this thesis, we focus on *B. amphitrite* induced fouling and hence a more specific introduction of barnacle biology is given.

1.3.5.1. Life cycle of barnacle

The lifecycle of the *B. Amphitrite,* includes six planktonic naupliar stages, a non-feeding cypris larval stage, and a sessile adult stage. The life history of the barnacle is shown in Figure 1.3. In *B. Amphitrite* the six ecdyses from the newly released nauplius to the cyprid are completed within 5-7 days at 25 ℃. Depending on culture conditions, cyprids will complete settlement within days to weeks to ensure successful metamorphosis to a sessile juvenile barnacles (Aldred and Clare 2008).

Prior to settlement, cyprids navigate from the water column to potential settlement locations, first exploring the surfaces using a temporary adhesive system and then attaching permanently with a discrete adhesive named permanent cyprid adhesive (Aldred and Clare 2008). Numerous surfaces may be explored and rejected before they spot the most suitable surfaces. During exploration, cyprids scrutinize the surfaces using paired antennules in a form of bi-pedal walking. They perform a tactile exploration of solid surfaces by forming temporary anchoring points with their antennules. This adhesion is mediated by secreted footprint protein (Phang et al. 2009). Cyprids are highly discriminatory during exploration and judge a surface's suitability based on criteria including texture, flow, local hydrodynamics, surface chemistry, and the presence of adult or cyprid conspecifics (Aldred et al. 2008; Rittschof et al. 1984; Roberts et al. 1991; Rittschof et al. 1998; Koehl 2007; Schumacher et al. 2007; Yule and Crisp 1983; Tegtmeyer and Rittschof 1989).

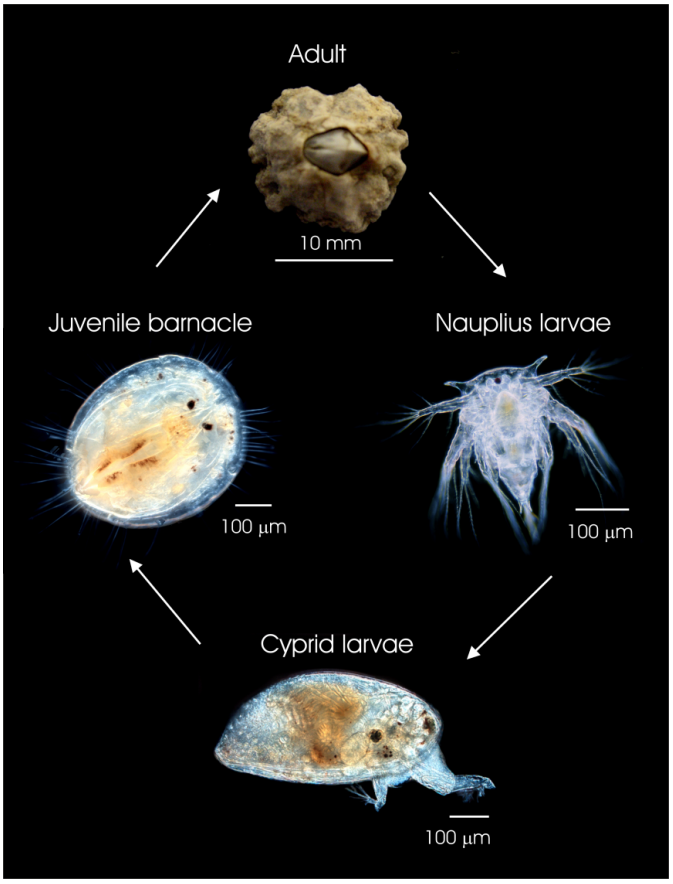

Figure 1.3. Life cycle of barnacle (Aldred et al. (2007)).

Once a settlement site has been selected, a liquid adhesive also termed permanent adhesive of cyprid is released from cement glands within the body through antennular cement ducts (Nott and Foster 1969; Walker 1971). As for the temporary adhesive tissue in the second antennular segment, the cyprid cement glands are composed of tissue that is epidermal in origin (Aldred and Clare 2008). The cyprid cement is deposited in a globular disc, fully embedding the third and fourth segments of the antennules. The cyprid is subsequently permanently attached during metamorphosis into a juvenile barnacle and then grows into the adult barnacle (Figure 1.3).

1.3.5.2. Barnacle adhesion process

There are at least four different adhesion mechanisms in the life cycle of barnacle, they are: temporary adhesive secreted during cyprid exploring, cyprid permanent cement of the settled cyprid, "pinhead" seta secretion at juvenile barnacle stage and adult barnacle cement at adult stage. During exploratory phase, cyprids explore the surface using its two antennules which adhere temporarily on surface by antennules consisting of dense cloak of minute cuticular villi. A thin layer of glycproteinaceous secretion is generated via the cuticular hairs. It subsequently provides a firm adhesion that allows the cyprid to temporarily attach to surface underwater. On locating a suitable attachment site, cyprids express a relatively larger volume of larval permanent cement from cement glands with the body through antennular cement ducts (Nott and Foster 1969; Walker 1971). This large blob of permanent cement embeds both antennules to prevent further translation. Approximately a week after metamorphosis, the basal area of the "pinhead" adheres to the substratum by a mechanism that is not yet clear. As the adult barnacle grows, the secondary cement glands are formed, adult cement is fully filled the gap between the barnacle base and the substratum. Adult barnacle cement is largely proteinaceous, which probably cross links on curing.

1.3.5.3. Cyprid larvae culture

Amphitrite cyprids were reared at the marine laboratory of the Tropical Marine Science Institute (TMSI), National University of Singapore. Adult *B. amphitrite*, collected from Kranji mangroves, Singapore, were kept in running 25-30 ℃ seawater in an open circulating marine aquarium and fed daily with freshly hatched Artemia. Larvae spawned from the adults were reared on an algal mixture of 1:1 v/v of *Tetraselmis suecica* and *Chaetoceros muelleri* at 25 ℃, at a density of approximate

5×10^5 cells/ml (Rittschof et al. 2003). Seawater and algae were replaced every two days to ensure an adequate food supply. Barnacle larvae developed into the cyprid stage within 5-7 days. The cyprids were stored at 4 ℃ and used for experiments after 3 days. Cyprids were acclimatized to room temperature for 30 min before initiation of the experiments.

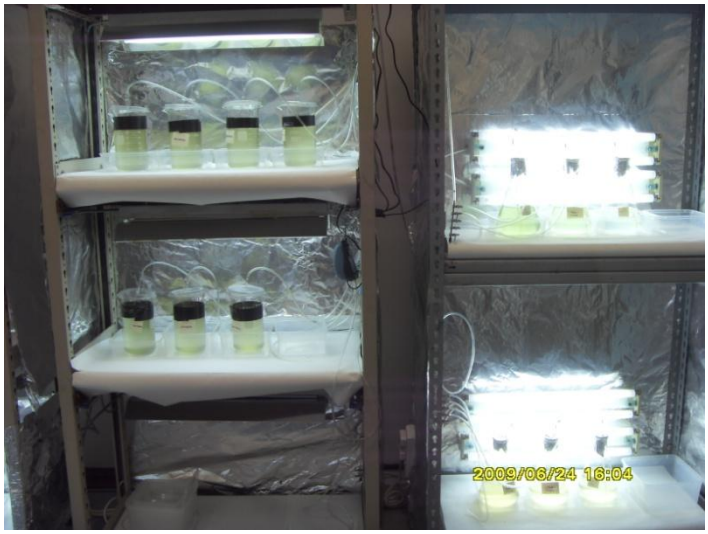

Figure 1.4. *A. Amphitrite* cyprids culture at Tropical Marine Science Institute (TMSI), National University of Singapore.

1.4. Strategies of fouling control

The problem of marine biofouling has long been recognized and various strategies have been applied to combat it. The most common methods used are antifouling coatings and physical cleaning. The latter, involving brushing, scraping have been traditionally used, however, these methods are not only time consuming but may also cause surface damages (Hodson et al. 2000). The most effective antifouling coating has used tributyltin (TBT) as a paint additive since 1960s. In 1970s, the introduction of self polishing copolymers (SPCs) containing copper, tin and other metallic compounds was widely accepted as a effective method for combating fouling (Phang et al. 2007). It is the most successful approach nowadays to prevent biofouling and

generates significant huge economic benefits. While biocides are highly effective (Billinghurst et al. 1998; Kem et al. 2003; Rudolf et al. 1997), they are generally very damaging to the environment and are consequently subject to regulations limiting their widespread implementation. As a consequence, more environmental friendly solutions to marine fouling control are required.

1.4.1. Biocides based methods

1.4.1.1. Copper

The detrimental effects of TBT imposed on the aquatic environment and potential effect on humans led to its eventual ban on all vessels since 2008 (IMO, 2001). As a consequence, copper has been increasingly used as the main biocide ingredient in antifouling coatings, although it was found effective in preventing biofouling with a long history (Yebra et al. 2004). Nowadays, most chemically active paint systems rely on the use of seawater soluble copper oxide (Cu_2O) pigment in combination with other biocides for the prevention of biofouling. The amount of copper used within any antifouling paint varied widely from 20% to 76%, although a great effort was put to reduce the proportion due to environmental concern. Natural background concentrations of copper in seawater are estimated within 0.5-3 μg/L, but concentrations up to 21 μ/L Cu have been found in contaminated areas (Brooks and Waldock 2009). A recent risk assessment on the use of copper as a biocide in antifouling paints considered the concentration, speciation and effects of copper in the coastal marine environment, and inputs from antifouling paints (Brooks and Waldock 2009). They concluded that copper toxicity may impose danger in isolated water bodies, such as enclosed marinas and harbours with little water exchange and high levels of boating activity and recommended development of environmentally friendly antifouling products that would limit the copper usage.

1.4.1.2. Booster biocides

Thanks to increased scepticism over the use of copper, together with relative high tolerance of macroalgae to copper, booster biocides were introduced to antifouling paints to improve their efficacy against these photosynthetic organisms (Voulvoulis et al. 1999). As a result, booster biocides increased the length and functionality of copper-based antifouling coating systems. The most commonly used booster biocides are categorised (Omae 2003; Voulvoulis et al. 1999). Among them, two of the key booster biocides (Irgarol 1051 and Diuron) have been regulated by the UK Health and Safety Executive, with Diuron banned from application and Irgarol restricted to application on vessels greater than 25 m in length (Chesworth et al. 2004; Lambert et al. 2006). The effectiveness of the copper-based coatings is restricted by the ability of the coatings to consistently leach the booster biocides. The concentrations of biocide released in free association paints requires better control and their persistence in marine sediments due to such mechanisms as incorporation within degraded paint particles need continued monitoring (Thomas et al. 2003; Thouvenin. et al. 2002). The use of booster biocides provides an interim solution and more effective antifouling strategies are required to combat marine fouling issues.

1.4.1.3. Natural biocides

As concerns on the biocide based coatings may impose danger to the marine environment, one suggested route is to exploit marine natural defenses utilized by marine organisms against epibionts, specifically, natural marine product antifoulants (Rittschof 2000). The development of effective and environmentally friendly antifouling compounds from natural sources has attracted much research interests among many research groups and commercial laboratories over the recent decades. Many antifouling substances have been extracted from seaweeds and sessile marine

invertebrates and the applications of those bioactive compounds in antifouling paints has been exploited (Fusetani 2004; Hellio and Yebra 2009). The antifouling compounds can be extracted from diverse marine organisms, such as, marine microorganisms, seaweeds and aquatic plants, marine invertebrates, and terrestrial natural products (Qian et al. 2010).

However, the compound must be synthesized in larger quantities at reasonable price, incorporated into the paint matrix, and passes the environmental evaluation that biocides go though. However, the lengthy time and the cost may limit the commercial alternatives to currently registered biocides (Yebra et al. 2004). Also, the supply of the natural compounds into commercial products is a major obstacle and the compounds show only a very narrow spectrum of antifouling activity (Qian et al. 2010). With these reasoning, together with the fact that it is not clear whether all the attachment mechanisms include chemosensory inputs, it may be concluded that attainment of natural metabolites with broad-spectrum activity seems an extremely difficult goal if not unfeasible (Yebra et al. 2004).

1.4.2. Non-toxic coatings

The detrimental or potential danger that biocides based coatings on marine environment prompt investment in the research and development of non-toxic alternatives such as fouling release coating (FRC), superhydrophillic zwitterionic polymers, textured surfaces, etc.

1.4.2.1. Fouling release coatings

Fouling release coatings (FRCs) have been developed as an alternative to biocide-containing coatings for decades and have been commercialized. The FRCs do not prevent organisms from attaching, but the interfacial bond is weakened so that

attached organisms are more easily removed by the hydrodynamic forces resulting from the ship movements through the water or other simple mechanical cleaning (Callow and Callow 2011; Larsson et al. 2010). The properties of FRCs are mainly represented by fluoropolymers and silicone polymers (Yebra et al. 2004). Fluoropolymers provide non-porous, low surface-free energy surfaces with non-stick characteristics, while silicone polymers improve the non-stick efficiency of fluoropolymers. The property of low surface energy facilitates the removal of marine adhesives as the mechanical locking of the glues is reduced which creates slippage and fouling release (Newby et al. 1995).

FRCs are primarily suitable for ships or surfaces which are exposed to fast flow, however, they are not suitable for use in many other circumstances, including static structures, and slow moving objects. In addition, the technology is still expensive, the coating exhibits poor adhesion to the substrate, are easily damaged and have poor mechanical properties (BradyJr 2001; Swain et al. 1998; Yebra et al. 2004).

1.4.2.2. Zwitterionic polymer coatings

In recent years, zwitterionic materials such as poly (sulphobetaine methacrylate) (polySBMA) and poly (carboxybetaine methacrylate) (polyCBMA) have been applied on the biofouling applications (Callow and Callow 2011). The chemical structures of pSBMA and pCBMA are shown in Figure 1.5. Surface coated with zwitterinoci groups are highly resistant to nonspecific protein adsorption, bacterial adhesion, and biofilm formation (Jiang and Cao 2010). The resistance of zwitterionic materials to the adsorption of proteins and cells is generally attributed to a strong electro statically induced hydration layer that creates a superhydrophilic surface. These materials are renowned due to their good chemical stability and low cost (Jiang and Cao 2010). In antifouling assays, polySBMA and polyCBMA have demonstrated

impressive fouling-resistance against proteins and mammalian cells (Aldred et al. 2010a). PolySBMA brushes grafted onto glass surfaces through surface-initiated atom transfer radical polymerization demonstrated significant resistance to the settling spores of marine fouling alga *Ulva linza* (Zhang et al. 2009). Both polySBMA and polyCBMA chemistries prevented settlement of *B. amphitrite* cyprids, and they did not generate toxic effects as all cyprids appeared to be healthy after the assay (Zhang et al. 2009). The mechanism of zwitterionic materials on the prevention of marine organisms may be explained by the secreted proteoglycan bioadhesives being unable to achieve a strong interfacial bond by excluding water molecules from the interface (Callow and Callow 2011). The future development of hydrolysable zwitterionic esters as coatings should provide a platform for the development of practical marine coatings (Jiang and Cao 2010).

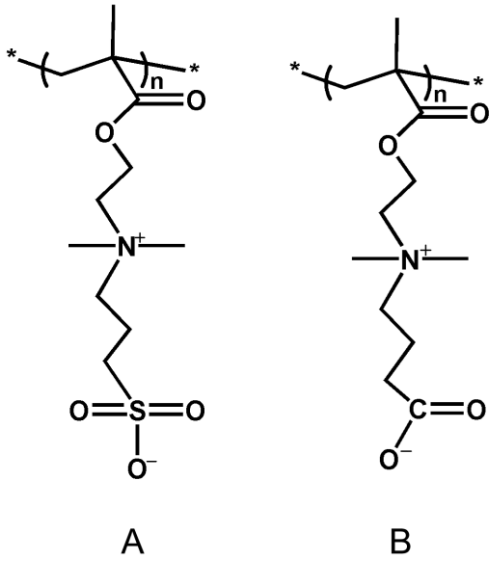

Figure 1.5. The chemical structures of (A) pSBMA; (B) pCBMA (Zhang et al. 2009)

1.4.2.3. Textured surfaces

Another environmentally benign and relatively new area of antifouling research is by the manipulation of surface topography or surface roughness of the coatings. Recently, antifouling (AF) strategies that exploit surface topography have typically been based on consideration of the length scale of the targeted fouling organisms (Schumacher et al. 2007). This length scale can range over several orders of magnitude from bacteria (< 1 μm) to barnacle cypris larvae (around 500 μm for *Balanus amphitrite*) (Schumacher et al. 2007). There are many studies which have examined surface modifications to reduce fouling organisms' settlement (Aldred et al. 2010b; Berntsson et al. 2000; Scardino et al. 2008). These generally involved etching micro-textures into a substrate of varying depths and widths.

In nature, several marine organisms with specific surface structures were found free of fouling. These natural antifouling surfaces attract great research interest over the past decades. The study and copying of these natural mechanisms is described 'biomimicry'. The term implies the use of the natural world as a model to base an engineering development or device upon or as a 'bottom- up' strategy for hierarchical structures (Callow and Callow 2011; Naik et al. 2003). The most well known polymer processes that may have antifouling potential is perhaps the shark skin mimic and the artificial topology inspired by the skin of shark (Sharklet^{TM}) with different arrangements combining pillars and ridges as shown in Figure 1.7 (Carman et al. 2006). Zoospore settlement was reduced by 85% on the finer (ca 2 mm) and more complex Sharklet AF^{TM} topographies (Carman et al. 2006). The result suggests that bio-inspired surface can inhibit the settlement of marine organisms. However, engineered microtopographies or artificially textured coatings only typically inhibit a subset of fouling organisms based on the size of the microstructures. To achieve

broad-spectrum fouling resistance, it appears that multiple strategies needed to be incorporated in the future, including nano-technology, natural product and surface chemistry. Furthermore, this technique is currently expensive and impractical for wide applications.

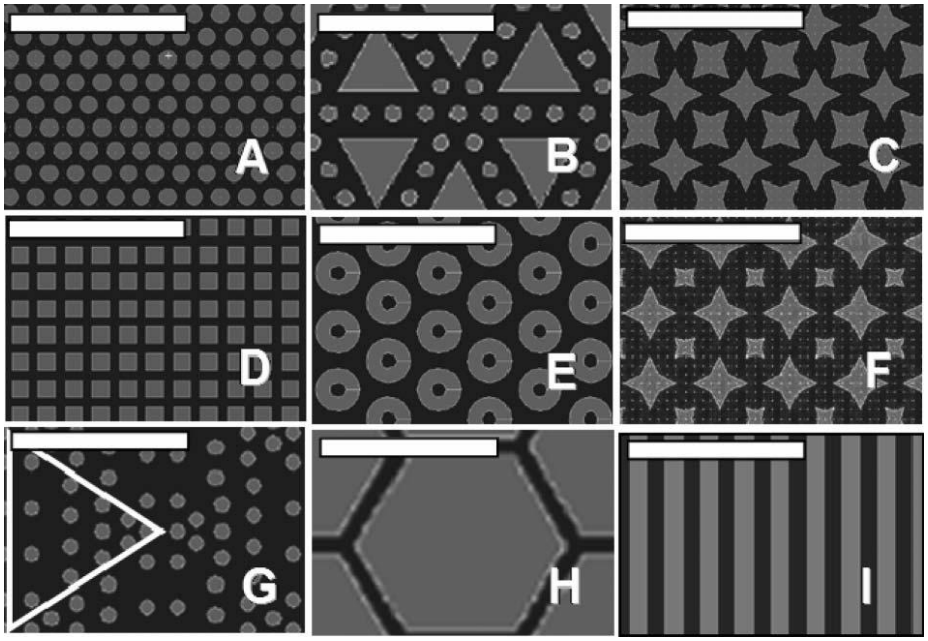

Figure 1.6. AutoCad sketches of proposed topographies. (A) 2 mm diameter, 2 mm spaced pillars; (B) triangles and 2 mm pillars; (C) 4 mm wide, 2 mm spaced stars; (D) 2 mm wide, 1mm spaced square pillars; (E) rings with 2 mm inner diameter and 6 mm outer diameter, spaced 2 mm apart; (F) 4 and 2 mm wide stars; (G) 2 mm diameter pillars spaced 1, 2 and 4 mm apart in a gradient array (repeat unit designated by triangle);(H) hexagons with 12 mmlong sides and spaced 2 mm apart; (I) 2 mm wide, 2 mm spaced channels. Scale bars=20 mm (Carman et al. 2006).

1.4.3. Physical methods

Other than the biocide and non-biocide coating based fouling control methods, effectiveness attributed to physical and mechanical ways has also been reported. Pulsed electric fields has been reported to inhibit cyprid settlement (Pérez et al. 2008). The result showed that with the amplitude of 10V and duration of 100ms, cyprid settlement was significantly inhibited. Low frequency sound and vibration were also found effectively to reduce barnacle cyprid settlement (Branscomb and Rittschof

1984; Choi et al. 2013). However, these frequencies fall within the audible spectrum of humans and thus are liable to generate noise pollution, limiting their application. A new direction for mechanical antifouling is to mimic natural grooming. This is the idea behind the HullBUG (Hull Bioinspired Underwater Grooming), an autonomous robot that will proactively pass over a hull while a ship is in port.

1.5. Effect of ultrasound on biofouling

Other than the aforementioned methods, ultrasound could also be a promising alternative. In this section, the applications of ultrasound on biofouling prevention are reviewed.

Sound is a travelling wave that is an oscillation of pressure transmitted through a solid, liquid, or gas, composed of frequencies within the range of hearing and of a level sufficiently strong to be heard, or the sensation stimulated in organs of hearing by such vibrations. Generally, mechanical vibrations create sound or pressure waves in an elastic medium, transferring energy into the medium and to any objects the sound make contact with. The typical human range for audible sound is from 20 Hz to 20 kHz; there are also ultrasonic waves and infrasonic waves that are beyond the human being audible ranges. Infrasound is the sound wave below 20 Hz while ultrasound, in its most basic definition, refers to the pressure waves with frequency of 20 kHz or higher, which is above the audible range of humans.

Normally, ultrasound is generated from ultrasonic transducers made of piezoelectric materials such as quartz or certain ceramics that resonate when electricity is passed through the material. The piezoelectric material can convert the electrical energy to mechanical energy in the form of ultrasound wave. The ultrasound wave propagates into the medium such as water and can be picked by the hydrophone.

1.5.1. Ultrasound applications on biofouling prevention

The applications of ultrasound on biofouling control have been extensively reported. Biofilm control and removal can be achieved by the application of ultrasound, and a optimum condition can be reached by the consideration of frequency and amplitude (Bott 2000). By operating ultrasound at 40 kHz for 10 s, biofilm could be removed and the efficiency was fourfold greater as compared to the swabbing method (Lagsir et al. 2000). Similarly, 87.5% of biofilms formed on water filled glass tubes could be removed using 20 kHz ultrasound treatment with pulsed operations (Mott et al. 1998).

The effectiveness of ultrasound was also found on the bacteria control. Ultrasound in the frequency range of 20-38 kHz significantly killed Bacillus species, and the efficiency was enhanced with increasing duration of exposure time and intensity (Joyce et al. 2003). Similarly, frequency of 26 kHz was found effectively in killing four mentioned bacteria (Scherba et al. 1991). Not only mortality effect, the bacteria growth inhibitory effect was also found. Gram-negative bacteria, in particular Escherichia coli, were significantly inhibited after ultrasound exposure (Monsen et al. 2009).

Likewise, ultrasound can be used on algae control. The effectiveness of ultrasound irradiation on algae removal was achieved at frequency of 40 kHz (Liang et al. 2009). Ultrasound cavitation plays significant role on algae removal, ultrasound frequency and intensity determines the removal efficiency (Giordano et al. 1976; Ma et al. 2005). Except ultrasonic cavitation, ultrasound induced resonant vibration was found to damage algae cell more easily when the applied ultrasonic frequency was close to the natural frequency of algae cell (Hao et al. 2004).

1.5.2. The application of ultrasound on barnacle prevention

The effect of ultrasound on barnacle induced marine fouling control has also been extensively studied. Laboratory studies have shown that frequencies in the orders of tens of kHz efficiently kill barnacle larvae (Mori et al. 1969; Suzuki and Konno 1970). In the field test, ultrasound frequency range between 20 to 100 kHz was effective in keeping an area free of fouling marine organisms (Fischer et al. 1981). More recently, a relative systematic study of ultrasound on barnacle cyprid settlement and mortality was explored using three frequencies and various exposure intensity and the most effective frequency on settlement inhibition occurred at 19.5 kHz (Kitamura et al. 1995). Also, ultrasound induced cavitation effect was used to pulverize barnacle nuaplii for the blasted water treatment and the pulverized ultrasound energy was estimated by calorimetric absorption (Seth et al. 2010). Nowadays, Shipsonic (Netherlands) and Ultrasonic Antifouling (UK) have commercialized ultrasound-based products, which are marketed for marine fouling prevention on berthed pleasure crafts.

1.6. Scope and objective of study

The thesis describes the use of ultrasound on the control of barnacle induced marine biofouling. The objective of this study is to explore the effects of ultrasound on barnacle cyprids and juvenile barnacles. The specific tasks are as follows:

To study the effect of ultrasound on barnacle cyprid settlement, mortality, exploration behavior, as well as the optimum parameters that generate the changed phenomenon;

To explore the possible mechanism that induces cyprid settlement inhibition;

To investigate low intensity, low frequency ultrasound on the prevention of cyprid settlement;

To explore the effect of ultrasound on barnacle cyprid footprints secretion and juvenile barnacles' adhesion strength;

To study the cavitation effects on the removal or damage of juvenile barnacles.

1.7. Thesis organization

In this chapter, an introduction on marine biofouling, especially barnacle induced marine biofouling is given, and strategies of antifouling are introduced, especially ultrasound based antifouling method, followed by the objective and organization of the thesis.

Chapter 2 presents the effects of ultrasound on barnacle cyrid settlement, exploration behavior and mortality using frequencies of 23, 63 and 102 kHz. Low frequency of 23 kHz shows more effective than the other two frequencies on settlement inhibition with the same ultrasound intensity.

Chapter 3 explores the possible mechanism behind ultrasound induced cyprid settlement inhibition using spectrum analysis method. And the results revealed that ultrasonic cavitation may be the possible mechanism.

Chapter 4 investigates low intensity ultrasound on cyprid settlement. And the results showed that, with low intensity exposure, significant inhibitory effects can be only achieved within the low frequency range of between 20 to 25 kHz. Also, the application of ultrasound treatment in an intermittent mode of "5 min on and 20 min off" at 23 kHz generates the same effect as with the continuous ultrasound application.

Chapter 5 studies the effect of ultrasound on cyprid footprints secretion and the adhesion strength of juvenile barnacles using AFM and Nano-tensile tester respectively. The results show that ultrasound treatment reduces cyprid footprint

secretion and juvenile barnacle adhesion strength. The findings suggest that the combination of ultrasound and fouling release coating may provide a more effective fouling control strategy.

Chapter 6 verifies the cavitation bubbles on the damage or removal of juvenile barnacles and observes bubble-barnacle interaction process using high speed photography.

Chapter 7 concludes the study and suggests some future work.

Chapter 2. Effect of ultrasound on cyprids and juvenile barnacles

In this chapter, effect of ultrasound on cyprid settlement, exploration behavior and juvenile barnacle growth was systematically studied. Settlement inhibition of barnacle (*Amphibalanus amphitrite*) cypris larvae resulting from exposure to ultrasound was studied using three frequencies (23, 63 and 102 kHz), applied at three acoustic pressure levels (9, 15, and 22 kPa) for exposure times of 30, 150, and 300 s. With the same acoustic exposure condition, the lowest settlement was achieved for 23 kHz, which also induced the highest cyprid mortality. Cyprid settlement following exposure to 23 kHz at 22 kPa for 30 s is reduced by a factor of two. Observing the cyprids' surface exploration revealed an altered behavior following exposure to ultrasound: step length was increased, while step duration, walking pace, and the fraction of cyprids exploring the surface were significantly reduced with respect to control cyprids (i.e. cyprids not exposed to ultrasound). The basal area of juvenile barnacles, metamorphosed from ultrasound-treated cyprids was initially smaller than unexposed individuals, but normalized over two weeks' growth. Thus, ultrasound exposure effectively reduces cyprid settlement, yet metamorphosed barnacles grow normally.

2.1. Introduction

Marine fouling significantly increases global carbon emissions by increasing fuel demand and generating additional maintenance costs, which can run into billions of dollars annually for marine industries (Yebra et al. 2004). Barnacles are among the most problematic macrofoulers, due to their size and their gregarious colonization of solid surfaces (Crisp and Meadows 1962).

The lifecycle of the striped barnacle, *Amphibalanus amphitrite* (= *Balanus amphitrite*: (Pitombo 2004), includes six planktonic naupliar stages, a non-feeding cypris larval stage, and a sessile adult stage. Barnacle fouling prevention research often focuses on dissuading or inhibiting cyprid settlement (Aldred and Clare 2008; Chambers et al. 2006), which is considered to be the key to preventing surface colonization by barnacles.

Cyprids are capable of swimming, which brings them into contact with solid substrates. They perform a tactile exploration of solid surfaces by forming temporary anchoring points with their antennules. The reactions of cyprids to environmental and surface cues generally translate into a behavioural response, which may correlate to settling affinity. Rittschof et al. (1984) classified the observed cyprid behaviour into specific categories while performing a settlement assay under flow. This adhesion is mediated by secreted footprint protein (Phang et al. 2009). Cyprids integrate their surface sensing with environmental cues in determining the final settlement choice (Aldred and Clare 2008; Aldred et al. 2008; Crisp 1955). Several studies have measured cyprid exploration behavior, correlating it with their settlement preferences. Cyprids were found to spend more time exploring smooth surfaces and tend to swim when exposed to micro-textured surfaces (Berntssona et al. 2000). The Etho Vision 3.0 software was developed to quantify total exploration time and the total distance

covered by cyprids during their substrate exploration (Marechal et al. 2004). Chaw and Birch (2009) developed a complementary fine scale microscopic observation of cyprid exploration, thus implementing a behavioral assay that quantifies the step length and step duration. This study revealed that cyprids explore hydrophilic surfaces using longer steps of shorter duration and correlated this behavior with a higher settling affinity on hydrophilic versus hydrophobic surfaces.

Several approaches have been explored for preventing barnacle cyprid settlement and extensively reviewed in the chapter of introduction. These strategies include biocides based methods (Standing et al. 1983; Clare et al. 1992; Kem et al. 2003; Rudolf et al. 1997), physical methods as electrical field (Pérez et al. 2008), low frequency sound waves (Branscomb and Rittschof 1984), fouling release coatings (Callow and Callow 2011; Larsson et al. 2010) and textured surfaces (Scardino et al. 2008; Schumacher et al. 2007).

Except for the above mentioned methods, ultrasound frequencies above 20 kHz, which are beyond the human audible range, are expected to offer a more widely accepted solution. The effectiveness of ultrasound on barnacle fouling prevention was also detailed reviewed (Kitamura et al. 1995; Seth et al. 2010; Suzuki and Konno 1970).

Although ultrasound is a promising marine fouling prevention tool, the scarcity of information regarding the required power and exposure time range limits its effective implementation. The application of ultrasound in marine fouling prevention will benefit from a better understanding of the impact of ultrasound on cyprid mortality and the inhibition of barnacle settlement. Thus, a comprehensive and systematic study of the influence of frequency, acoustic pressure and exposure time on cyprid settlement, in combination with a cyprid exploration behavioral assay, is needed to

provide essential information for the application of ultrasound in marine fouling prevention. From prior studies, Mori et al (1969) and Suzuki and Konno (1970) found that ultrasound frequencies of the order of tens of kHz efficiently kill barnacle larvae. Fischer et al (1981) also found that devices emitting in the 20-100 kHz range maintain solid surfaces clear of fouling organisms. More recently, Kitamura et al (1995) reported a higher efficiency for 19.5, versus 28 or 50 kHz. Taking into account the transducer's resonant frequencies, 23, 63, and 102 kHz were selected for this study. In light of previous reports, these frequencies cover an adequate range for marine fouling prevention.

The present study examines the efficiency of three frequencies (23, 63, and 102 kHz), and the influence of exposure time and acoustic pressure on barnacle cyprid settlement. Moreover, it quantifies the effect of ultrasound exposure on cyprid mortality and cyprid exploration behavior. Finally, it explores the growth of juvenile barnacles, which were metamorphosed from ultrasound-treated cyprids.

2.2. Materials and methods

2.2.1. Ultrasonic irradiation system

A diagram of the experimental setup is shown in Figure 2.1. A sinusoidal wave from a function generator (Agilent 33210A, USA) is fed into a power amplifier (HSA4051, Japan). This signal is used to drive an 80 mm ceramic piezoelectric transducer (Fuji Ceramics, Japan) at selected resonant frequencies of 23, 63, and 102 kHz. The transducer rested at the bottom of a transparent acrylic water tank with its emission axis pointing vertically upwards.

An open polyethylene snap-cap vial (Ref. 18 09 0906, Alpha analytical, Singapore) was placed with its axis horizontal at a height of 20 mm above the transducer. The

acoustic pressure inside the vial was measured using a hydrophone (GRAS 10-CT, G.R.A.S Sound & Vibration, Denmark) and adjusted to the desired value. The vial was then removed and rinsed with 1 µm filtered seawater (FSW, passed through 5 and 1 µm double open filter cartridges: Cole-Palmer, 255482-43 and 255481-43, respectively). 60-70 cyprids in 10 ml FSW were then placed in the vial, which was capped and re-positioned at the same location above the transducer.

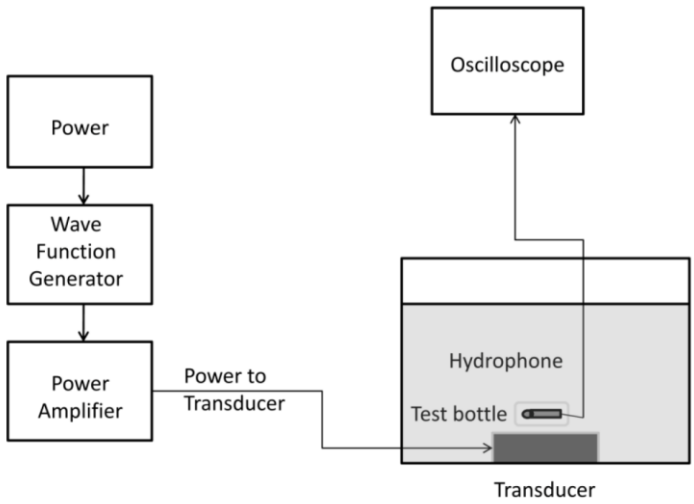

Figure 2.1. Schematic diagram of the ultrasound system.

2.2.2. Cyprid settlement and mortality assay

The effect of ultrasound on cyprid settlement was studied under three frequencies: 23, 63 and 102 kHz. To study the effect of acoustic pressure on settlement, cyprids were exposed to ultrasonic pressures of 9, 15, and 22 kPa for 30 s. To assess the affect of exposure time, cyprids were exposed for 30, 150 and 300 s at an acoustic pressure of 20 kPa. The ultrasound treated and control (no ultrasound exposed) cyprids were incubated in their respective capped vials for 24 hrs at 28 ℃, on a 15:9-hour light/dark cycle. All settled cyprids were counted, including those that were permanently attached but not metamorphosed and fully metamorphosed barnacles.

The effect of ultrasound on cyprid mortality was also quantified. In this assay, 50-70 cyprids were transferred to FSW-filled polyethylene snap-cap vials and exposed to three frequencies: 23, 63, and 102 kHz for exposure times of 30, 150, and 300 s, at the fixed acoustic pressure of 20 kPa. After 24 hrs, the vials were emptied into a counting tray and dead cyprids were scored as described in Kem et al. (2003). The mortality of control cyprids (no ultrasound exposed cyprids), was recorded for comparison. Both settlement and mortality assays were conducted in triplicate.

2.2.3. Cyprid exploration behavior assay

Cyprid exploration behavior tests were performed on ultrasound-treated cyprids and control cyprids. As no significant cyprid settlement differences were observed following exposure to 63 and 102 kHz ultrasound (see Results below), the cyprid exploration behavior assays were conducted with 23 and 102 kHz, which represent the lowest and highest frequencies, respectively. An acoustic pressure of 20 kPa was applied to separate batches of cyprids for times of 30 and 300 s' duration. These were then transferred to a FSW-filled polycarbonate multi-well plate **(**Nalge Nunc International, USA**)** and the behavior of 15-20 individual cyprids for each condition was recorded using the imaging method described in Chaw and Birch (2009). As above, the behavior of control cyprids was measured in the same way. After a 2 min acclimation period, the observation and recording time was set to 5 min (Marechal et al. 2004). Image analysis was used to determine the step length, defined as the distance between two sequential temporary anchoring points, and the step duration, defined as the time elapsed from the detaching of a trailing antennule to its reattachment, forming a new temporary anchoring point. Step length and step duration data were pooled for all cyprids within each condition (Chaw and Birch

2009). The cyprid walking pace was defined as the number of steps taken by cyprids in 5 mins.

The cyprid exploration rate was calculated as a ratio of the exploring cyprids to the total number of cyprids. A microscope (IX51, Olympus, Japan) was used at low magnification (4 x 10) to generate a field of view covering one well of the plate. After adding 50-60 cyprids to each well and allowing 2 mins for acclimation, the number of exploring cyprids was counted over a period of 5 mins. Cyprids exploring the surface were scored only once, even if they resumed surface exploration after swimming.

2.2.4. Barnacle growth assay

To examine if cyprid exposure to ultrasound compromises the growth of metamorphosed barnacles, these were cultured in the laboratory and their growth compared with that of barnacles developed from control cyprids (not exposed to ultrasound). Cyprids treated with frequencies of 23, 63, and 102 kHz for 300 s at acoustic pressure of 20 kPa, respectively, were transferred to Petri dishes (Alpha analytical, Singapore), where they were allowed to settle. Metamorphosed juvenile barnacles were maintained in an aquarium with running seawater, with supplemental feeding using the same algal mixture as for the nauplii culture for 3 h per day. The underside of 20-25 juvenile barnacles within each Petri dish was photographed every 2 days over a two-week period (Skinner et al. 2007) using a digital camera (Olympus E330, Japan) attached to a microscope (Olympus SZX 10, Japan). The images were processed with ImageJ software (Version 1.43), which used edge contrast to define the perimeter and thereby calculate the total basal area.

2.2.5. Statistical analysis

All statistical comparisons were performed using GraphPad Prism 5 (GraphPad Software Inc.). Two main factors were considered in cyprid settlement, mortality, and exploration behavioral assays: ultrasound frequency and acoustic pressure; or exposure time and frequency. Data was analyzed with a two-way analysis of variance (ANOVA) to evaluate significant influence of these parameters. This was followed by a one-way ANOVA together with a Tukey post test to determine differences between treated and control cyprids. Barnacle growth rate data were analyzed with a one-way ANOVA, followed by a Tukey post test. All data are reported as mean $\pm$ standard error (SE). For all comparisons, p-values ≤ 0.05 were considered as statistically significant.

2.3. Results

2.3.1. Cyprid settlement assay

Ultrasound exposure significantly reduced cyprid settlement compared to untreated control cyprids (One way ANOVA, $p < 0.05$). Tukey pair-wise comparisons revealed that all ultrasound treatments differed significantly from the untreated control ($p < 0.05$), as shown in Figure 2.2. Significant differences were also found among ultrasound frequencies (Two-way ANOVA, $p < 0.05$; Figure 2.2). The number of settled cyprids was lowest for cyprids exposed to 23 kHz (Tukey test, $p < 0.05$), with no significant difference between 63 and 102 kHz at equal exposure times (Tukey test, $p > 0.05$).

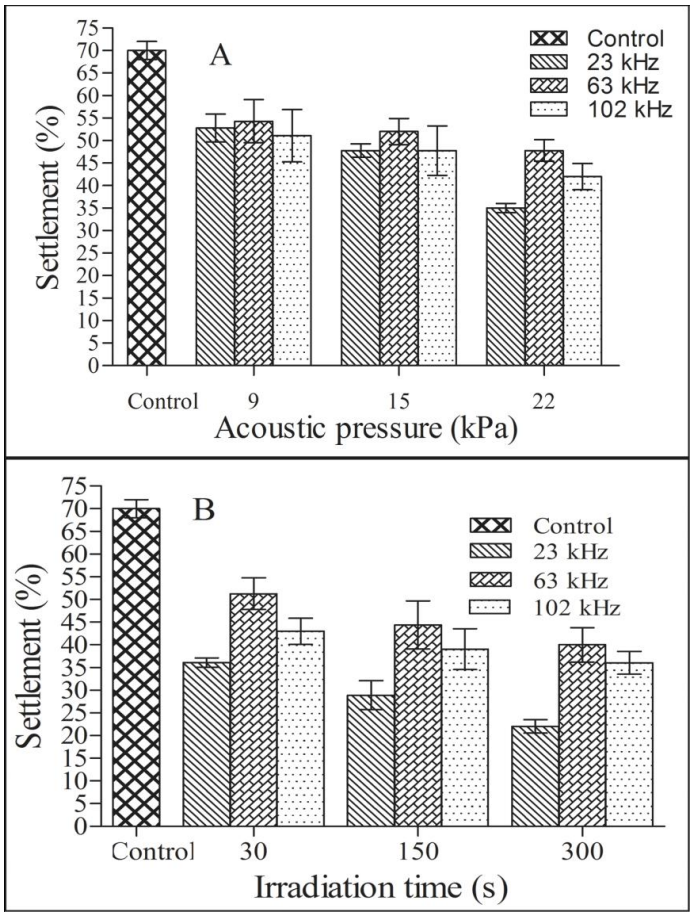

Figure 2.2. The effect of ultrasound exposure on cyprid settlement. (A) Tested acoustic pressures of 9, 15, and 22 kPa for an exposure time of 30 s. (B) Exposure time of 30, 150, and 300 s at a pressure of 20 kPa.

Settlement differed significantly with acoustic pressure levels (Two-way ANOVA, $p = 0.0008$), with higher acoustic pressure leading to lower settlement (Tukey test, $p < 0.05$, Figure 2.2A). At 23 kHz, an acoustic pressure of 22 kPa applied for 30 s reduced settlement by a factor of two (Figure 2.2A). Different settlement was similarly observed with exposure times (Two-way ANOVA, $p = 0.001$). Settlement

decreased with ultrasound exposure and was lower than control cyprids (Tukey test, $p < 0.05$, Figure 2.2B).

2.3.2. Cyprid mortality

Mortality assays showed that exposure to ultrasound increases cyprid mortality (One-way ANOVA, $p < 0.05$), with both exposure time and frequency having a significant effect (Two-way ANOVA, $p < 0.05$, Figure 2.3). For 63 and 102 kHz, a significant increase in mortality was not recorded for 30 and 150 s' exposure (Tukey test, $p > 0.05$). Increased mortality was observed for 300 s' exposure (Tukey test, $p < 0.05$) and no differences were observed in mortality induced by 63 and 102 kHz (Tukey tests, $p > 0.05$). 23 kHz induced the highest mortality rates (Tukey test, $p < 0.05$) and its effect increased with exposure time (Tukey test, $p < 0.05$). 23 kHz applied for 300 s at an acoustic pressure of 20 kPa led to a three-fold increase in cyprid mortality (Figure 2.3).

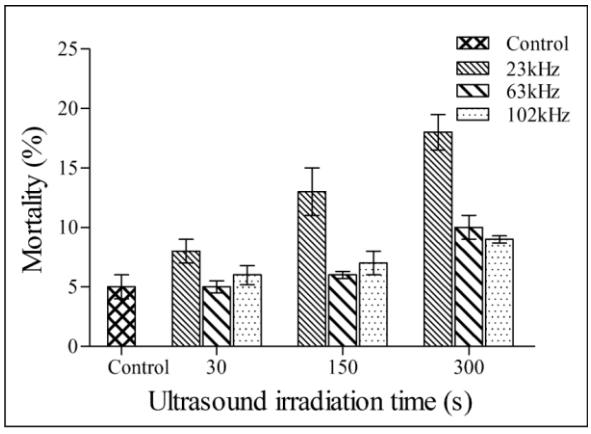

Figure 2.3. The effect of ultrasound exposure on cyprid mortality at an acoustic pressure of 20 kPa.

2.3.3. Cyprid exploration behavioral assay

For cyprids exposed to ultrasound, step length and step duration data yielded a distinguishable response. Figure 2.4 shows histograms of control and ultrasound-treated cyprids and Table 2.1 reports mean ± SE values extracted from these data. Step duration, exploration rate, and walking data are summarized by the histograms shown in Figure 2.5.

Cyprid exploration behavior was significantly affected by ultrasound frequency (Two-way ANOVA, $p < 0.01$). From Figure 2.4, step lengths smaller than 230 µm were not observed on control cyprids, while step lengths smaller than 170 µm were obtained for ultrasound treated cyprids. From Table 2.1, the mean step length was significantly reduced for cyprids exposed to ultrasound (One-way ANOVA, $p < 0.05$). However, there was no significant difference in the step lengths of cyprids subjected to 23 or 102 kHz ultrasound (Tukey test, $p > 0.05$).

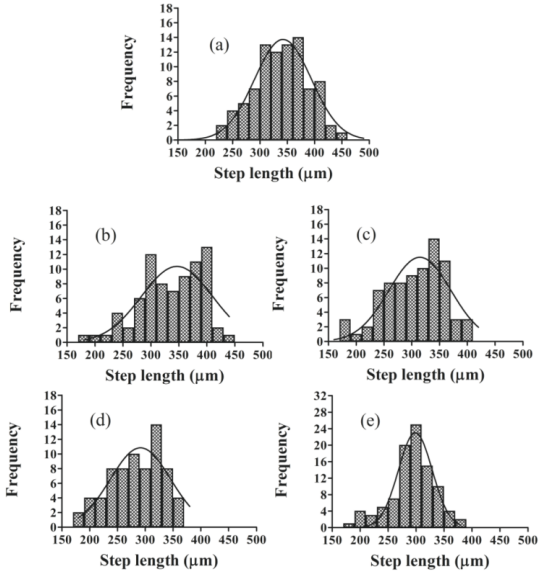

Figure 2.4. Histograms of step length data for: (a) untreated control cyprids; (b) and (c): cyprids exposed to 23 kHz for 30 and 300 s, respectively; (d) and (e): cyprids exposed to 102 kHz for 30 and 300 s, respectively. Ultrasound was applied with an acoustic pressure of 20 kPa.

Table 2.1. Step length for control cyprids and cyprids exposed to an ultrasound pressure of 20 kPa.

Ultrasound treatments	Average step length ± SE(μm)
Control	341 ± 5
23 kHz for 30 s	300 ± 6
23 kHz for 300 s	305 ± 6
102 kHz for 30 s	288 ± 8
102 kHz for 300 s	291 ± 4

Step duration increased with ultrasound exposure time (Two-way ANOVA, $p < 0.0001$; Figure 2.5a), with insignificant differences between frequencies with 30 s' exposure time (Tukey, $p > 0.05$). At 300 s' exposure, 23 kHz increases step duration significantly more than 102 KHz (Tukey test, $p < 0.05$). Ultrasound exposure also diminished the cyprid walking pace (Two-way ANOVA, $p < 0.0001$; Figure 2.5b). This reduction followed a similar trend to the step duration changes: the influence of 23 and 102 kHz was indistinguishable for 30 s' exposure and 23 kHz was more effective than 102 kHz, when ultrasound was applied for 30 s (Tukey test, $p < 0.05$, Figure 2.5b). The cyprids' exploration rate decreased with ultrasound exposure time (Two-way ANOVA, $p = 0.0074$; Figure 2.5c) and followed the same trend: 23 and 102 kHz generated an indistinguishable effect at 30 s' exposure time, while 23 kHz generated a more substantial reduction than 102 kHz for 300 s' exposure time (Tukey test, $p > 0.05$).

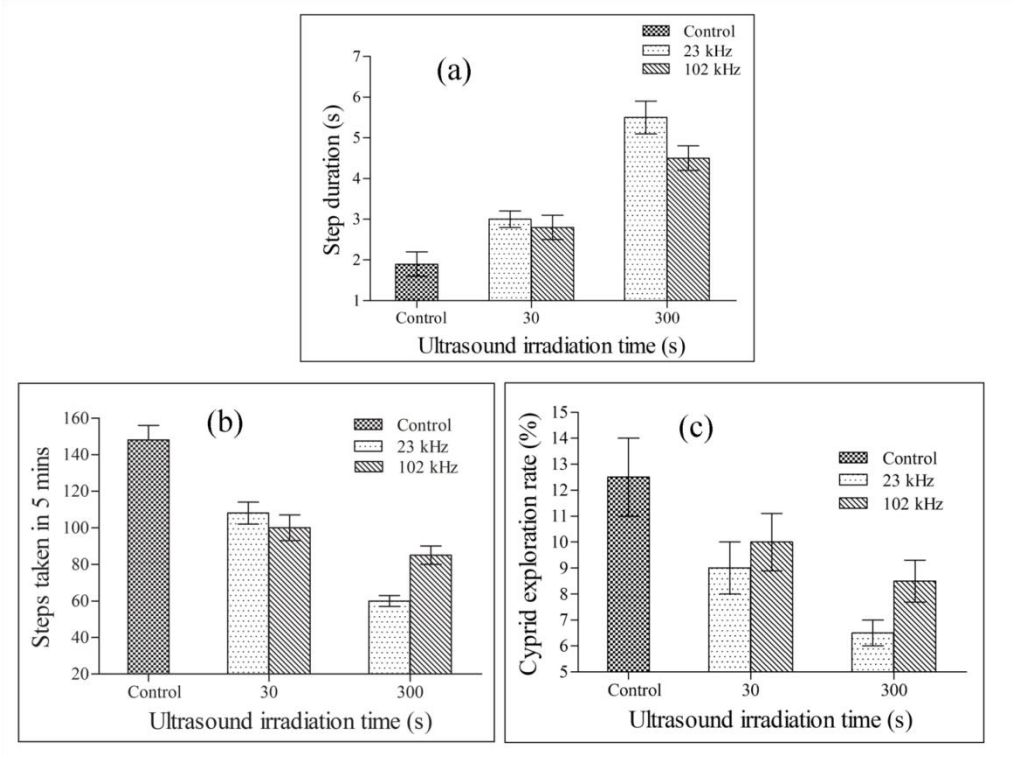

Figure 2.5. Histograms of cyprid behavior data for: (a) Step duration; (b) Walking pace (c) Exploration rate. Ultrasound was applied with an acoustic pressure of 20 kPa.

2.3.4. Barnacle growth assay

Barnacles newly metamorphosed from ultrasound-treated cyprids initially showed smaller basal areas than those metamorphosed from control, untreated cyprids (One-way ANOVA, $p < 0.05$, Figure 2.6). There were no differences in size between the newly metamorphosed adults obtained from cyprids exposed to 23, 63, and 102 kHz ultrasound frequencies, all applied at 20 kPa for 300 s (Tukey test, $p > 0.05$). For all barnacles, the basal area increased with time. After 10 days' culture, the differences in basal area between ultrasound-treated and control barnacles were reduced and no longer significant (Tukey test, $p > 0.05$).

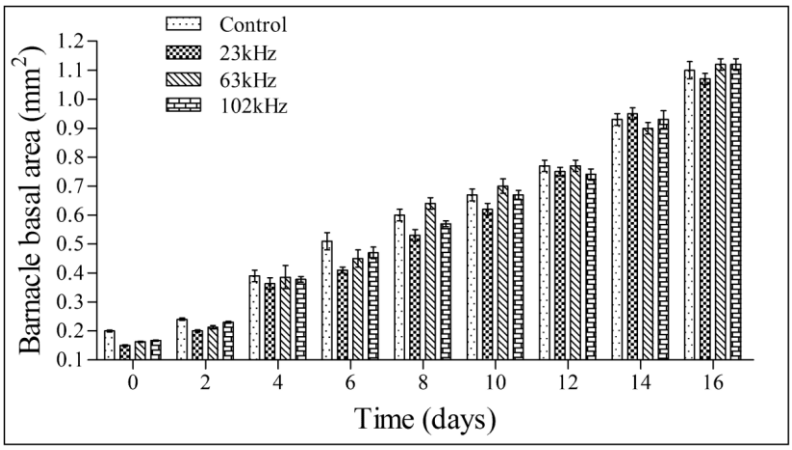

Figure 2.6. Growth of juvenile barnacles, metamorphosed from untreated control cyprids and cyprids exposed to ultrasound frequencies of 23, 63, and 102 kHz, for 300 s with an acoustic pressure of 20 kPa.

2.4. Discussion

Cyprids exposed to ultrasound exhibited lower settlement rates and higher mortality. Settlement inhibition was enhanced with increasing acoustic pressure and longer exposure times, which suggests a progressive degradation of the cyprids condition, although no obvious visible damage was observed. Of the ultrasound frequencies used, 23 kHz was most effective, with 63 and 102 kHz generating a similar, lower response. Cyprid mortality did not increase significantly when cyprids were exposed to 63 or 102 kHz for up to 150 s and it only increased moderately for cyprids exposed to these frequencies over 300 s. Interestingly, for these two frequencies, settlement rates are reduced significantly for the different exposure times but did not induce higher mortality. The most effective configuration was obtained with application of 23 kHz at 20 kPa for 300 s. This reduced cyprid settlement by a factor of two and induced a three-fold increase in their mortality. Kitamura et al. (1995) previously reported an increased efficacy of lower ultrasound frequencies, in the region of 20 kHz, and that the impact of ultrasound increased with total irradiation. Their study also confirms the lethal effect of ultrasound exposure, with an enhanced impact at

19.5 kHz. These results are consistent with the data reported in this study and other similar work by Mori et al. (1969) and Suzuki and Konno (1970).

Ultrasound treatment presents several benefits over chemical-based biocidal strategies. Biocide-based antifouling coatings function through the gradual release of molecules from the coating's surface, a portion of which may accumulate in, and adversely affect, the marine environment (Chambers et al. 2006). In contrast, ultrasound exposure does not engender a cumulative effect, as molecules are not released into the marine environment. Ultrasound as a method of fouling prevention confers additional advantages. It can be applied at will in a highly controlled manner, as opposed to biocides that are released continuously based on the chemistry of the coating (Chambers et al. 2006). For example ultrasound could be applied in a regimented pulsed fashion, as has been described for electric fields (Pérez et al. 2008), or could be turned on while in port and turned off once a ship has reached cruising speed, thus potentially saving power and other resources. Moreover, ultrasound may be conveniently applied to surfaces with low liquid shear forces (e.g. low-flow areas of the hull and the sea chest), where fouling-release non-stick coatings have limited effectiveness. Undoubtedly, a thorough assessment of the effect of ultrasound on the marine environment would be prudent before its widespread implementation. With an optimized engineering design, its implementation will ideally be confined to surface treatment, while limiting the propagation of sound waves into the marine environment.

The decreased settlement and increased mortality observed following exposure to ultrasound is likely a result of physical injury to the cyprid. Ultrasound pressure fluctuations are efficiently transmitted through liquids and can dissipate their energy in biological tissues, which can be altered and damaged by this process (Brondum et

al. 1998). High intensity ultrasound, which develops significant levels of cavitation, can be used to disintegrate barnacle larvae (Seth et al. 2010). Cavitation induced by ultrasound has been cited as responsible for compromising the viability of several organisms, including bacteria and algae growing on solid substrates (Scherba et al. 1991; Liang et al. 2009; Lagsir et al. 2000). Cavitation is followed by implosion, which generates high liquid shear forces. Micro-streaming, induced by gas bubbles generated during cavitation, is also capable of injuring cells. These liquid shear forces can damage organisms. Given that cavitation threshold generally increases with ultrasound frequency (Ma et al. 2005; Hao et al. 2004; Kratochvil et al. 2006), this may explain the enhanced efficiency of 23 kHz for compromising cyprids viability. Further exploration of the ultrasound-induced physical damage is expected to shed light on the causes underlying the cyprids' reduction in settlement and their increased mortality.

Interestingly, exposing cyprids to ultrasound also alters their subsequent surface exploration behavior. Given the similar response generated by 63 and 102 kHz, only 23 and 102 kHz frequencies were used in these experiments. While the step length was changed significantly following ultrasound exposure, significant differences in step length were not observed either between 23 to 102 kHz or when the exposure time was increased from 30 to 300 s (Table 2.1). In contrast, both frequency and exposure time generated significant changes in step duration, walking pace, and exploration rate. Following ultrasound exposure, step duration increased and both walking pace and exploration decreased. All three parameters followed similar trends: the influence of ultrasound increased with exposure time, with 23 and 102 kHz applied for 30 s generating the same change, while 23 kHz was more effective than 102 kHz, when applied over a period of 300 s (Figure 2.5). This increasing change of the exploration behavior with ultrasound exposure may be indicative of a

physiological change in the cyprid's condition. As observed in the settlement and mortality assays, 23 kHz generates the largest impact.

A previous study by Chaw and Birch (2009) observed that cyprids exploring a surface that is less favoured for settlement decrease their step length and increase their step duration, which may be considered as performing a more detailed and prolonged inspection of the surface. Cyprids exposed to ultrasound, which compromises their viability, also decreased their step length and increased their step duration when exploring the same surface. However, the cause and mechanism leading to this change in behavior may be different. Specifically, a change in surface properties cannot directly be compared with ultrasound-induced damage to the cyprid's condition. With the possibility that the exploration behavior on a less favoured surface was caused by weakened temporary adhesion points, the likelihood of ultrasound exposure weakening cyprid adhesion to the surface can be surmised. However, no adhesion data has been gathered from the cyprid behavior assays to validate this hypothesis. With respect to settlement, the reduced exploration rate and walking pace exhibited by cyprids exposed to ultrasound generate fewer temporary anchoring points in a given time. This behavior may lead to a lower surface density of footprint protein, which acts as a settlement-inducing cue (Aldred et al. 2008; Aldred and Clare 2008).

Metamorphosis of cyprids exposed to ultrasound yields barnacles with a smaller basal area than those from control cyprids. Exposure to ultrasound has been shown capable of accelerating or inhibiting the growth of organisms (Ahn et al. 2003; Matsuura et al. 2003; Pitt and Ross 2003). As the juvenile barnacles grew over two weeks, with regular feeding, the size of barnacles of the two populations converged. Thus, despite

a clear reduction in cyprid viability following ultrasound exposure, barnacles metamorphosed from these larvae are able to compensate and grow normally.

Ultrasound could therefore be applicable for barnacle fouling prevention by using an efficient transducer, which can generate an acoustic pressure of about 20 kPa at a frequency just above the audible threshold of 20 kHz. As illustrated in the present study, even short exposure times are efficient for reducing cyprid settlement, by half at 30 s and down to one-third after 5 mins' exposure.

2.5. Conclusion for chapter 2

Exposure to ultrasound significantly affected barnacle cyprid settlement, viability, and exploration behavior. Both the highest efficacy against settlement and the highest mortality was shown for 23 kHz; when exposed to ultrasound at 23 kHz for 300 s at a pressure of 20 kPa settlement was reduced by a factor of two and mortality was increased by a factor of three. These changes are probably a consequence of the organisms sustaining physical damage, presumably induced by cavitation and the liquid shear forces it generates. Juvenile barnacles, metamorphosed from cyprids exposed to ultrasound, grew normally. Further studies are needed to elucidate any damage induced by ultrasound to the cyprid's carapace and its antennules, including their sensory organs and attachment discs. These may shed light on the mechanisms responsible for reduced cyprid viability and settlement inhibition. The use of ultrasound shows significant promise as a fouling prevention technology, particularly as a replacement for biocidal coatings on surfaces with low shear flow. By implementing a proper understanding of the mechanisms of action in engineering design, this should allow optimizing of the ultrasound application focus, while limiting any unwanted environmental effects, which is expected to produce a practical and environmentally-safe antifouling prevention strategy.

Chapter 3. The exploration of the mechanism of ultrasound on barnacle cyprid settlement inhibition

In chapter 2, ultrasound showed ability to reduce cyprid settlement and increase cyprid mortality. In this chapter, the possible mechanism of ultrasound on cyprid settlement inhibition was explored. The inhibitory effect of ultrasound on barnacle (*Amphibalanus amphitrite*) cyprid was investigated under three excitation frequencies (23, 63, and 102 kHz). The linear regression models were built to study the effect of ultrasound pressure and exposure time on cyprid settlement. The negative slopes of the linear regression lines indicate reduced settlement with increased exposure time and acoustic pressure. The excitation frequency of 23 kHz was found to be the most effective on settlement inhibition, with 63 and 102 kHz exhibiting similar but weaker response. Separately, ultrasonic cavitation was investigated and confirmed in the filtered seawater (FSW) and partially degassed filtered seawater (PDFSW) via the acoustic spectrum analysis. The cavitation energy was found to be double in FSW than in PDFSW at 23 kHz with the acoustic pressure of 20 kPa. The much higher settlement reduction and stronger cavitation in FSW at 23 kHz suggest that cavitation is a possible if not most likely mechanism for the cyprid inhibition. The cavitation induced force may lead to physical damage to the cyprids which subsequently will result in much higher mortality. The cavitation effect was proven to be stronger at 23 kHz than the other two frequencies with the same acoustic energy, which might explain the enhanced efficiency on settlement reduction.

3.1. Introduction

In Chapter 2, it was found that ultrasound exposure reduced cyprid settlement and changed cyprid exploration behavior. In liquids or biological tissue, energy transmitted by the propagation of ultrasonic pressure fluctuations can induce biological changes as a result of ultrasound induced thermal and non-thermal effects (Brondum et al. 1998). The thermal biological effect is not considered in our thesis as no temperature elevation was detected during experiments. The other mechanisms for non-thermal biological effect include ultrasound wave, cavitation or the combination of both (Heng et al. 2009; Moholkar et al. 2000). Ultrasound wave induced radiation force, radiation torque, and micro-streaming are capable of deforming and disrupting biological tissues, disintegrating biological structures and enhancing enzyme-mediated thrombolysis (Holland et al. 2000; Nyborg 1982; Soltani et al. 2008). The ultrasonic cavitation here refers to formation, growth and collapse of vapour or gas bubbles under influence of ultrasound and the bubbles can undergo either a stable cavitation with bubbles oscillatory motion or a transient cavitation with bubble collapse (Apfel 1997; Frohly et al. 2000). Ultrasound cavitation has been reported to be the main factor for bacterial growth inhibition, algae removal and biofilm disintegration (Ahn et al. 2003; Liang et al. 2009; Lagsir et al. 2000). The ultrasound cavitation is affected by many factors such as dissolved gas, hydrostatic pressure, ambient temperature, liquid viscosity, ultrasound frequency and acoustic intensity (Avvaru and Pandit 2009; Mason and Lorimer 2002). It was verified that cavitation could only occur when the cavitation threshold was met. The cavitation threshold here refers to the minimum pressure required for a cavitation occurs (Kanegsberg and Kabegsberg 2011). Studies showed that cavitation threshold was increased in a degassed condition and more ultrasound energy was required for cavitation to occur (Atchley et al. 1988; Mason and Lorimer 2002).

The use of ultrasound wave irradiation was found to be an effective approach to solve the barnacle induced marine fouling problem (Guo et al. 2011b; Kitamura et al. 1995; Mori et al. 1969; Seth et al. 2010). While these reported studies have shown a clear promise of ultrasound as a marine fouling prevention strategy, there is a lack of information regarding the power threshold and the specific frequencies for effective operations. Moreover, ultrasound applications in marine fouling prevention will benefit from a better understanding of the mechanisms responsible for cyprid mortality or reduced barnacle settlement on solid surfaces. This present chapter would attempt to explore the ultrasound irradiation condition for settlement inhibition with different ultrasonic parameters, including power, frequencies and exposure time. Moreover, the mechanism responsible for the settlement inhibition would be studied with the acoustic emission spectrum method, together with the settlement and mortality comparison in FSW and PDFSW.

3.2. Material and methods

3.2.1. Ultrasonic irradiation system

The experiments were carried out with the ultrasound irradiation system that is similar as described in Figure 2.1, and the experimental process is as described in section 2.2.1. The acoustic signal picked by hydrophone, however, was analyzed differently. In section 2.2.1, the ultrasound signal was transmitted directly to the oscilloscope to be converted to the acoustic pressure according to the receiving sensitivity of the hydrophone. In this chapter, however, the ultrasound signal from hydrophone was transmitted to the data acquisition system (USB-5132, N.I. Ltd., USA) and was fed to a computer. The ultrasound signal was recorded and analyzed with the software LABVIEW 2009 (N.I. Ltd., USA) for the spectrum analysis. Again, three frequencies of 23, 63 and 102 kHz were studied.

3.2.2. Cyprid settlement and mortality assay

The inhibitory effect of ultrasound on cyprid settlement was studied under three ultrasonic excitation frequencies, namely, 23, 63 and 102 kHz. Cyprids were treated with various acoustic pressure and exposure time. After ultrasound irradiation, the exposed and control (no ultrasound exposure) cyprids were incubated in their respective capped vials for 24 hours at 28℃ with a 15-hour light and 9-hour dark cycle. All settled and metamorphosed barnacles and cyprids that were permanently attached but not yet metamorphosed were counted (Kem et al. 2003). The dead cyprids were also scored to quantify ultrasound exposure induced cyprid mortality. The settlement and mortality of the control cyprids were recorded for comparison. Both Settlement and mortality assays were conducted in triplicate.

3.2.3. Cyprid inhibition mechanism investigation

For evaluating ultrasound induced cyprid inhibition mechanism, two kinds of liquids were employed: one was filtered seawater (FSW) and the other was partially degassed filtered seawater (PDFSW). The PDFSW was achieved by vacuuming the FSW with a rotary vane vacuum pump (Pfeiffer Balzers, Germany) for 10 minutes. To conduct the settlement and mortality assay in PDFSW, the tap water used in the water tank was also replaced by 10-minute degassed tap water.

As 23 kHz was observed to be the most effective on cyprid settlement inhibition among the three frequencies (see Results below), only this particular frequency was employed for the settlement inhibition mechanism study. Acoustic pressures of 5, 10, 15, 20, 30 kPa were used for an exposure time of 150 s to compare the settlement and mortality in FSW and PDFSW. Experiments on the cyprids in both FSW and PDFSW

conditions were performed in triplicate, and the settlement and mortality results were compared.

3.2.4. Ultrasonic emission spectrum analysis and cavitation energy estimation

Randomicity is the primary characteristic of the ultrasonic cavitation bubble activity and the ultrasonic emission spectrum is normally used to analyze the signal (Llyichev et al. 1989; Frohly et al. 2000; Mohokar et al. 2000; Liang et al. 2006; Ashokkumar et a. 2007; Avvaru and Pandit 2009). To compare the difference of ultrasound signal in FSW and PDFSW, the power spectrum density analysis was carried out with online Fast Fourier Transform (FFT) analysis using graphical interface programming done with LABVIEW 2009.

The ultrasonic power spectral density analysis is generally done using Welch method (Petosić et al. 2009; Liang et al. 2006). It is a nonparametric method to analyze the power spectrum of ultrasonic signal. The Welch method has been extensively documented (Welch et al. 1967; Kay SM, Marple SL 1981; Ubeyli et al. 2003). Briefly, the signals are divided into overlapping segments, windowed by a specific window function, periodograms are calculated and then average of the periodograms is calculated. In our study, the overlapping ratio is 50% and Hamming window is applied.

Welch's method is an improvement on the standard periodogram spectrum estimating method and on Bartlett's method (Barbe et al. 2010; Bartlett 1948). For example, it alleviates the discontinuities and reduces the spread of the spectral energy into the side lobes by windowing; it reduces the variance of the periodogram method by averaging; it improves the smoothness of the spectrum (Welch et al. 1967; Barbe et al. 2010). However, the Welch method has its drawbacks: the variance is a

monotonically decreasing function of the fraction of overlap; it requires the estimation of a number of parameters, particularly the window size; it requires many replications to obtain smoothing (Jokinen et al. 2000; Law 1983).

The energy of an ultrasound signal is comprised of two parts: the energy due to ultrasound wave itself and the cavitation energy due to the cavitation activity (that is, the oscillation and collapse of the bubbles) (Mohokar et al. 2000; Avvaru and Pandit 2009). At low acoustic intensity, the acoustic spectrum was found to be only due to the driving frequency caused by bubbles oscillating proportionally to the pressure variation (Avvaru and Pandit 2009). When the intensity exceeded the cavitation threshold, the acoustic spectrum was comprised of the driving frequency, harmonics, sub-harmonics and ultra-harmonics of the driving frequency, as well as broad band frequency (Ashokkumar et a. 2007). The harmonics in the spectrum are explained in terms of forced non-linear bubble oscillations and the broad band noise spectrum is explained due to the shock wave emitted by transiently collapsing bubbles (Frohly et al. 2000).

There are two forms of energy in ultrasound cavitation field: one is nonlinear energy due to the nonlinearity of the medium and cavitation, while the other is linear energy of fundamental ultrasonic wave (Liang et al. 2006; Moholkar et al. 2000). The nonlinear energy is mainly due to cavitation (Liang et al. 2006; Moholkar et al. 2000). Therefore, the nonlinear energy (cavitation energy) can be approximately obtained by subtracting the energy of the fundamental wave (linear energy) from the total energy of acoustic field (Liang et al. 2006; Frohly et al. 2000).

For separating the linear energy (fundamental wave) and nonlinear energy (cavitation energy), a program of ultrasonic emission spectrum analysis with LABVIEW 2009 was written. The program is based on Welch method to estimate power spectrum density of ultrasound signal. In this program, the duration of signals is 100 ms and the frequency resolution f_0 is fixed at 10 Hz for the three driving frequencies (23, 63 and 102 kHz). When calculate the power spectrum density using Welch method, the application of window function will induce energy leakage. That is, the energy of the original signal at a particular frequency will spread to a frequency band (Liang et al. 2006). For this reason and also the profile of the spectrum, the energy in the $(f_0 - 2d_f)$-$(f_0 + 2d_f)$ band is used to estimate the fundamental wave (f_0) (linear energy) by an integration of the spectrum in a linear scale, approximately. The parameter f_0 is the fundamental frequency (driving frequency) and d_f is the frequency resolution of the spectrum.

The output voltage RMS value of the hydrophone represents the amplitude of the acoustic pressure and its squared value is the total ultrasonic energy correspondingly. The cavitaion energy can be approximately calculated by subtracting the fundamental wave energy from the total energy.

3.2.5. Data analysis

All statistical comparisons were performed using GraphPad Prism 5 (GraphPad Software Inc.). Factors which affect the cyprid settlement and mortality in this work were frequency, ultrasonic pressure and ultrasound exposure time. Settlement and mortality data were analyzed with linear regression analysis and the equations of the regression lines were constructed to predict the effect of ultrasonic pressure and exposure time on settlement and mortality. To evaluate the effect of degassed treatment, t-tests were conducted to compare the settlement and mortality data in

FSW and PDFSW in control groups. All data was reported as mean ± standard error (SE). For all comparisons, p-values ≤ 0.05 were considered as statistically significant.

3.3. Results

3.3.1. Cyprid settlement assay

Each of the three frequencies exhibited a somewhat linear reduction in cyprid settlement with increased acoustic pressure (Figure 3.1). The slopes of linear regressions established for the data of (23 and 63 kHz) and (23 and 102 kHz) were found to differ significantly with the p values of (p=0.0165) and (p=0.009), respectively. However, the slopes of linear regression equations for 63 and 102 kHz showed no significant difference (p=0.5346) together with no significant difference of the intercepts (p=0.4586). It can thus be concluded that 23 kHz was more effective in influencing cyprid settlement than the other two frequencies, and there was no difference found between 63 and 102 kHz. Settlement in general was reduced with increased acoustic pressure. However, there was no settlement reduction at all the test frequencies when the pressure was 5 kPa compared with the control data (t-test, p > 0.05).

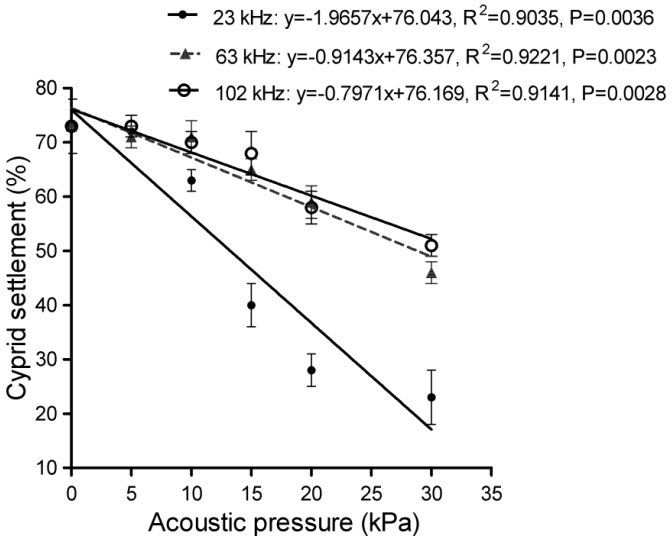

Figure 3.1. Cyprid settlement as a function of acoustic pressure. Symbols indentify values from three frequencies (23, 63 and 102 kHz). The exposure time was fixed at 150 s and the ultrasound pressure was set at 0 (control), 5, 10, 15, 20 and 30 kPa, respectively.

The effect of ultrasound exposure time on cyprid settlement is shown in Figure 3.2. The settlement reduction was found to scale fairly linearly with time. The excitation frequency of 23 kHz was also found to induce more settlement reduction than the other two mentioned frequencies.

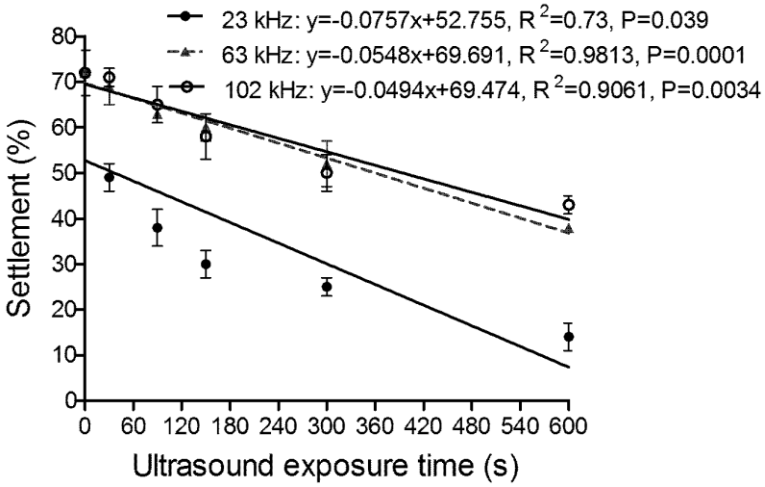

Figure 3.2. Cyprid settlement as a function of exposure time. The ultrasound pressure was fixed at 20 kPa and the exposure time was set at 0 (Control), 30, 90, 150, 300 and 600 s, respectively.

3.3.2. Settlement and mortality comparison between FSW and PDFSW

There was no significant difference in settlement and mortality between FSW and PDFSW in the control groups (Figure 3.3; t-test, $p > 0.05$). This suggests that degassed treatment does not affect cyprid living pattern. Therefore, it is considered reasonable to employ the degassed treatment for the ultrasound induced settlement inhibition mechanism study.

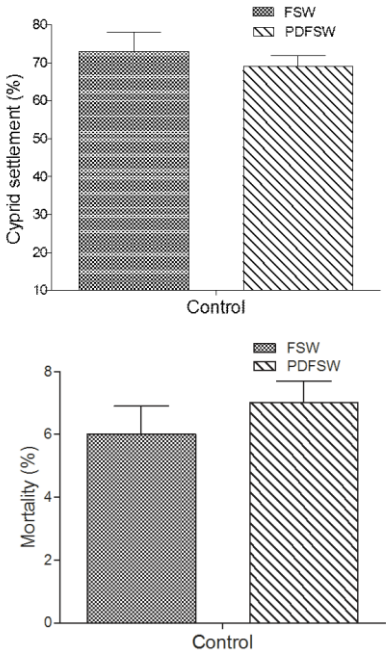

Figure 3.3. Settlement and mortality comparison between FSW and PDFSW in control groups. "Control" indicates no ultrasound exposure.

Cyprid settlement exhibited a linear reduction with acoustic pressure in both FSW and PDFSW condition (Figure 3.4). The slopes of linear regressions established between FSW and PDFSW at 23 kHz differed significantly ($p=0.031$). With the same ultrasound exposure, more settlement reduction was achieved in FSW.

The linear regression models were also applied to study cyprid mortality versus acoustic pressure (Figure 3.5). The increased mortality was found to scale linearly

with pressure in both FSW and PDFSW. The slopes of linear regressions established between FSW and PDFSW at 23 kHz differed significantly (p=0.01). More significant cyprid mortality was achieved in FSW. It was showed that at 5 kPa, no significant difference was observed in both mortality and settlement when compared with control data (t-test, $p > 0.05$).

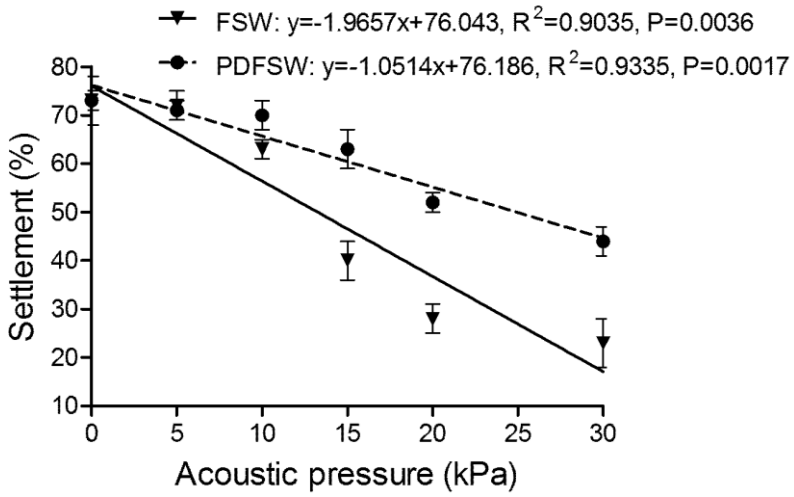

Figure 3.4. Settlement comparison between FSW and PDFSW after ultrasound treatment. The excitation frequency was 23 kHz and the acoustic pressure was set at 0 (Control), 5, 10, 15, 20 and 30 kPa. The exposure time was fixed at 150 s.

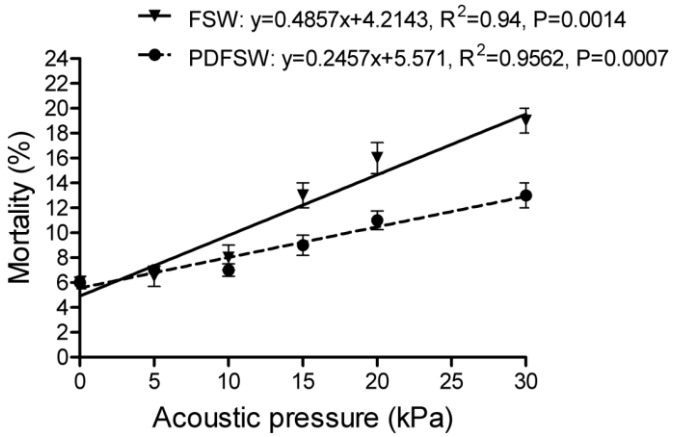

Figure 3.5. Cyprid mortality comparison between FSW and PDFSW after ultrasound treatment. The excitation frequency was 23 kHz and the acoustic pressure was set at 0 (Control), 5, 10, 15, 20 and 30 kPa. The exposure time was fixed at 150 s.

3.3.3. Ultrasonic spectrum and cavitation energy analysis

The ultrasound spectrum in FSW and PDFSW was analyzed with power spectrum density analysis (Figure 3.6). Under the driving frequency of 23 kHz, the spectrum of FSW and PDFSW was a combination of two components: the line spectrum containing a fundamental line (23 kHz), harmonics (46, 69 kHz, etc.) and the broadband component superimposed on the line spectrum (Figure 3.6). The line spectrum was attributed to non-linear movement of stable cavitation-induced bubbles. The broad band noise, however, was due to collapsing bubbles induced shock wave emission by transient cavitation behavior. It is clear that ultrasound cavitation occurred in both FSW and PDFSW. However, the cavitation effect was much stronger in FSW and could be evaluated by the nonlinear energy (Figure 3.7).

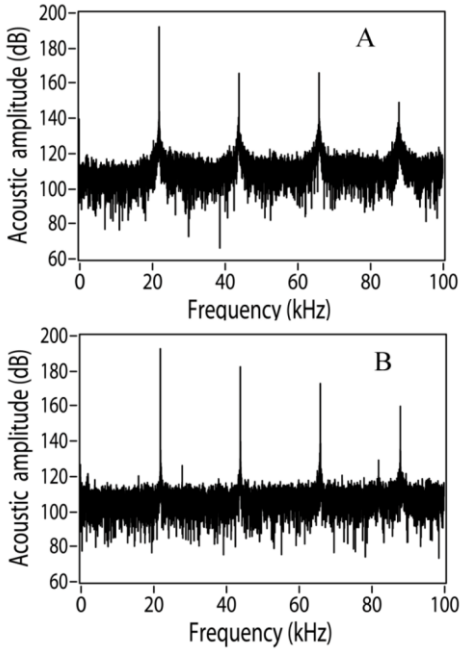

Figure 3.6. Ultrasound power spectrum density comparison between FSW and PDFSW condition. The acoustic pressure was 20 kPa and the excitation frequency is 23 kHz. “A” is the ultrasound spectrum in FSW; “B” is the ultrasound spectrum in PDFSW.

The nonlinear energy as a function of total acoustic energy was presented in Figure 3.7. On the x-axis are the values of ultrasonic energy corresponding to the ultrasound pressure of 5, 10, 15, 20 and 30 kPa, respectively. The y-axis is the cavitation energy (nonlinear energy). It can be deduced that 5 kPa is the threshold for cavitation as no harmonicas are observed at this amplitude together with no nonlinear energy in both FSW and PDFSW (Figure 3.8 and 3.7). With the same exposure, cavitation intensity is much stronger in FSW than in PDFSW. At the pressure of 20 kPa, the cavitation energy in FSW was 0.041 V^2. However, the corresponding energy in PDFSW was only 0.018 V^2. The nonlinear energy in PDFSW is also increased with acoustic intensity, but at a much lower rate than in FSW.

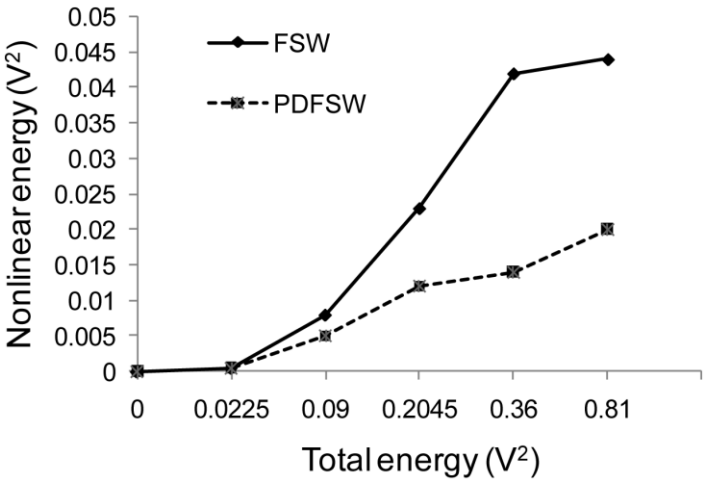

Figure 3.7. Nonlinear energy in FSW and PDFSW at 23 kHz. The x-axis was the total ultrasonic energy represented by V^2 corresponding to different acoustic pressures (5, 10, 15, 20, 30 kPa), and the y-axis was the nonlinear energy of cavitation which was also represented by V^2.

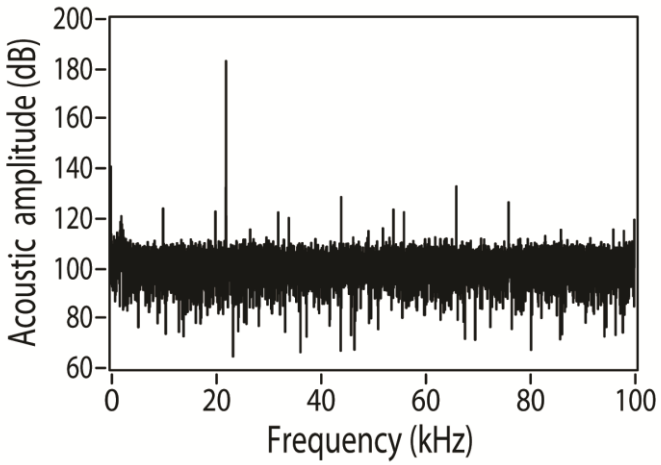

Figure 3.8. Ultrasound power spectrum density of 23 kHz at the acoustic pressure of 5 kPa in FSW condition.

3.4. Discussion and conclusion for chapter 3

The ultrasound irradiation induced barnacle cyprid settlement inhibition was investigated under three excitation frequencies (23, 63, and 102 kHz). The linear regression models were constructed to study the effect of ultrasound pressure and exposure time on settlement. The negative slopes of the linear regression lines indicate the reduced settlement with increased exposure time and acoustic pressure. Of the three frequencies, 23 kHz is found to be the most effective, with 63 and 102 kHz inducing similar but weaker response. These results are in general agreement with the reported work of Guo et al. (2011). Kitamura et al. (1995) also reported similar findings as lower frequency in the region of 20 kHz was more effective to induce lethal effect on barnacle nauplii, and increased settlement reduction was achieved with higher ultrasonic irradiation.

The ultrasonic spectrums of FSW and PDFSW at 23 kHz with the acoustic pressure of 20 kPa in Figure.3.6 were quite similar to the reported findings (Segebarth et al. 2002; Hao et al. 2004). Under the excitation frequency, the acoustic cavitation spectrum comprised of various frequencies: driving frequency, harmonics of the

driving frequency and the broadband frequency (or broad band "noise") associated with transient bubbles collapse (Avvaru and Pandit 2009; Frohly et al. 2000). Both harmonics and broadband noise were observed in FSW and PDFSW which confirmed that cavitation did occur in these liquids. However, cavitation was much stronger in FSW, which was consistent with the reported findings by Atchley et al. (1988) and Mason et al. (2002). Their studies showed that cavitation was difficult to achieve under degassed condition and more ultrasound energy was required for the cavitation to occur. The cavitation intensity can be easily evaluated by the nonlinear energy. It was found that with the same ultrasound pressure of 20 kPa, the nonlinear energy in FSW was $0.041V^2$ and the corresponding energy in PDFSW was only $0.018\ V^2$ (Figure 3.7). Since the total acoustic energy remained the same in FSW and PDFSW, the more significant reduced settlement in FSW is therefore attributed to ultrasonic cavitation effect.

The reduced settlement observed could be the result of physical injury inflicted on the cyprids due to ultrasonic cavitation. Small non-equilibrium bubbles contained in the liquids would undergo oscillation or implosion as a result of cavitation which could produce high shear stress and liquid jets that could physically damage nearby organisms (Fong et al. 2006; Hao et al. 2004; Seth et al. 2010). The bubbles could also induce micro-streaming in the surrounding liquid that could induce damaging high shear stress to the biological species present (Mitragotri 2005). Ultrasound cavitation-induced shear stress, shock wave and liquid micro-jets have been applied for bacterial growth inhibition, algae removal and biofilm disintegration (Ahn et al. 2003; Liang et al. 2009; Lagsir et al. 2000). High intensity ultrasound, which develops significant cavitation, has also been used to disintegrate barnacle larvae for the ballast water treatment (Seth et al. 2010). In that report, they quantified the energy needed to pulverize the barnacle larvae. However, the power they reported was very

much higher than our experimental values because of their criterion on pulverization leading to crushed larvae observed. In our experiments, no apparent injury on cyprids was observed after ultrasound treatment. The findings of more settlement reduction and stronger cavitation in the FSW indirectly confirm that cavitation is the mechanism for cyprid inhibition. The cavitation induced force might easily lead to physical or even physiological damage to the cyprids which subsequently reduce the ability to settle.

Though our direct observation under the microscope did not detect any injury following ultrasonic exposure, the mortality results shed light on the inherent ultrasonic cavitation induced damage. More cyprid mortality was observed with ultrasonic irradiation, and the trend of the mortality increase is consistent with the increase in nonlinear energy (Figure 3.5 and 3.7). Similar to the settlement result, more mortality was achieved in FSW than PDFSW with the same acoustic energy. The observed settlement and mortality patterns in the FSW and PDFSW suggest that although direct ultrasound wave radiated force may also be responsible for the cyprid settlement inhibition, the effect is much less significant than cavitation.

The cyprid inhibition effectiveness for different excitation frequencies differed significantly even though the ultrasound power was kept at the same level (Figure 3.1 and 3.2). Kitamura et al. (1995) reported similar result as lower frequency of 19.5 kHz was more effective on barnacle larvae mortality than the other two higher frequencies. This can be possibly explained by the effect of ultrasound frequency on cavitation. In general, cavitation would occur more readily at lower frequencies and its threshold would increase with ultrasound frequency (Kratochv Í and Morntein 2006; Ma et al. 2005), which are consistent with our findings. The cavitation effect was detected for all the three excitation frequencies with the same acoustic energy

(Figure 3.9). However, cavitation was much stronger at 23 kHz than at 63 and 102 kHz, with the calculated corresponding cavitation energy calculated as 0.041, 0.023, 0.019 V^2, respectively.

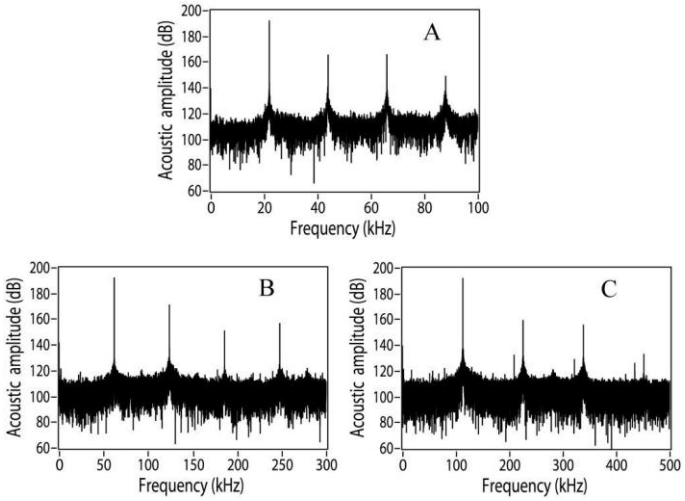

Figure 3.9. Ultrasound power spectrum density comparison among the 23, 63 and 102 kHz in FSW condition with the ultrasound pressure of 20 kPa.

For the range of acoustic energy used, there is a general linear trend of increased acoustic energy with reduced settlement. However, to achieve the inhibitory effect, there is an ultrasound intensity threshold that must be met. No cyprid settlement inhibition was observed at all the three excitation frequencies when the pressure was at 5 kPa (Figure 3.1) and no harmonics detected in the frequency spectrum indicated that no cavitation had occurred (Figure 3.8), together with the essentially zero nonlinear energy (Figure 3.7). Therefore, to ensure the presence of inhibitory effect, the applied acoustic pressure should be higher than 5 kPa.

The effectiveness of ultrasound on cyprid settlement reduction suggests that it can potentially be a strategy for barnacle induced marine fouling prevention. It possesses several benefits over biocide-based methods. The most predominant factor is that it can be applied in a highly controlled manner, whereas the biocides may have to be

released continuously for chemical based coating. However, a full and thorough assessment of the effect of ultrasound on the marine environment would still be required before its application.

Chapter 4. Investigation of low intensity ultrasound on barnacle cyprid settlement

In chapter 2 and 3, ultrasound was found to inhibit cyprid settlement effectively and the possible mechanism was explored to be ultrasonic cavitation. The increased cyprid mortality revealed that the application of relative high pressure ultrasound may impose danger to other marine organisms, although the impact may be significantly reduced with proper design and a controlled operation mode. To minimize the cavitation effect, the possibility of using low intensity ultrasound on the barnacle induced marine biofouling prevention was investigated in this chapter. The results found that low frequency and intensity ultrasound was demonstrated as an effective inhibitor of barnacle cyprid settlement. When the same substratum vibration amplitude (10.05 nm) and acoustic pressure (5 kPa) were applied, ultrasound at a frequency of 23 kHz significantly reduced cyprid settlement. The mechanism appeared to differ from the ultrasonic cavitation induced inhibition previously reported as no increased mortality was observed, and no change in the exploratory behavior of cyprids was observed when they were exposed to this continuous ultrasonic irradiation regime. The application of ultrasound treatment in an intermittent mode of “5 min on and 20 min off” at 20-25 kHz and at low intensity of 5 kPa produced the same effect as with the continuous application of 23 kHz. This energy efficient approach to the use of low frequency, low intensity ultrasound may present a promising and efficient strategy regarding irradiation treatment for antifouling applications.

4.1. Introduction

Ultrasound has been reported to prevent barnacle induced fouling (Kitamura et al. 1995; Seth et al. 2010). Guo et al (2011a) demonstrated that with the acoustic pressure of 20 kPa, frequencies of 23, 63 and 102 kHz operated with a short duration of 5 min will significant inhibit barnacle settlement. The mechanism responsible for the inhibition appears to be a result of ultrasonic cavitation, which could induce physical or physiological impact to cyprids, resulting in the reduced settlement (Guo et al. 2011b). Although the relatively high intensity ultrasound showed promise as an AF strategy, its impact on other non-target marine organisms may limit its application. As acoustic energy attenuates less over the same distance in water than in air, sound waves can propagate long distances with little reduction in acoustic energy in water (Slabbekoorn et al. 2010). Thus the application of high intensity ultrasound would not only affect the target organisms, but also impact other (non-fouling) marine organisms. In addition, high intensity ultrasound applications require high performance actuators, increasing the safety concerns during application and incurring additional cost in energy consumption and maintenance. Therefore, the development of low intensity or low power ultrasound for antifouling prevention appears to be an attractive proposition.

Low intensity ultrasound is defined as ultrasound operated at acoustic pressures below the cavitation threshold, which is the specific acoustic pressure above which cavitation occurs (Dicker et al. 2010). High intensity ultrasound is associated with irradiation treatments where acoustic pressures induce cavitation effects. With low intensity ultrasound, forces arising from shock wave and micro-stream which may cause injury to cyprids, are not generated. There are few reports on the effects of low intensity sound on cyprid settlement. Branscomb and Rittschof (1984) described the

application of low amplitude, low frequency sound waves, but the frequencies tested were within the audible spectrum of humans. Fish hearing ability has been reported to be in the range of 30-5000 Hz (Slabbekoorn et al. 2010), and the application of these levels of low frequency sound may cause undue and unintended stress on the fish and other marine organisms (Smith et al. 2004; Wysocki et al. 2006).

This study examined the effect of three sound frequencies viz. 23, 63 and 102 kHz at low amplitudes, on cyprid behaviour and settlement. The effect of substratum vibration and acoustic pressure on cyprid settlement was investigated. Finally, the effectiveness of continuous versus intermittent modes of ultrasound application was explored.

4.2. Material and methods

4.2.1. Ultrasound irradiation setup

The schematic of the ultrasonic experimental setup is given in Figure 4.1. The sinusoidal signal transmitted from the function generator (Agilent 33210A, USA) was fed into the power amplifier (HSA4051, Japan), and used to drive the parallel connected PZTs (piezoelectric transducers, Hangzhou Applied Acoustics Research Institute, China). An open cylindrical glass vial with a height and diameter of 20 mm was glued to each transducer. In the experiments, 2 ml of filtered seawater (FSW; 1 mm filtered) were transferred into each vial; the depth of seawater was 5 mm. A small 1 mm diameter needle hydrophone (Precision Acoustics, UK), with a sensor situated at the tip was used to measure the pressure without affecting the acoustic field. The measuring points were set 0.5 mm above the bottom of the vial and the acoustic pressure measured can be regarded as pressure experienced by the cyprids during settlement.

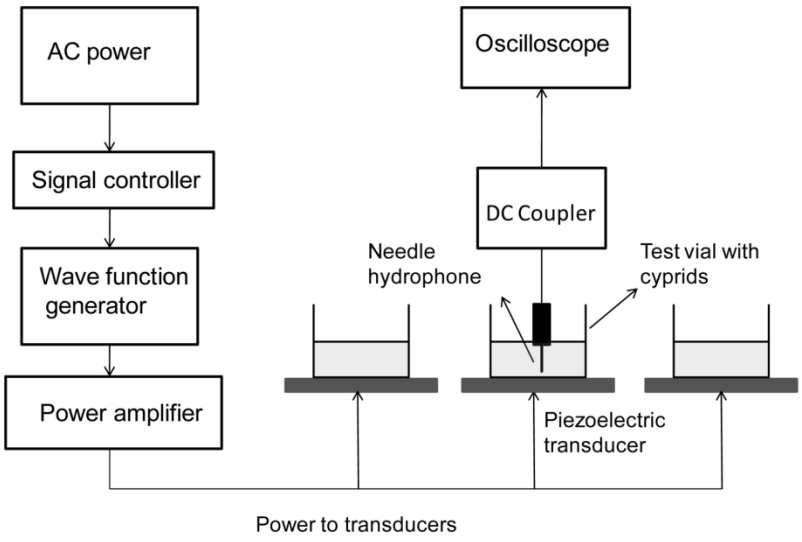

Figure 4.1. The Schematic diagram of the ultrasound irradiation system.

4.2.2. The choice of ultrasound amplitude

The signal from hydrophone was transmitted to an oscilloscope (Agilent 35670A, USA). The data were then digitized and stored in a computer database. The ultrasound signal was recorded and analyzed with the software LABVIEW 2009 (N.I. Ltd., USA).

The acoustic spectrum analysis method is usually applied to study the ultrasonic signal (Frohly et al. 2000; Moholka et al. 2000; Liang et al. 2006; Guo et al. 2011b). At low acoustic intensity, the acoustic spectrum comprises mainly of the driving frequency. When the intensity exceeds the cavitation threshold, the acoustic spectrum includes the driving frequency, harmonics, sub-harmonics and ultra-harmonics of the driving frequency, as well as broad band frequencies due to transient cavitation (Liang et al. 2006; Moholkar et al. 2000). Ultrasonic cavitation induced shock waves,

high temperature and liquid jets can cause physical damage to surrounding materials and organisms (Mason and Lorimer 2002; Suslink and Nyborg 1988).

As demonstrated by Guo et al. (2011b), at amplitude of 5 kPa with an exposure of 150 s, no inhibitory effects were found at any of the frequencies tested, and no increased mortality was detected. In this study, low intensity ultrasound with continuous exposure for 24 h at the same 5 kPa amplitude was tested. The resulting ultrasonic spctrum of 23, 63 and 102 kHz at this amplitude are given in Figure 4.2 and the sharp peaks observed in each spectrum were the driving frequencies. The spectrums obtained comprised only the driving frequencies, indicating that no cavitation effects were generated (cf. Frohly et al. 2000; Moholkar et al. 2000).

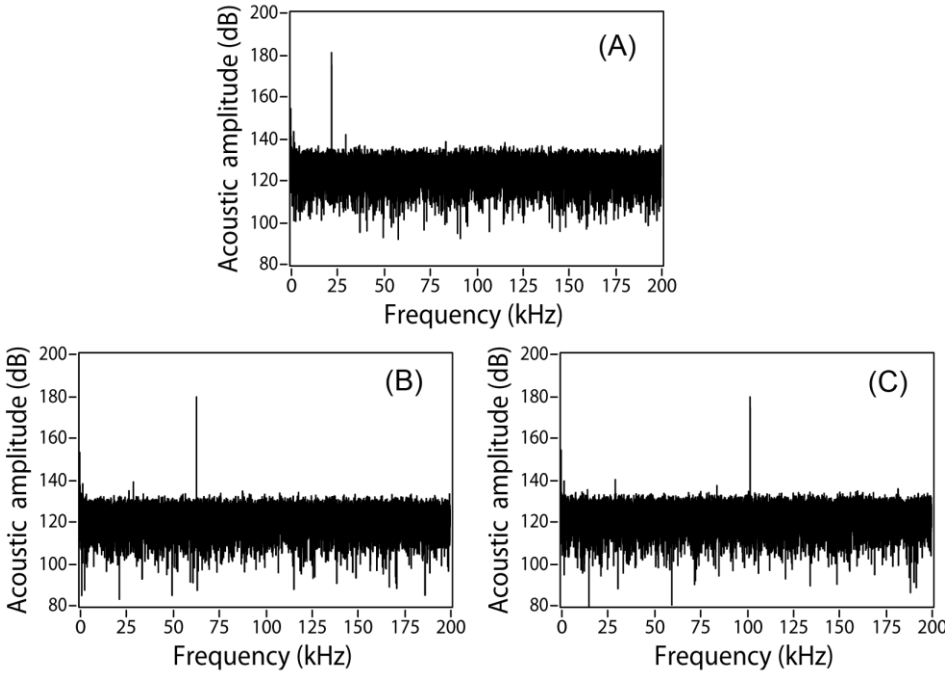

Figure 4.2. Ultrasound power spectral density at the acoustic pressure of 5 kPa. A is the spectrum of 23 kHz, B is the spectrum of 63 kHz, and C is the spectrum of 102 kHz.

4.2.3. Cyprid settlement and mortality assay

The effects on cyprid settlement in response to ultrasound treatment were studied using frequencies of 23, 63, and 102 kHz. Three sets of experimental devices (as shown in Figure 4.1) operating at different frequencies were set up; nine PZTs connected to replicate glass vials were set up for each frequency. After exposure for 5 min, three vials were detached. The next set of three vials was removed after 12 h and the remaining three vials after 24 h. All tests were conducted with the acoustic pressure of 5 kPa. Cyprids from the same batch were used and the three setups were run simultaneously. In the experiments, 60-70 cyprids were used in each vial. Thiyagarajan et al. (2002) demonstrated that the gregarious behavior of cyprids did not interfere with settlement rate at cyprid densities of 5-200 per 5ml. For both control and ultrasound-treated cyprids, the vials were covered during the experiment to prevent evaporation. The control vials were incubated at 28 ℃, on a 15:9 h light/dark cycle for 24 h. After the irradiation treatments, cyprids were incubated in their respective covered vials. After 24 h from the start of the experiment, all the cyprids in the different treatments were examined under a stereo microscope (Nikon SMZ 1500, Japan). All settled cyprids were counted, including those that were permanently attached, but not metamorphosed as well as fully metamorphosed barnacles. The number of dead cyprids was also counted. Settlement and mortality in the control vials (cyprids not subjected to ultrasound treatment) were recorded for comparison.

4.2.4. Effect of low intensity, continuous ultrasound on cyprid behavior

A close-range microscopy recording method for examining cyprid behavior was described in Chaw and Birch (2009) and Chaw et al (2011). Step length, defined as the distance between two sequential temporary anchoring points, and walking pace, defined as the number of steps taken in a given time of 5 min (Guo et al. 2011a) can be quantified and used to define cyprid exploration behavior under different conditions. Observations of cyprid exploration behavior were performed to assess the condition of cyprids exposed to ultrasound. Unlike the study of Guo et al (2011a) where cyprid exploration behavior was examined after the cyprids were exposed ultrasound irradiation, in this chapter, the vials with the working transducers were observed under a stereo microscope (Nikon SMZ 1500, Japan) and the exploratory patterns of cyprids recorded during irradiation. Cyprid behavior was recorded after a 30 min acclimation period of ultrasound exposure. For each frequency, 8-12 videos of 'walking', ie exploring, cyprids were recorded for 5 min and the results were analyzed.

The number of cyprids exploring the surface in each vial was also counted. After adding 50-60 cyprids to each vial and allowing 30 min for acclimation, the number of exploring cyprids was enumerated over a period of 10 min. To avoid repetition, once a cyprid was observed walking, a micropipette was used to remove it. For ease of comparison, the fraction of cyprids exploring the surface was quantified for each treatment. The analysis at each frequency and the controls was conducted in triplicate.

4.2.5. Substratum vibration and acoustic pressure analysis

In the experiments, it was observed that with the same acoustic pressure of 5 kPa, only at a frequency of 23 kHz was significant inhibitory effect observed. Two additional experiments were conducted to elucidate whether the inhibitory effects were a result of substratum vibration or effects of the acoustic pressure in the liquid.

The acoustic pressure in the vial was evenly distributed on the surface (Figure 4.4), hence the ultrasonic wave in the vials may be assumed to be a plane wave (Kinsler et al. 1982). Taking into account reflection and neglecting damping effects, the acoustic pressure p in a certain position can be expressed by the equation:

$$p=p_i e^{j(\omega t-kX)}+ p_r e^{j(\omega t+k X)} \quad (1)$$

$$u=p/\rho_0 c_0 \quad (2)$$

$$u=r\omega \quad (3)$$

where p_i is the pressure of incident wave and p_r is the pressure of reflective wave, ρ_0 is the density of seawater, c_0 is the sound velocity in the seawater, u is the particle velocity of liquid, ω is ultrasound frequency, k is the wave number defined by $k=\omega/c$, and r is the particle vibration displacement.

In the above experimental setup, on the vial substratum-liquid interface, the normal velocity of the substratum should be the same as the velocity of particles in the liquid. With measurement points 0.5 mm from the substratum and assuming no damping effects, the substratum particle velocity would be approximately the same as that of the liquid particles. As described by Equations (1)-(3), the substratum vibration displacement is directly related to the acoustic pressure in the liquid.

The substratum vibration measurement was conducted with a scanning vibrometer (Polytec, Inc., USA). In the first experiment, by adjusting the driving voltage, the acoustic pressure at each frequency (23, 63 and 102 kHz) was set to 5 kPa. The vial substratum vibration displacement transmitted from the PZT with the corresponding voltages at each frequency was measured. A cyprid settlement experiment was conducted in this configuration with continuous irradiation for 24 h at the fixed acoustic pressure of 5 kPa.

In a second experiment, by adjusting the driving voltage, the substratum vibration at each frequency was adjusted to 10.05 nm, which was the vibration amplitude of 23 kHz when the acoustic pressure was 5 kPa. The acoustic pressures at the corresponding voltages were measured with a needle hydrophone. Likewise, a settlement experiment was conducted with continuous irradiation for 24 hrs with the fixed substratum vibration displacement set at 10.05 nm.

4.2.6. Intermittent ultrasonic irradiation

It has been reported that pulsed or intermittent ultrasound applications can be used to eliminate bacteria and clean fouled membrane filters (Cai et al. 2009; Rediske et al. 2000), and this would reduce energy consumption and damage, without compromising the cleaning effects.

The hypothesis for the present study was that an effective inhibitory effect may also be obtained with cyclical ultrasonic operations. Instead of activating the transducers continuously, the ultrasound was switched on and off for a desired period. To generate an intermittent treatment, the signal controller was used to provide the function generator with a desired switching on/off signal, resulting in the transducers being excited to emit an intermittent ultrasound wave into the water column. Such a

mode of operation minimizes power consumption and potentially prolongs the lifespan of ultrasonic devices. In the present study, five types of operational modes were applied and tested (Figure 4.3). For example for mode (A), the signal controller provides the function generator with the controlled signal, enabling the function generator to operate cyclically with an on-period of 1 min and off-period of 2 min continuously for 24 h. The PZTs then generate and deliver the ultrasound wave in the respective cyclic manner into the water column containing cyprids.

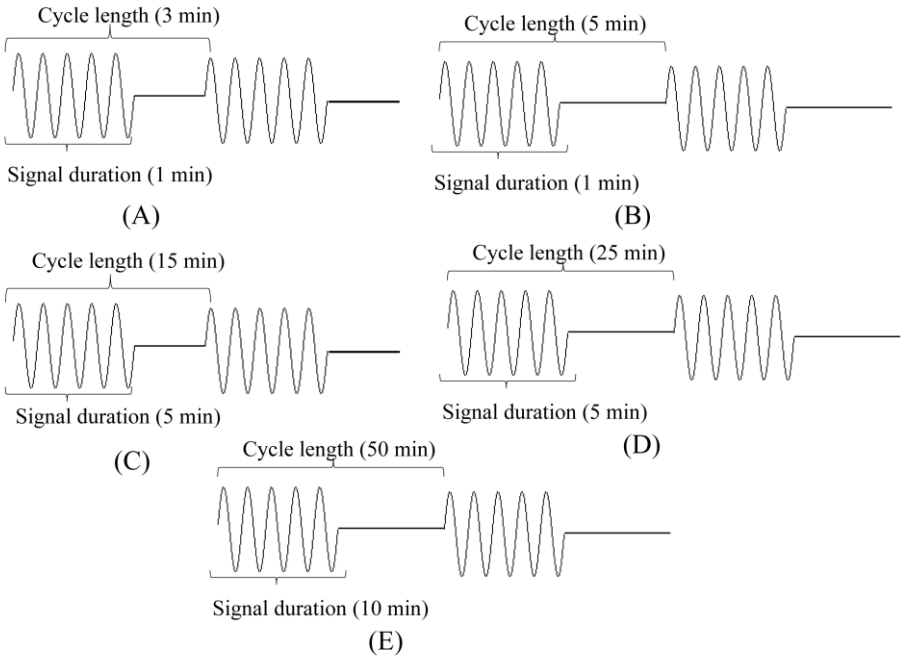

Figure 4.3. Operating settings for cyclic ultrasound irradiation. A signal duration of 1 min coupled to cycle length of 3 min translates to an intermittent pattern of 1 min of irradiation followed by 2 min no irradiation. The same definition is applied for the other operation modes.

4.2.7. Efficient frequency band on cyprid settlement

Low frequency application of 23 kHz exhibited significant inhibitory effect on cyprid settlement. However, it was surmised that the inhibitory effect should not only work at a particular frequency, but within a frequency range. An additional settlement test was therefore conducted for the frequency range of 20-30 kHz. A swept sine wave signal, with linear spacing, was used to drive the PZTs working at frequency range across 20-25 kHz and 25-30 kHz with acoustic amplitude of 5 kPa, respectively.

4.2.8. Statistical analysis

Normality tests of settlement and mortality data were performed with a Kolmogorov-Smirnov test using Sigma Stat 3.5 (Systat Software, Inc., San Jose, CA, USA); the results indicated that parametric tests were appropriate for the data analysis. For the continuous mode, two main factors were considered in cyprid settlement and mortality, namely exposure time and frequency. Data were analyzed with a Two-Way analysis of variance (ANOVA) to evaluate significant influence of these parameters. This was followed by a One-Way ANOVA together with a Tukey *post hoc* test to determine differences between treated and control cyprids. For the other tests, data were analyzed with a One-Way ANOVA, followed by a Tukey *post hoc* test. All data were reported as mean $\pm$ standard error (SE). For all comparisons, p-values ≤ 0.05 were considered as statistically significant.

4.3. Results

4.3.1. Acoustic pressure distribution measurement

The acoustic pressure was adjusted to the desired value of 5 kPa at a height of 0.5 mm above the vial bottom. Although there were pressure variations along x and y directions at different measurement points (Figure 4.4), the maximum difference was within 10%, and the distinction was considered insignificant. Owing to the symmetry of the vial, the acoustic pressure was considered evenly distributed in the horizontal direction. As a result, cyprids at different locations on the same surface would be exposed to the same acoustic amplitude. The same acoustic pressure distribution results were found for frequencies of 63 and 102 kHz.

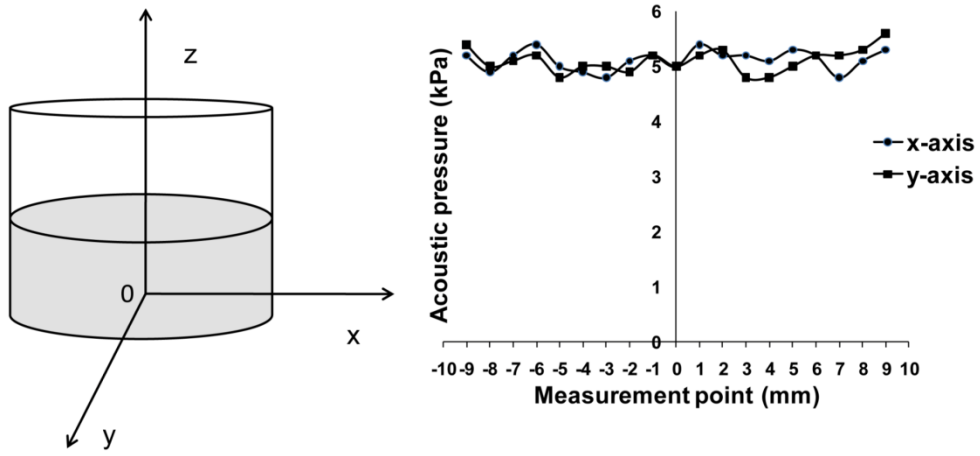

Figure 4.4. Distribution of acoustic pressure in the horizontal direction at a height of 0.5 mm above the bottom of a vial at a frequency of 23 kHz. The depth of FSW was 5 mm.

4.3.2. Effect of continuous irradiation on cyprid settlement and mortality

Cyprid settlement was found to vary significantly between the test frequencies (Two-Way ANOVA, $p < 0.05$; Figure 4.5). As observed in Guo et al (2011a), settlement was significantly reduced for cyprids exposed to the continuous irradiation at 23 kHz (One-Way ANOVA, $p < 0.05$), while no inhibitory effects were achieved for cyprids exposed to 63 and 102 kHz (Tukey test, $p > 0.05$). Continuous irradiation at 23 kHz significantly inhibited settlement; few juvenile barnacle observed attached to the bottom of the test vials. At frequencies of 63 and 102 kHz under the same exposure time and acoustic amplitude, no inhibitory effect was observed (Figure 4.6).

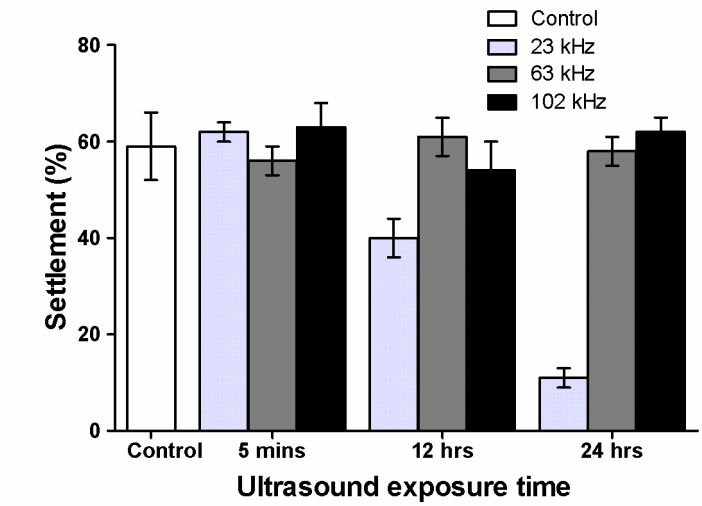

Figure 4.5. The effect of ultrasound exposure time and frequency on settlement. The acoustic amplitude was set at 5 kPa.

Settlement differed significantly with exposure time (Two-Way ANOVA, $p < 0.05$; Figure 4.5, Table 4.1). No inhibitory effect was observed for cyprids exposed to ultrasound for 5 min (Tukey test, $p > 0.05$), which was consistent with the result of Guo et al. (2011b). Although settlement reduction was achieved at 23 kHz for 12 h

exposure, the change was small. On the other hand, with continuous exposure of 24 h, settlement reduction was five-fold (Figure 4.5).

Table 4.1. Two-way ANOVA for the influence of frequency and exposure time on cyprid settlement.

Source of variation	Df	Mean square	F value	P value
Frequency	2	1027	44.81	< 0.0001
Exposure time	3	530.7	23.16	< 0.0001
Interaction	6	590.7	25.77	< 0.0001

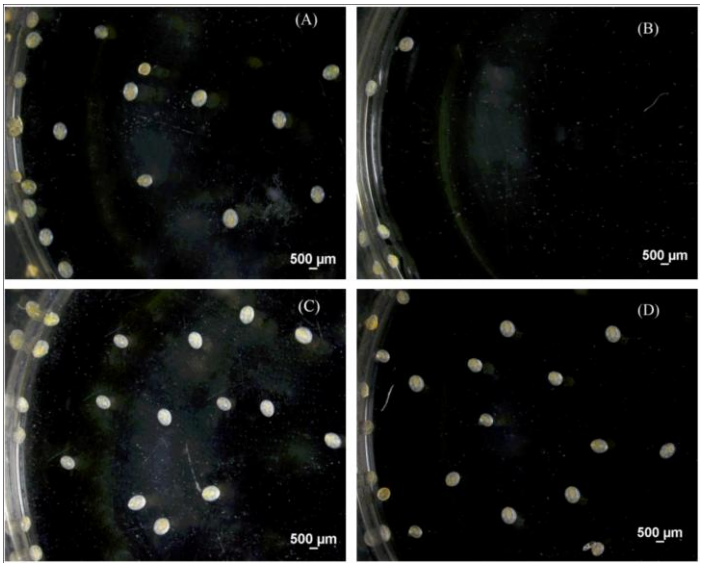

Figure 4.6. Images of the bottom of test vials after continuous ultrasound exposure for 24 h at frequencies of 23 (B), 63 (C) and 102 (D) kHz. (A) shows the control.

No significant increase of mortality was detected for any of the test frequencies under 24h continuous irradiation (Tukey test, $p > 0.05$; Figure 4.7), indicating that ultrasound exposure under these regimes was not lethal to cyprids. As irradiation for 24 h was needed to prevent settlement, it is probable that the irradiation treatment did not damage the cyprids, but prevented permanent attachment to the substratum.

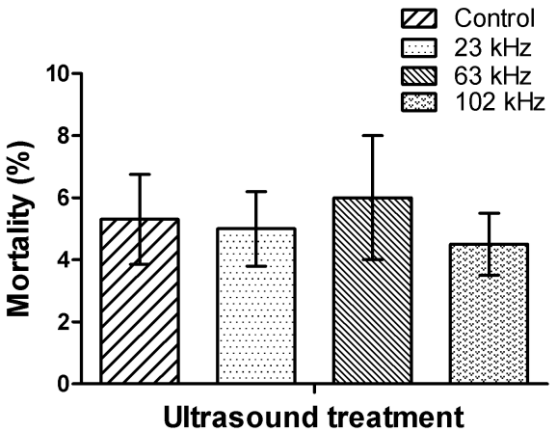

Figure 4.7. Cyprid mortality at different ultrasound frequencies. The acoustic pressure was set at 5 kPa for 24 h.

4.3.3. Observations of cyprid exploration

There was no difference observed in the numbers of cyprids exploring the surface when they were subjected to the different irradiation treatments. No significant difference in cyprid exploration behavior was observed among the different frequencies tested (One Way ANOVA, $p > 0.05$, Table 4.2). With continuous ultrasound exposure at the pressure of 5 kPa, there was no difference between treated and control groups (Tukey test, $p > 0.05$). This result differs from observations in Guo et al. (2011a), where cyprid exploration behavior was affected by ultrasound treatment at 20 kPa.

Table 4.2. Cyprid exploration behavior in response to different ultrasonic exposures. The acoustic amplitude was set at 5 kPa.

	Control	23 kHz	63 kHz	102 kHz
Cyprid step length (um)	329±7	342±11	323±9	337±13
Steps taken in 5 min	140±10	155±7	139±15	147±8

4.3.4. Substratum vibration and acoustic pressure on settlement inhibition

At the same acoustic pressure of 5 kPa, the substratum vibration amplitude for each frequency differed. The vibration amplitude was highest at 23 kHz with 10.05 nm, whilst amplitudes of 4.35 and 3.1 nm were obtained for 63 and 102 kHz respectively (Figure 4.8a). Significant inhibitory effects were only observed for cyprids exposed to the acoustic pressure of 5 kPa for 24 h at 23 kHz (One-Way ANOVA, Tukey test, $p < 0.05$, Figure 4.8b). No inhibitory effects were observed for the other two frequencies (Tukey test, $p > 0.05$).

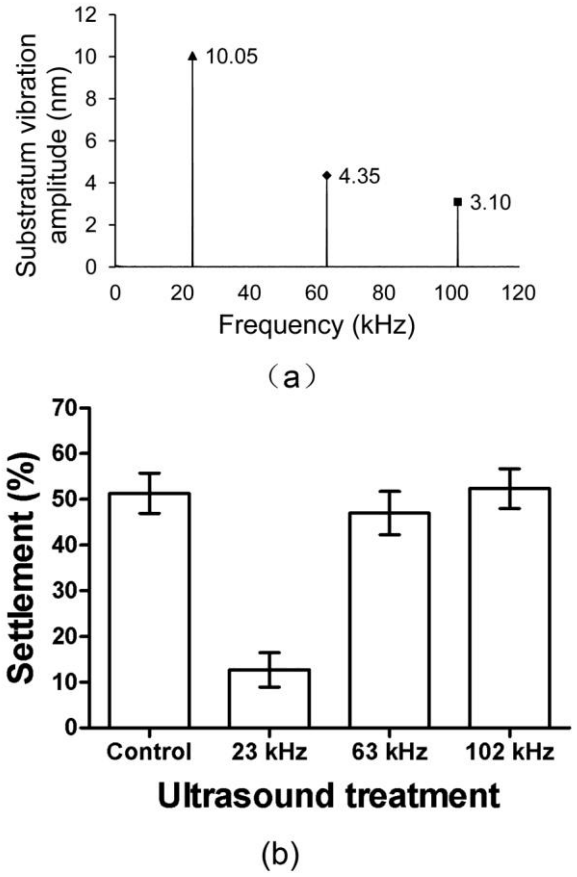

Figure 4.8. Substratum vibration *vs* cyprid settlement at frequencies 23, 63 and 102 kHz with the same acoustic pressure of 5 kPa: (a) substratum vibration amplitude; (b) cyprid settlement.

At the same vibration amplitude of 10.05 nm, settlement inhibition was achieved for all the frequencies tested (Tukey test, $p < 0.05$, Figure 4.9b). However, 23 kHz showed the most pronounced inhibition of settlement (Tukey test, $p < 0.05$). Although the surface vibration was the same, the resultant acoustic pressures at 63 and 102 kHz would be larger than at 23 kHz (Figure 4.9a). Acoustic cavitation is likely to have occurred at 63 and 102 kHz and this was verified by the harmonics detected in the ultrasound spectrum (Figure 4.10).

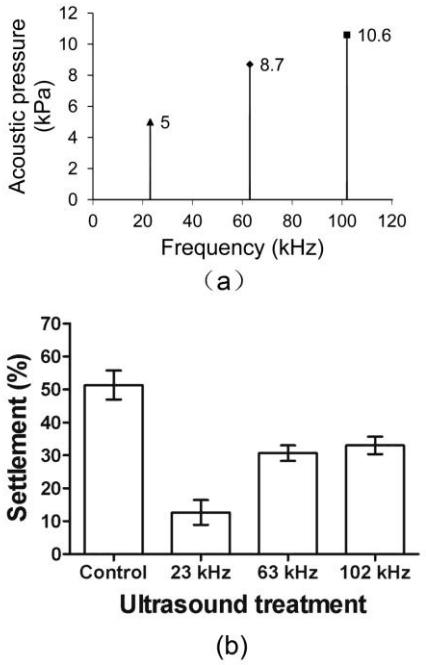

Figure 4.9. Acoustic pressure *vs* cyprid settlement at frequencies of 23, 63 and 102 kHz at the same substratum vibration of 10.05 nm. (a) acoustic pressure; (b) cyprid settlement.

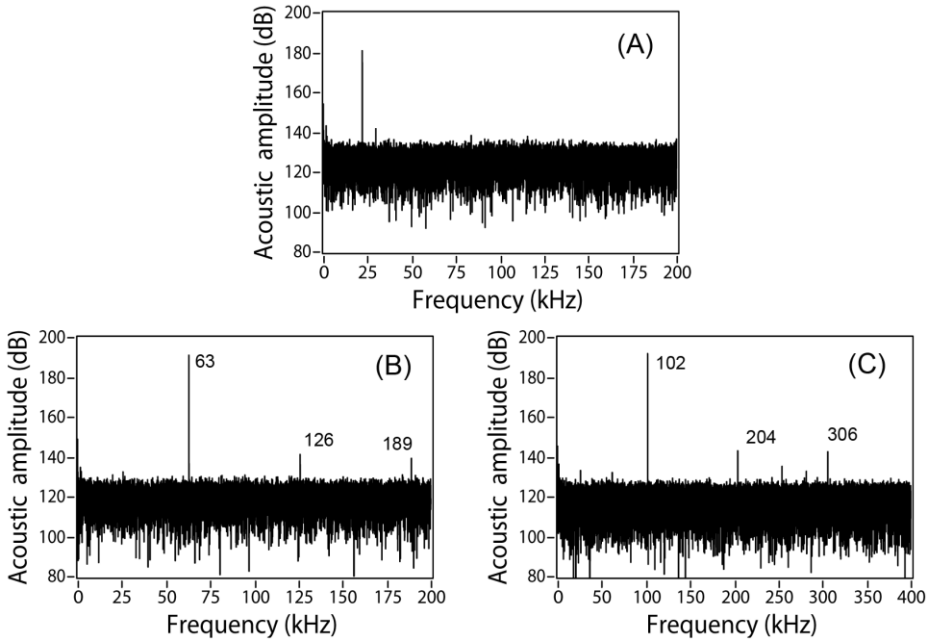

Figure 4.10. Acoustic spectrum of 23 (A), 63 (B) and 102 (C) kHz, at a substratum vibration of 10.05 nm.

4.3.5. Cyprid settlement under different cyclical irradiation modes

As an inhibitory effect was only observed with 23 kHz, the response of cyclical application of ultrasound on settlement was further examined for this frequency. Ultrasound exposure with various operation modes significantly reduced settlement compared to the control (One-Way ANOVA, $p < 0.05$, Figure 4.11). The cyclical mode of "10 min on 40 min off" was found to exhibit much less inhibitory effect than the continuous irradiation (Tukey test, $p < 0.05$). The other cyclical operation modes, however, achieved the same inhibitory effects as for the continuous mode (Figure 4.11, Tukey test, $p > 0.05$), all of which have reduced settlement approximately by a factor of five compared to the control.

Although operation mode of "1 min on, 4 min off" consumed the same energy as mode of "5 min on, 20 min off" over the duration of 24 h, the latter was preferred as more frequent operation of the device could reduce its lifespan.

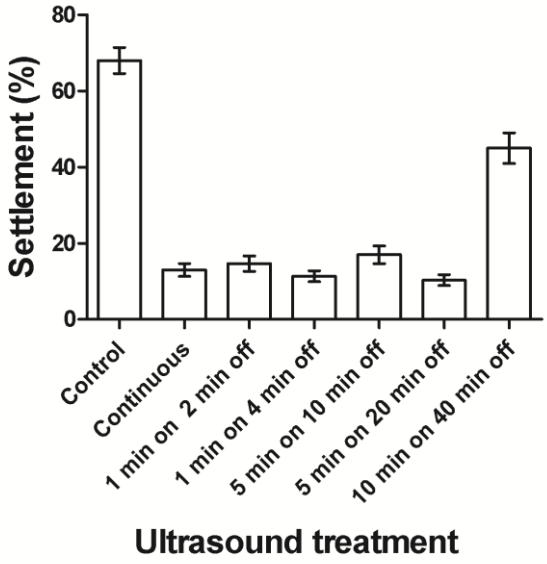

Figure 4.11. Comparison of various cyclical irradiation modes on cyprid settlement at a frequency of 23 kHz and acoustic amplitude of 5 kPa.

4.3.6. Efficient frequency band on cyprid settlement

There was no significant difference between cyprids exposed to 23 kHz and frequency bandwidth of 20-25 kHz (Tukey test, $p > 0.05$, Figure 4.12). Frequency range of 25-30 kHz also generated inhibitory effects, however, with a lower inhibitory effect than 23 kHz (Tukey test, $p < 0.05$).

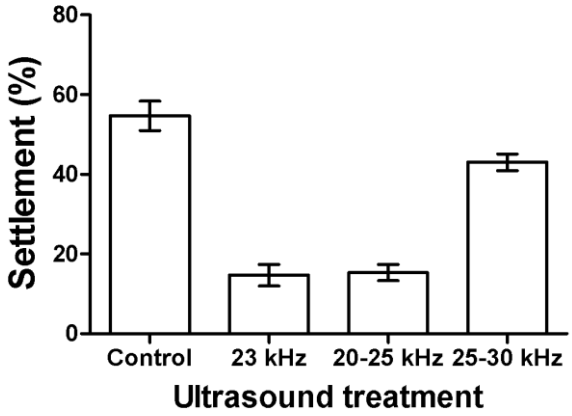

Figure 4.12. Effective frequency band on settlement. The experiments were conducted at the acoustic amplitude of 5 kPa with the continuous exposure of 24 h. The result at 23 kHz is compared with frequency ranges of 20-25 kHz and 25-30 kHz.

4.4. Discussion

It has been demonstrated previously that low frequency ultrasound can reduce barnacle settlement effectively. Kitamura et al. (1995) reported that a frequency of 23 kHz resulted in greater inhibition of cyprid settlement than two higher frequencies viz. 63 and 102 kHz, under the same acoustic pressure of 20 kPa. The mechanism of settlement inhibition was found to be ultrasonic cavitation which induced physical injury and increased cyprid mortality (Guo et al. 2011b). High intensity ultrasound resulting in cavitation effects has been cited as the main factor reducing viability of several organisms, including bacteria, algae and barnacle nauplii (Liang et al. 2009; Lagsir et al. 2000; Seth et al. 2010). Groves et al. (2009) also suggested that ultrasound cavitation may be responsible for the antifouling effects observed for their ultrasonic devices.

How low frequency, low intensity ultrasound affects the settlement of cyprids among the test frequencies is not clear. In this study, lower amplitudes of 5 kPa were applied. As the spectrum of the frequencies at 5 kPa were comprised mainly of the driving frequencies, it is probable that with this amplitude, cavitation effects are absent (Liang et al. 2006; Avvaru and Pandit 2009) and thus not a dominating factor contributing to settlement inhibition (cf. Guo et al. 2011b). The results of this study demonstrated settlement inhibition at 23 kHz, but at higher frequencies of 63 and 102 kHz, no inhibition was observed. This concurs with the earlier observation for 20 kPa (Guo et al. 2011a). However, for the present study, there was no observed difference in mortality between treated and control cyprids, which suggested that cavitation effects may not have contributed to the reduction of cyprid settlement.

Given the experimental setup, it is plausible that substratum vibration arising from the excitation of piezoelectric actuators may have compromised the cyprids' ability to

attach to the surface. Direct ultrasonic vibration has been reported as means of protecting submerged marine structures (Shigihara and Kobayashi 2002). Donskoy et al. (1996) also found that low frequency sound and sound-excited vibrations were useful to prevent settlement of zebra mussels. As described by the expressions (1)-(3) given above, there is a direct relationship between acoustic pressure and substratum vibration displacement. At the same acoustic pressure, lower frequencies achieve higher vibration amplitude; likewise, with the same substratum vibration amplitude, higher frequencies result in higher acoustic pressures. In general the results support this, although due to the equipment detection limitations, the values measured were not always proportional to the frequencies.

The net impact on cyprid settlement may be a result of compound effects, beyond the effect of substratum vibration alone. The strongest inhibition of settlement was observed at 23 kHz in both conditions, when acoustic pressure was set at 5 kPa, and when substratum amplitude was controlled at 10.05 nm. This result suggests that the inhibitory effect may not only be related to amplitude, but also to ultrasound frequency. The inhibitory effect was also found not only limited at a particular frequency, but within a frequency band. Therefore, to achieve cyprid reduction with ultrasonic strategy, low frequency band of 20-25 kHz is recommended.

During exploration, cyprids utilize their antennular sensory setae to gather information from environmental stimuli such as water currents and substratum properties (Aldred et al. 2010a; Maruzzo et al. 2011). In the present study, it was noted that continuous exposure to ultrasound treatment at 5 kPa did not alter cyprid exploratory behavior, whereas cyprid exploration behavior varied significantly for cyprids exposed to ultrasound with amplitude of 20 kPa in a short exposure (Guo et al. 2011a). Maruzzo et al. (2011) described the action of antennular setae during

exploratory behavior and the size of setae was found much larger than the substrate vibration amplitude. It may be surmised that with 5 kPa, the substratum vibration amplitude would be in nanometers (Figure 4.a) and may be too small to be detected by the sensory setae. On the other hand, an inhibition effect may result from the acoustic wave in the liquid. In the treatment vials, the inertia force arising from the substratum vibration may be estimated by the equation, $F_i=mr\omega^2$, whilst the force caused by acoustic wave in the liquid may be estimated with $F_a= ps$, where p is the acoustic pressure and s is the cross sectional area of cyprids. Assuming a maximal cyprid mass of at least 37.7 μg (*Semibalanus balanoides*; Holland and Walker 1975) with a cross sectional area of approximately $1x10^{-7}$ m^2 (*Balanus improvisus*; Larsson et al. 2010), under a pressure of 5 kPa, the acoustic wave induced force would be much larger than the inertia force due to substratum vibration. It may be possible then that a liquid-born acoustic wave may also have contributed to the inhibitory effect. The acoustic wave may have interacted with the dynamic behavior of the cyprids in a phenomenon known as resonance, resulting in detachment of the cyprids attached by temporary adhesive laid down during exploration. Crisp et al. (1985) demonstrated that the force needed to detach a cyprid attached by temporary adhesive is 30 times less than that required to detach larvae which have laid down permanent adhesive.

As energy consumption is an important consideration for use of ultrasound as a practical marine AF strategy, intermittent application is favored. The effect of intermittent treatment was examined in this study and found to be a useful means of providing effective reduction in barnacle settlement. Further cost savings in operations may be achieved by maximizing on-off cycles. For example, it was found that with “1 min on and 4 min off” and “5 min on and 20 min off”, the same inhibitory effects were achieved with the same energy demand, but equipment lifespan would increase significantly if the devices were not switched on and off as

often. The operation mode of "10 min on 40 min off" was the least effective. This result may be related to the organism's settlement behavior. Cyprids begin secretion of permanent adhesive soon after attachment, and the adhesive cures rapidly with maximum adhesive strength obtained in 3 h (Berglin et al. 2001; Phang et al. 2006).

For intermittent patterns with short off periods, the excitation of ultrasound either in the water or at the water-substratum interface may be perceived by cyprids as an unpleasant site to settle. For a period of 40 min without irradiation, it is plausible that the cyprids were still able to complete settlement and permanent adhesion and thus the external ultrasound failed to overcome the adhesion strength of cyprid permanent adhesive.

4.5. Conclusion for chapter 4

Combining the results of cyprid exploration, settlement and mortality, it was concluded that the low intensity ultrasound method was advantageous compared to high amplitude ultrasound as an AF method. Ultrasound based AF techniques offer several benefits over chemical-based biocidal strategies, which are encumbered by issues of environmental pollution (Chambers et al. 2006). The major constraints of ultrasound applications have been energy demand and possible effects on non-target populations in the vicinity of application. With proper design, a low frequency, low amplitude ultrasound system could be operated economically. Furthermore, with low amplitudes, it is plausible that the system would have lower impact on other marine organisms as the range of transmittance is limited.

Chapter 5. Effect of ultrasound on cyprid footprints and juvenile barnacle adhesion strength on a fouling release material

In this chapter, atomic force microscopy (AFM) was used to analyze the effect of ultrasound on barnacle cyprid footprints (FPs), which are protein adhesives secreted when the larvae explore surfaces. Cyprids were exposed to 23 kHz ultrasound treatment at 20 kPa for 5 mins. The ultrasound treated cyprids were found to secrete less FP and the FP appeared to spread a larger area than that laid by untreated cyprids. The adhesion strength of the newly settled (day 0) barnacles metamorphosed from ultrasound treated cyprids on silicone substrate was reduced compared to barnacle settled from cyprids not exposed to ultrasound. However, no difference in adhesion strength was observed in the 4-8 day old juvenile barnacles. The evidence from this study suggests that ultrasound treatment results in a reduced cyprid footprint secretion and affects the subsequent recruitment of barnacles onto a substrate by reducing the ability of larval and early settlement stages of barnacles from firmly adhering to the substrate. Ultrasound may offer a means to enhance the performance of fouling release substrates by reducing the ability of early settlement stages of barnacles from firmly adhering to the substrate.

5.1. Introduction

In earlier chapters, it has been demonstrated that both low and high intensity ultrasound can prevent barnacle cyprid settlement (Guo et al. 2012; Guo et al. 2011a; Guo et al. 2011b). The mechanism for reduction in settlement in response to low intensity and low frequency (20-25 kHz) ultrasound is still unknown. However, the probable mechanism of high intensity ultrasound on cyprid settlement inhibition has been attributed to ultrasonic cavitation (Guo et al. 2011a), in which the cavitation induced forces have reduced the cyprid settlement and changed its exploration behavior.

The lifecycle of the barnacle, *Amphibalanus amphitrite* (= *Balanus amphitrite*: Pitombo 2004), includes planktotrophic nauplius stages, a non-feeding cypris larval stage, and a sessile adult stage. The pre-settlement cypris stage actively explores surfaces and metamorphoses into the juvenile barnacles once a suitable site is found. Surface exploration is conducted using the antennules, in a form of bi-pedal 'walking', which appears to be affected by the surface texture, material properties, chemical clues, and presence of adult or cyprid nonspecific (Aldred and Clare 2008; Schumacher et al. 2007; Yule and Crisp 1983). During exploration, secretion is deposited as footprints (FPs) through the antennular attachment discs and these have been implicated to act as settlement cues for other exploring cyprids (Aldred and Clare 2008; Crisp et al. 1985). The FP has been described as a temporary adhesive, as it enables reversible attachment to surfaces (Crisp et al. 1985; Dreanno et al. 2006; Matsumura et al. 1998). A settlement-inducing protein complex (SIPC), which functions also as a settlement cue, has been found to be present in FPs (Matsumura et al. 1998; Dreanno et al. 2006). It has also been reported that surfaces which were easier for the adsorption of FPs would lead to higher settlement (Phang et al. 2009).

Fouling release coatings (FRCs) are now widely used for the antifouling (Aldred and Clare 2008; Callow and Callow 2011). The FRCs do not prevent organisms from attachment, but the interfacial bond between the organism and coating is weak. As a result, the attached organisms are more easily removed by the hydrodynamic forces created from a vessel's movement through the water, or by other simple mechanical cleaning (Aldred and Clare 2008; Larsson et al. 2010). The cyprid larval stage and juvenile barnacles have previously been proposed as appropriate experimental models for evaluation of antifouling performance (Larsson et al. 2010). It was found that attachment strength played a significant role on the marine organisms' settlement. For surfaces with higher settlement, stronger forces were required to detach the organisms. The settlement of Mytilus alloprovincialis was found positively correlated to adhesion strength (Carl et al. 2012). Also, barnacle cyprids were found preferring to settle on the substratum where the possibility of subsequent removal is least likely to occur (Aldred et al. 2010). Ultrasound has shown the ability to reduce or enhance the protein secretion (Ishibashi et al. 2010; Ruan et al. 2010). Based on the preliminary results of easier removal of the newly metamorphosed barnacles from ultrasound treated cyprids, it is surmised that ultrasound may also have reduced or delayed the secretion of juvenile barnacle cement, which affected barnacles' adhesion strength. Since ultrasound has shown ability to reduce cyprid settlement (Guo et al. 2011b), if ultrasound is also able to reduce the adhesion strength of attached barnacles, by the combination of strategies of FRCs and ultrasound, a more thorough and efficient antifouling method may be achieved. This is especially important for the gigantic vessels with the cruising speed that are not sufficient to produce the required dynamic force to detach the fouling organisms.

Since cyprid settlement and exploration behavior were significantly changed by ultrasound exposure with high amplitude (Guo et al. 2011a), it is surmised that

ultrasound treatment may affect cyprid's FP secretion, and barnacle adhesion strength may in turn be affected. In this chapter, we explored the effect of ultrasound on cyprid's FPs and juvenile barnacle adhesion strength using AFM and Nano-tensile tester, respectively, so as to learn how ultrasound might affect cyprids and gain a better understanding of the mechanism behind the ultrasound induced inhibitory effects.

5.2. Materials and methods

5.2.1. Surface preparation

Enhanced FP absorption has been demonstrated on the NH_2 terminated glass microscopy cover slips (Phang et al. 2008; Phang et al. 2009). In this chapter, the same surfaces were used to evaluate ultrasound on cyprid temporary adhesive protein secretion. To study the effect of ultrasound on juvenile barnacle adhesion strength, the medical grade silicone sheeting (Bioplexus, USA) was used and cleaned following the provided instructions before use.

To coat the surfaces, the glass microscopy cover slips were firstly immersed in 5% decon 90 solution and cleaned using ultrasonic clean-tank for 20 mins. The use of Decon 90 solution to effectively clean surfaces for increasing surface density of silanol groups and/or prior to silanization has been well documented in the previous literature (Bi et al. 2007; Hartono et al. 2008). The slips were then rinsed thoroughly with ultrapure water and dried with nitrogen gas. The Amino (NH_2-) terminated surfaces were obtained by immersing the cleaned slips in 5% 3-aminopropyl triethoxysilane (APTES) solution and were put in the shaker (GFP MBH, Germany) for 30 mins. After that the surfaces were rinsed with ultrapure water thoroughly and dried using nitrogen gas.

Static water contact angles (CAs) of NH_2 terminated surfaces and silicone plates were measured at 25℃, using the sessile drop method with a 2 µl water droplet, in a telescopic goniometer (model 100-00-(230), Rame-Hart, Inc., Mountain Lake, NJ, USA). To measure the contact angle of coated cover slips, eight samples were replicated and the averaged contact angle was 55°± 2.4° and the value was approximately consistent with reported results by Phang et al. (2008) and Phang et al. (2009). The contact angle of silicone substrate was 94°.

5.2.2. Ultrasound experimental setup

The set up for the ultrasonic experiment is similar as described in Figure 2.1. As low frequency of 23 kHz exhibited most significant effect on barnacle cyprid settlement and exploration behavior (Guo et al. 2011a), in the present study, only this frequency was chosen, with the pressure set at 20 kPa. The cyprids were then subjected to ultrasound exposure for 5 mins.

5.2.3. Cyprid settlement assay and juvenile barnacle culture

Cyprid settlement was performed with a 'no choice' assay, as described in Aldred et al. (2010b). The experiments were conducted on the medical grade silicone substrates (Bioplexus, USA). Thiyagarajan et al. (2002) demonstrated that the gregarious behavior of cyprids did not interfere with settlement rates at cyprid densities of 5-200 per 5ml. After ultrasound exposure, 500 µl volume of FSW, containing approximately 15-20 cyprids, was deposited on each sliced silicone plate (2x2 cm), forming a droplet on the surface. The surfaces were placed in Petri dishes and sealed with paraffin to prevent water evaporation. The assay was incubated at 26°C for 48 h, on a 15 h light and 9 h dark cycle. The cyprids were then examined under a stereo microscope (Nikon SMZ 1500, Japan), and the number of cyprids which had settled

and metamorphosed into barnacles was enumerated. To evaluate ultrasound effect, eight replicate silicone substrates were prepared for both ultrasound treated and control cyprids.

5.2.4. Footprint observation using AFM

The schematic of the AFM setup for cyprid FP measurement is shown in Figure 5.1 and the working principle and protocol are as described in Phang et al. (2006). In this study, the AFM scanning was conducted using a Dimension D3100 atomic force microscope (Veeco/Digital Instruments (DI), Santa Barbara, CA). Since cyprid FP morphology showed no significant difference in air and in FSW (Phang et al. 2009; Phang et al. 2010), but imaging in air provided higher resolution, in the present study, the AFM scanning was conducted in air with tapping mode. The NH_2 terminated cover slips were mounted on the glass sides prior to experiments. Cyprids were transferred to the modified cover slips using a micropipette. Cyprid exploration was monitored by a stereo microscope equipped with video capture software NIS-Elements BR 3.2 (Nikon Instech Co., Ltd., Japan). The explored areas were marked on the back of glass slides and the videos of the 'walking' were captured for the ease of FP searching during scanning. The cyprid was subsequently removed and the surface was rinsed with ultrapure distilled water and dried with nitrogen gas to minimize the contamination. Before exploration, cyprids were allowed 5 mins' acclimatization after ultrasound exposure and the observation time for both control and ultrasound treated cyprids were within 40 mins. AFM images were taken in air using the intermittent-contact mode with silicon cantilevers having a spring constant of 30 N/m (Nanosensors, Germany).

To evaluate the effect of ultrasound on cyprid footprints, six footprints of both control and ultrasound treated cyprids were analyzed and all the footprints were obtained from different individual cyprid.

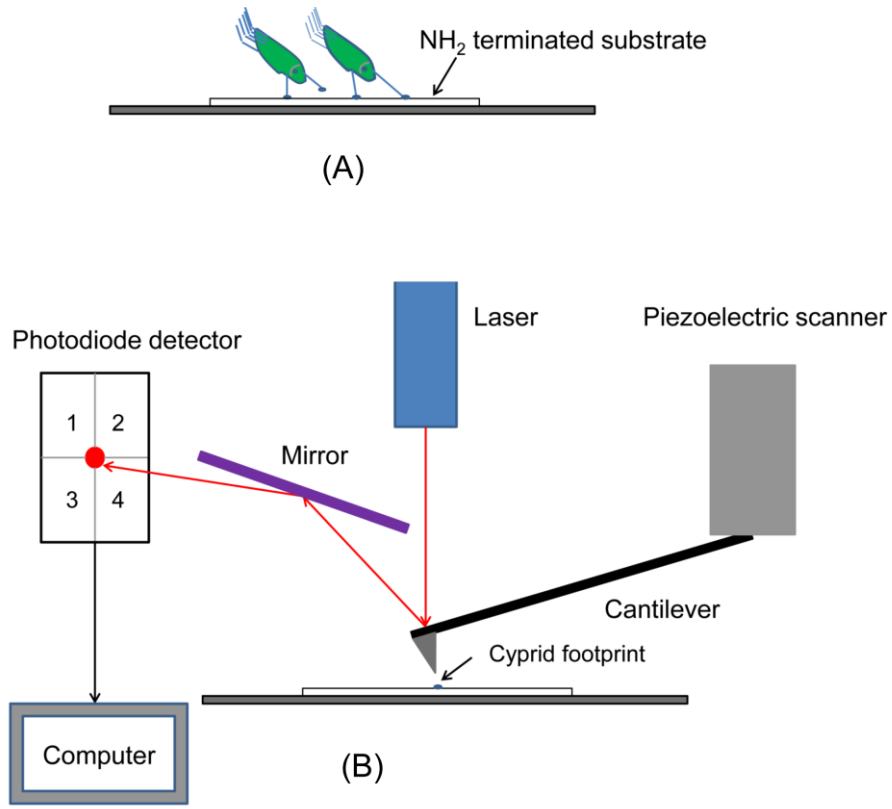

Figure 5.1. The schematic of AFM on barnacle cyprid footprint scanning. (A) Cyprid explored the NH_2 terminated cover slip and left footprint on it; (B) the morphology of footprint was scanned by AFM D3100.

5.2.5. Barnacle adhesion strength measurement

Measurement of barnacle adhesive force was conducted using a calibrated Nano-tensile tester (Nano Bionix System, MTS, USA), and the schematic of the experimental setup is shown in Figure 5.2. The sliced silicone substrates (2x2 cm) with barnacles settled were clamped in the lower grip. A micro steel fibre with diameter of 80 μm and length of 10 mm was clamped in the upper grip. The fibre was controlled and lowered until it was slightly above the top of barnacle shell. Then the

tip of the fibre was wetted with a small drop of superglue (Selleys Pty Ltd, Australia) and lowered to touch the top of barnacle shell. The glue was allowed to dry for about 30 s and the force required to dislodge the barnacle was then measured. During experiments, barnacle plate was wetted using FSW. To study the effect of pulling velocity on barnacle detachment force measurement, two strain rates were chosen, one was $1.0x10^{-4}$ s^{-1}, representing lower pulling velocity and the other was $1.0x10^{-2}$ s^{-1}, representing faster pulling velocity. The preliminary results revealed that no significant detachment forces were detected with the above mentioned velocities, therefore, in our study, only strain rate of $1.0x10^{-2}$ s^{-1} was chosen. Similar results were found by Berglin et al. (2001), who found pulling velocities did not affect barnacle attachment force measurement. After detachment, the coatings were rinsed using ultra-pure distilled water and observed under a stereo microscope with image capture software (Nikon Instech Co., Ltd., Japan). Only the forces that completely removed barnacles were recorded and ten replicates for each group barnacles were measured.

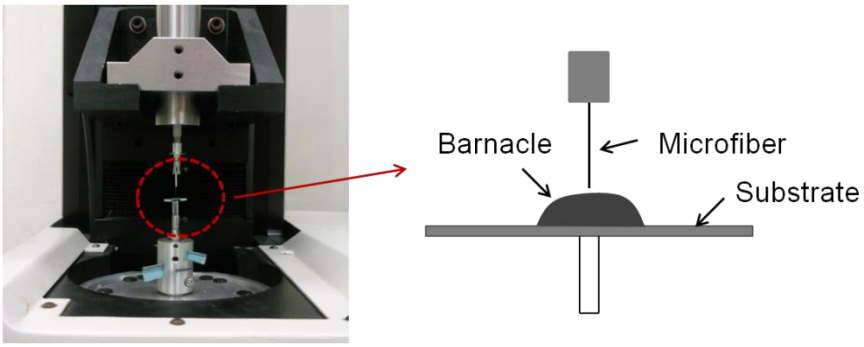

Figure 5.2. The schematic of Nanotensile tester on barnacle adhesive force measurement.

To conduct the adhesion strength measurement, the basal areas of barnacles were required. The images of barnacles before experiments were photographed using a stereo microscope with image capture software. The images were processed with

ImageJ software (Version 1.43), which used edge contrast to define the perimeter and thereby calculate the total basal area. Barnacles metamorphosed from ultrasound treated and control cyprids were reared and fed daily with algal mixture of 1:1 v/v of *Tetraselmis suecica* and *Chaetoceros muelleri* at a density of approximately $5x10^5$ cells /ml. Adhesion strength measurements were conducted on the newly metamorphosed barnacles (day 0) to day 8 barnacles.

5.2.6. Data analysis

The statistical comparisons were performed using GraphPad Prism 5 (GraphPad Software Inc.). Data of barnacle adhesive forces/strength were analyzed with a two-way analysis of variance (ANOVA) to evaluate the significant influence of ultrasound and age effect. Then a one-way ANOVA together with a Tukey *post hoc* test was conducted to determine differences within each treatment. Data of settlement and cyprid footprints were analyzed using t-test. All data are reported as mean ± standard error (SE). For all comparisons, p-values ≤ 0.05 were considered as statistically significant.

5.3. Results

5.3.1. Cyprid settlement

The settlement of control and ultrasound treated cyprids is shown in Figure 5.3. Significant difference was observed between ultrasound treated and control cyprids (t-test, $p < 0.001$). After treatment with 23 kHz for 5 mins at 20 kPa, settlement was reduced significantly from 43.5% to 16% (Figure 5.3).

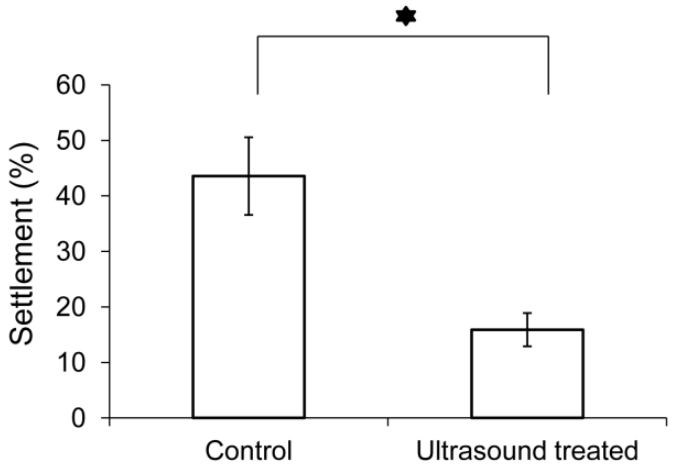

Figure 5.3. Cyprid settlement comparison. Error bars here are standard errors. The asterisk here represents statistically significant difference.

5.3.2. Images of FPs on NH_2 terminated surfaces

The barnacle cyprid FP height images obtained by AFM are shown in Figure 5.4. Entire footprints and sections of footprints with higher magnification were imaged. For cyprids exposed to ultrasound, the FP exhibited difference in morphology compared with that of control cyprids. FP secreted by ultrasound treated cyprids had a larger spreading area than that deposited by control cyprids, however, FP from control cyprid was found to be much thicker (t-test, $p < 0.05$; Figure 5.4, Table 5.1). The fibrillar structure of the FP was observed from both ultrasound treated and

control cyprids, and only section of higher magnification of footprints from ultrasound treated cyprid is shown in Figure 5.4C.

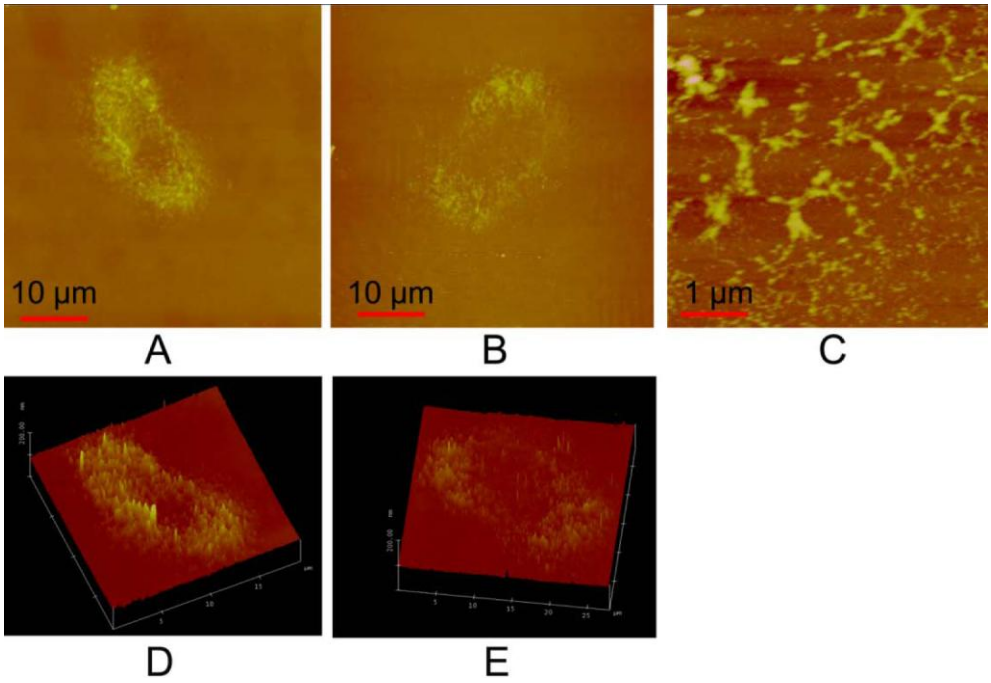

Figure 5.4. The morphological comparison of FP from ultrasound treated and control cyprids on NH_2 terminated surfaces. A is the FP of control cyprids; B is the FP of ultrasound treated cyprids; C is the magnificantion of FP; D and E are 3D images of FP from control and ultrasound treated cyprids.

The geometrical data extracted from AFM scanned FPs are presented in Table 5.1. The mean FP spread area from ultrasound treated cyprid was 1142 μm^2, which was larger than the FP area of control cyprids of 778 μm^2. The route-mean-square (RMS) thickness of the footprints, calculated from AFM results, was used to evaluate cyprid footprint thickness. This value was half of that measured for the control, and the volume of FP secreted by ultrasound treated cyprids was 9.4 μm^3, which was one third less compared to the control cypirds (Table 5.1).

Table 5.1. The morphological information of FP comparison obtained by AFM

Footprint type	Mean footprint area (μm^2)	RMS footprint thickness (nm)	Footprint volume (μm^3)
Ultrasound treated	1142 ± 92	8.7 ± 0.6	9.4 ± 0.62
Control	778 ± 54	16.3 ± 1.1	12.6 ± 1.2

5.3.3. Adhesion strength comparison

A typical force-displacement curve of day 0 barnacle measured using Nano-tensile tester is shown in Figure 5.5. The recorded force curve exhibited an approximately linear elastic regime upon contact until detachment occurred (when the force drop significantly). Figure 5.6 shows the detachment forces obtained with juvenile barnacles which had been pre-treated with ultrasound. Both ultrasound treatment and barnacle age contributed to the adhesive forces measured for the juvenile barnacles (Two-Way ANOVA, $p < 0.05$; Figure 5.6A). The forces needed to dislodge the barnacles were found to increase significantly with age (Tukey test, $p < 0.05$). For the newly metamorphosed barnacles (day 0), a higher detachment force was required to dislodge the control barnacles (Tukey test, $p < 0.05$) compared to barnacles reared from ultrasound treated cyprids. The averaged detachment force for the ultrasound treated barnacles (day 0) was 6.37 ± 1.4 mN, as compared to that measured for the controls (11.65 ± 2.3 mN). Similar results were found on day 2 barnacles (Tukey test, $p < 0.05$). However, no significant difference in detachment force was found after 4 days' in culture (Tukey test, $p > 0.05$; Figure 5.6A).

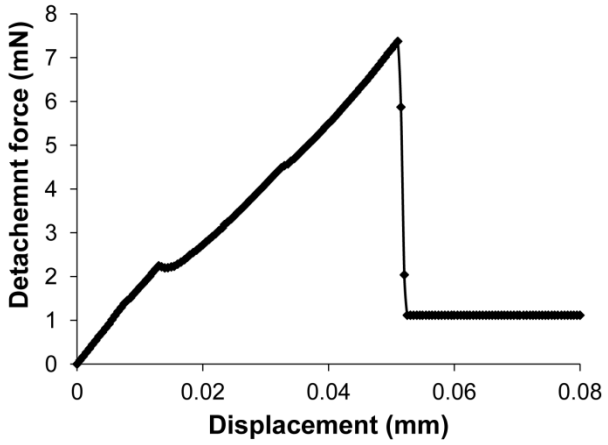

Figure 5.5. Representative force displacement curve of day 0 barnacle metamorphosed from ultrasound treated cyprid.

The adhesion strength was caculated by dividing the detachment forces over the basal areas of juvenile barnacles. The results revealed that adhesion strength was reduced after ultrasound exposure for the day 0 and day 2 barnacles (Figure 5.6B; Tukey test, $p < 0.05$). For day 0 barnacles, the averaged adhesion strength of the juvenile barnacles metamorphosed from control cyprids was $0.83 \pm 0.07 \times 10^5$ Pa, while the adhsion strength of barnacles from ultrasound treated cyprids was $0.7 \pm 0.03 \times 10^5$ Pa. The adhesion strength measured increased to $1.33 \pm 0.11 \times 10^5$ Pa and $1.13 \pm 0.067 \times 10^5$ Pa, respectively, for the day 2 barnacles. There was also no difference detected after 4 days' in culture (Tukey test, $p > 0.05$; Figure 5.6B).

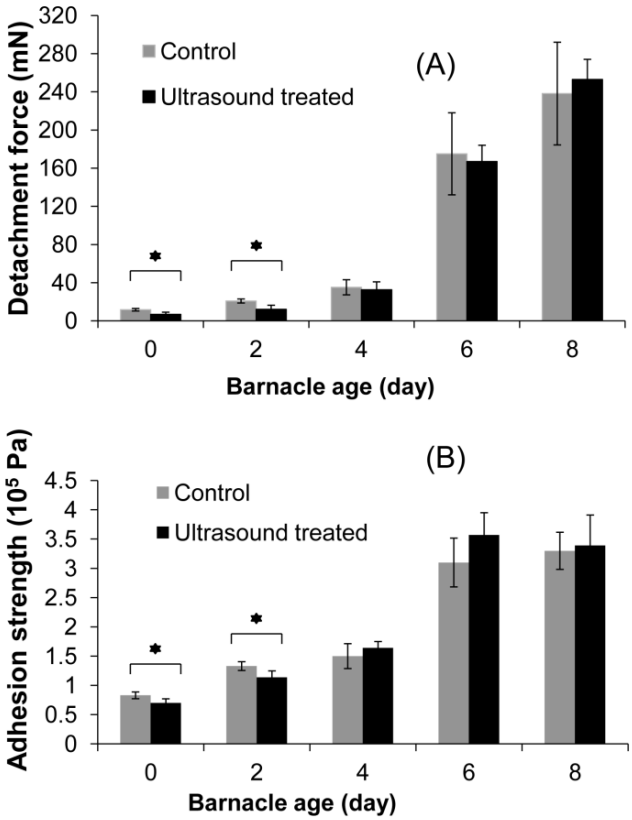

Figure 5.6. The detachment force and adhesion strength comparison of barnacles metamorphosed from control and ultrasound treated cyprids. The asterisks here represent statistically significant difference. The error bars here are standard errors.

The images of barnacles before and after pulling experiments were captured using microscope equiped with image capturing software. The dislogement areas were gentlly rinsed using distilled water and imaged after drying. Since no differences in surface failure modes were detected between ultrasound treated and control barnacles, only the images of control barnacles are shown in Figure 5.7. For the newly metamorphosed barnacles to the day 6 barnacles, the whole animals including the thin barnacle plates were completely removed, suggesting that the failure occurred between barnacle adhesive and the substrates. Therefore, the values measured could be regarded as the adhesion strength. However, for the day 8 barnacle, partial barnacle basal plates were still found to be attached on the surface after detachment. This may suggest that partial cohesive failure occurred within barnacles, which meant

that the adhesion strength between barnacle plates and surfaces exceeded the cohesion strength within the barnacle part. Therefore, the value measured could not be treated as the adhesion strength but take on a value lower than that.

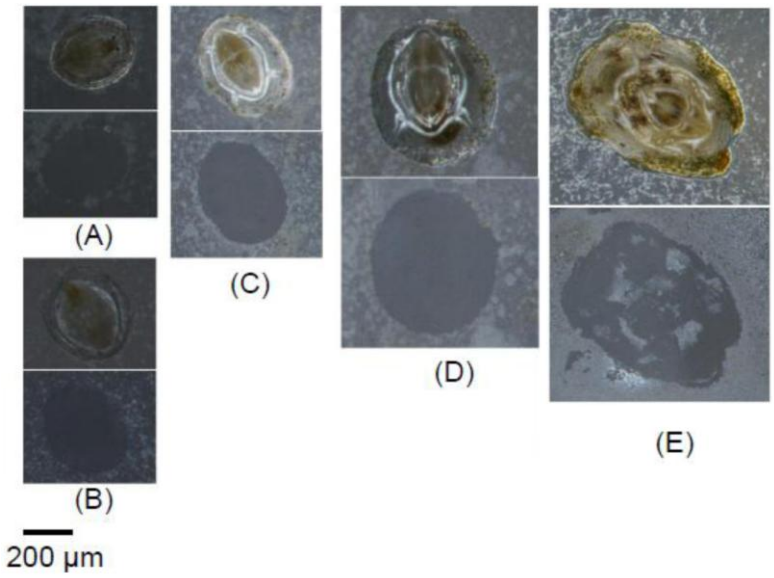

Figure 5.7. Microscopy images of surfaces after removal of different age barnacles. (A) is the image of day 0 barnacle, (B) is the image of day 2 barnacle, (C) is the image of day 4 barnacle, (D) is the image of day 6 barnacle and (E) is the image of day 8 barnacle.

5.4. Discussion

Cyprid settlement on silicone substrate was significantly inhibited with ultrasound treatment. The ability of ultrasound to prevent cyprid settlement has been previously reported (Guo et al. 2011a; Kitamura et al. 1995), and it has been shown that ultrasound intensity exceeding the ultrasound cavitation threshold could reduce cyprid settlement by cavitation generated forces (Guo et al. 2011b). In this study, we investigated how ultrasound may also induce biological changes in cyprid settlement.

The interaction of cyprid temparory adhesive protein with the explored surfaces was studied using AFM. It was observed that the FP morphology differed significantly between ultrasound treated and control cyprids (Figure 5.4). The area of FP from

ultrasound treated cyprids was larger than that of control cyprids. The thickness of FP, however, was half of that of control cyprids. Also, the estimated volume of FP was one third less than the FP from control cyprids. Different FP morphologies have also been observed when FP was deposited on different property surfaces (Phang et al. 2008), and this was explained that a highly charged bioadhesive can displace water and spread more easily on a hydrophobic surfaces. However, the possible reason for the larger area of FP from ultrasound treated cyprids could be the sliding of the antennules while in contact with the substrates, as a result of ultrasound exposure. It may also due to ultrasound induced lower viscosity of FPs, which needs further exporation using contact mode AFM testing. This result agreed with previous study of ultrasound on cyprid exploration behavior (Guo et al. 2011a), which found that cyprid would exhibit a more hesitated and unstable 'walking' after ultrasound treatment. Ultrasound cavitation generated forces could alter cyprid exploration behavior and consequently, affecting the FP secretion. The ability of ultrasound affecting protein secretion was also reported. In a study of ultrasound on photodynamic antimicrobial therapy, Ishibashi et al. (2010) found that ultrasound can reduce cell surface protein secretion; whereas Ruan et al. (2010) indicated that the exposure of ultrasound can enhance the adhesion protein secretion in mesenchymal stem.

The FP released on the explored surfaces from the paired attachment discs is used to adhere temporarily while 'walking' on the substrate (Walker 1987). In addition to serving as a temporary adhesive, FP also played the role as pheromone that induced settlement (Matsumura et al. 1998; Dreanno et al. 2006). As a result, substrates that were explored by previous cyprids were prone to attract more settlement (Clare et al. 1994). Barnacle settlement inducing protein complex (SIPC), a settlement pheromone, isolated from barnacle extract, has been demonstrated to induce gregarious settlement

of conspecific cyprids (Crisp and Meadows 1963; Clare and Matsumura 2000; Dreanno et al. 2006). Studies showed that SIPC exists in the FP protein deposited on the substrates during cyprid exploration (Matsumura et al. 1998; Dreanno et al. 2006), which may suggest the ability of FP to increase cyprid settlement. As observed in Figure 5.4, FP had a relatively larger spread area after ultrasound exposure. However, both density and volume of temparory adhesive protein were reduced. Since settlement can be increased by the presence of SIPC, the reduced settlement after ultrasound treatment may be attributed to lower concentration of temparory adhesive protein, as hypothesized by Phang et al. (2009), which suggested that the lower FP concentration on hydrophobic surface could lead to less settlement.

The barnacle detachment measurement was conducted using a Nano-tensile tester on different age barnacles and the surface failure modes were observed under microscope. The results concur with findings conducted by Berglin et al. (2001), for PMMA and PDMS substrates. In their study, the surface failure mode of newly metamorphosed barnacles appeared to be cohesive failure within barnacle base plate. That is the adhesion interaction between juvenile barnacle secreted adhesive and surface has exceeded the cohesive force within the barnacle part (Berglin et al. 2001). The present findings, conducted on the medical grade silicone substrates, showed that newly metamorphosed barnacles could be completely detached. These forces may be regarded as reflecting the juvenile barnacle adhesive strength. However, for the day 8 barnacle (Figure 5.7), after detachment, the surface failure mode transited from adhesive failure between barnacle adhesive and surface, to the cohesive failure within the barnacle base plate. Therefore, in this case, the forces measured for the older barnacles could not be regarded as barnacle adhesive forces, and this may explain why there is no force difference detected between barnacles from control and ultrasound treated cyrids.

The adhesion strength of the newly attached barnacles was affected by ultrasound. With the application of ultrasound on cyprids, the adhesion strength for newly metamorphosed barnacles was lower (0.7×10^5 Pa) than the adhesion strength of untreated control barnacles (0.83×10^5 Pa). However, this difference in adhesion strength diminished after 4 days' in culture, suggesting that the animals are able to recover from the treatment to secrete normal glues. Since ultrasound can reduce or enhance the protein secretion (Ishibashi et al. 2010; Ruan et al. 2010), it is probably that ultrasound may have reduced or delayed the secretion of juvenile barnacle cement. For the day 8 barnacle, the force measured could not be regarded as the adhesion strength as cohesive failure within barnacle base plate was detected (Figure 5.7). This might be explained that as barnacles grow; more cement is generated, which significantly enhance the ability of attachment. Reduced adhesion strength may alter the settlement and recruitment of marine organisms on to surfaces, and it has been reported that marine organisms prefer to settle on sites with minimal possibility of removal (Aldred et al. 2010; Carl et al. 2012). This appears some consistence with our results, which found ultrasound treated cyprids demonstrated a lower settlement and the adhesion strength of the metamorphosed barnacles were also samller than the control barnacles.

The ability of ultrasound to reduce cyprid settlement as well as to reduce the adhesion of juvenile barnacles may be useful for enhancing the performance of fouling release coatings to prevent fouling. The hydrodynamic forces imposed by a vessel moving through the water is usually sufficient to remove any hard fouling adhering to fouling release coatings. However, these surfaces are highly susceptible to fouling when the vessels are moving slowly. We have demonstrated that ultrasound can reduce cyprid settlement, as well as reduce the adhesion strength of recently settled barnacles. It seems plausible then that ultrasound may be useful to enhance the performance of

fouling release coatings by offering protection during periods of low movement. A combination of antifouling strategy consisting of ultrasound method and fouling release coatings may provide a more effective and economical strategy to reduce barnacle based marine biofouling.

5.5. Conclusion for chapter 5

In this chapter, we demonstrated that juvenile barnacle metamorphosed from ultrasound treated cyprids initially produce weaker glues on settlement, and this difference persists for up to 4 days. Our results also indicate that ultrasound exposure alter the cyprid FP secretion. Applied in combination with fouling release coatings, the results suggests that ultrasound may potentially be used to enhance antifouling performance of fouling release coatings.

Chapter 6. The effect of cavitation bubbles on the removal of juvenile barnacles

In this chapter, the effect of cavitation bubbles on the removal of juvenile barnacles was investigated using high speed photography. Using spark generated bubbles, the interaction between barnacle and cavitation bubble was examined in detail. The liquid jet generated by the bubble collapse was observed to be directed towards barnacle at different impact intensities, which is related to the dimensionless distance H' (H'= H/R_m), where H is the distance between bubble formation point and the top of barnacle, and R_m is the maximum bubble radius. At lower values of H', higher speed liquid jet was produced; consequently a larger impact pressure was generated. In general, barnacles are more easily removed at younger stages. In older barnacles, the liquid jet impact was only able to remove the barnacle shells, leaving the base plate attached to the surface. This study indicates that cavitation can be used to remove attached barnacles, and it would be more efficient if it is applied during early stages of fouling, before the formation of hard calcareous structures.

6.1. Introduction

In the previous chapters, the effects of ultrasound on barnacle cyprids were extensively studied, however, it is difficult to ensure total prevention of barnacle attachment. And the problem may still exist due to barnacles' rapid propagation and gregarious nature. Therefore, cleaning or removal of the attached barnacles is also considered important on barnacle fouling control. Different methods of removal of the attached hard foulers, such as barnacles, have been introduced to enhance performance of antifouling coatings. Chemical methods such as acid cleaning solution have been used for cleaning barnacle fouled surfaces (Dolez and Love 2002). However, the strong corrosive nature of acid mixtures is hazardous for handling and results in toxic discharges. While systems such as Ecospeed® focus on aggressive hull cleaning, gentle hull grooming methods are being developed to maintain foul-release coatings (Tribou and Swain 2010; Ralston and Swain 2009). This is beneficial for ships that spend long time in port or for slower moving vessels, and is compatible with existing technologies. However, the deployment of machinery and operators may damage the coating, and if it is applied to antifouling coatings, may release undesirable amounts of biocide. Cavitating water jet technology may provide an attractive and environmentally safe alternative to mechanical grooming. This approach assumes that the energy from the collapse of a bubble generated under pressure over a tiny area will result in localised shear stress, which may be directed to remove fouling. This phenomenon is related to the generation of water hammer pressure, i.e., pressure caused by a rapid change in fluid velocity in a given physical system (Ghidaoui et al. 2005). Cavitation induced liquid jet has been shown to detach the bacteria, clean surface dirt and remove biofouling films (Mason et al. 1996; Bayoudh et al. 2005; Mason et al. 2003).

In our earlier work, we explored the use of ultrasound as a means for controlling barnacle cyprid settlement (guo et al. 2011b; Seth et al. 2010). Although ultrasound induced cavitation may induce larval mortality, no evidence has been presented thus far to demonstrate directly the effect of cavitation bubbles on the organisms. In this chapter, we investigate the effect of ultrasound and spark generated bubble jet on the attached barnacles. A liquid jet impact was created by a single spark generated bubble in a controlled manner close to a hard boundary (Badarinath et al. 2011; Shrestha et al. 2009). The interaction between ultrasonic cavitation bubbles and barnacles was investigated. A spark generated bubble was created to study the dynamic behavior of a single bubble within a free field and near a surface boundary. The process of interaction between a single bubble and a barnacle subject was documented using high speed camera. By varying the distance between bubble initial position and the top of barnacle, the threshold distance for barnacle damage was estimated, enabling the calculation of the threshold pressure for barnacle removal. Finally, barnacle removal efficiency was examined for barnacles of different sizes.

6.2. Materials and methods

6.2.1. Barnacle culture

Larvae of barnacle *Amphibalanus amphitrite* were reared at 26°C, fed with an algal mixture of 1:1 v/v of Tetraselmis suecica and Chaetoceros muelleri at a density of approximately 5x105 cells/ml (Rittschof et al. 2003). Barnacle larvae metamorphosed to cyprids within 5-7 days. And the cyprids were then transferred to settle on glass slides at 26°C. Seawater and algae were replaced every two days to ensure an adequate food supply. In the experiments, barnacles cultured for up to 20 days were tested. Adult barnacles were reared on a diet of brine shrimp and mixed algae.

6.2.2. Ultrasonic experimental setup

The schematic of ultrasonic experimental setup is shown in Figure 6.1. A transparent glass water tank, with size of 180 mm × 190 mm × 200 mm, was used for the experiment. The tank was filled with clean tap water up to a height of about 140 mm. A sinusoidal wave from the function generator (Agilent 33210A, USA) was magnified using the power amplifier (HSA4051, Japan), which was used to drive the ultrasound transducer (Fuji ceramics, Japan). Barnacles settled on the glass substrates were placed directly facing the transducer. The working frequency of this transducer was set at 27 kHz and the ultrasonic signal was picked by the hydrophone (Bruel & Kjear Ltd., Type 8103, Denmark). To avoid possible cavitation induced damage to the hydrophone, the signal was recorded at a distance away from the cavitation concentration area and the pressure measured was recorded at 50 kPa. The ultrasound signal was digitalized and analyzed with the software LABVIEW (N.I. Ltd., USA).

A high speed camera (Photron Fastcam–APX Ultima Imager) was used to record the interaction between bubbles and barnacles. A continuous light source (MLDS250–Iwasaki Electric Co. Ltd) was placed behind the setup for illuminating purpose and a tracing paper was used to ensure the evenness of light intensity. In the ultrasound experiments, two groups of barnacles were used: the first set consisted of newly metamorphosed barnacles (day 0) of 0.38±0.06 mm in base plate diameter, and the other set consisted of 10-day old barnacles of 2.30±0.13 mm diameter. The experiments were repeated four times and the measurement uncertainties reported in this paper are given as standard errors.

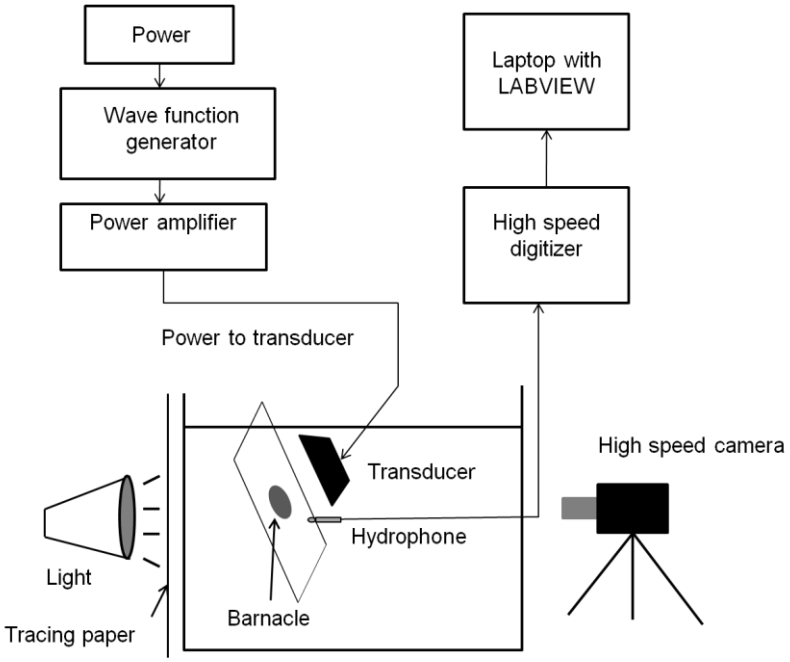

Figure 6.1. The schematic of ultrasonic experimental setup.

6.2.3. Experimental setup for the spark generated bubbles

The schematic of the experimental setup is shown in Figure 6.2. The same tank as ultrasonic experiment in Figure 6.1 was used and was filled with tap water having a height of 140 mm. To produce the spark-generated bubbles, a electric circuit was used, which comprised of a DC supply, a 1KΩ resistor, a capacitor of 4700 μF, a two way switch and a pair of crossed electrodes (100 μm in diameter). The capacitor was first charged to a pre-determined voltage with the resistor in the circuit. Then the circuit was shorted with the two-way switch. A spark was subsequently generated and a bubble comprising of gas and vapor was produced. To study the bubble dynamics in free-field, the crossed electrodes were adjusted to be at a distance of least 10 times the maximum of the bubble radius away from the tank walls or other free surfaces to reduce the effect on bubble dynamics. In the absence of boundary effect, the bubble would oscillate spherically and it was considered as free-field bubble. To study the bubble-barnacle interaction process, juvenile barnacle that settled on the glass slide

was placed vertically below the electrode crossing point (Figure 6.2). A high speed camera (Photron Fastcam-APX Ultima Imager) was used to capture bubble dynamics and bubble-barnacle interaction. A light source was also used for illumination. The images were calibrated using a ruler which was imaged at the focal point of the camera, and was used for subsequent data analysis.

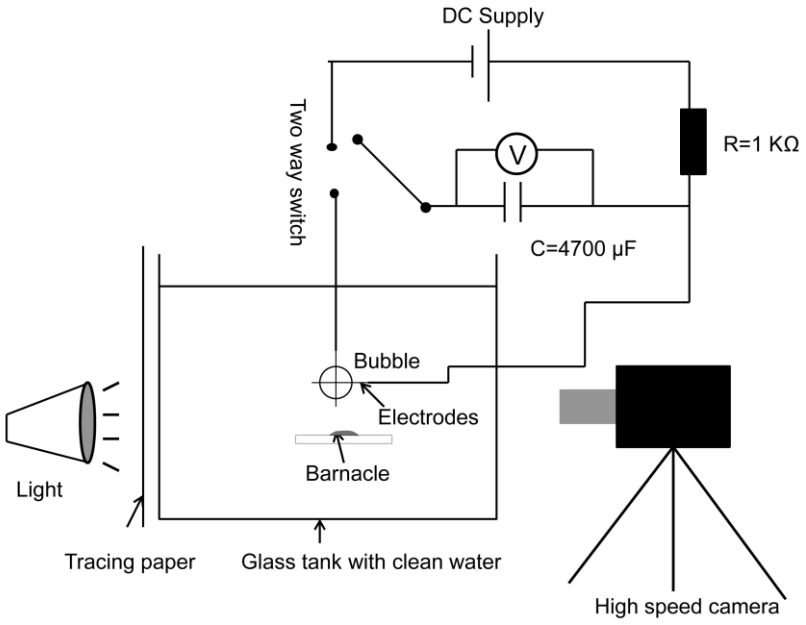

Figure 6.2. Experimental setup of spark generated bubbles on barnacles

To have a better view of bubble-barnacle interaction, a small modification was made on the setup which is shown in Figure 6.3. The surface with the settled barnacles was not placed vertically facing the camera but with a tilted angle of 45^{o}. In this arrangement the interaction between liquid jets and barnacles can be viewed. The electrodes crossing point was adjusted towards the barnacles on the surface. As such, the bubble was created perpendicular to the position of the barnacles on the plate.

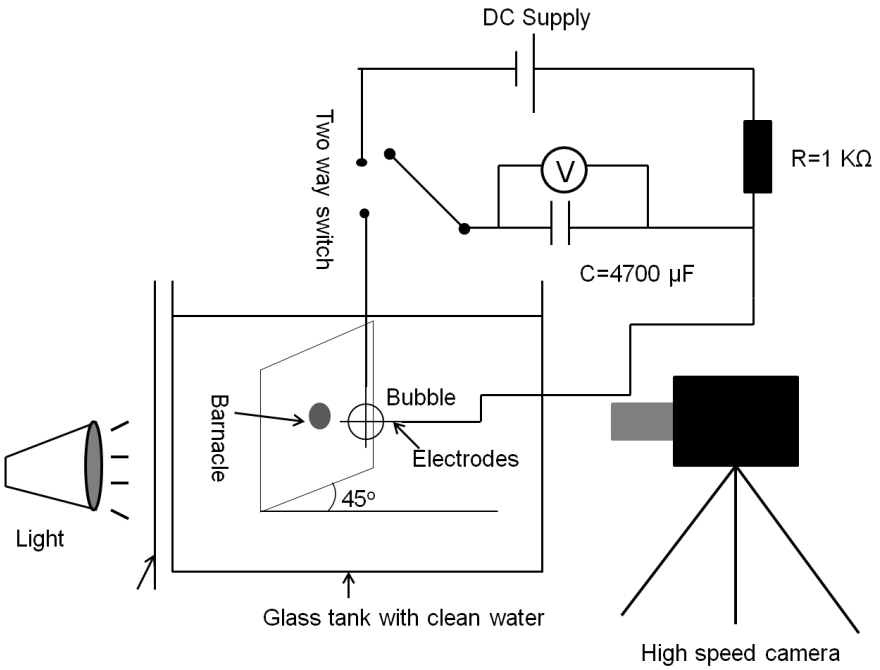

Figure 6.3. The experimental setup for the observation of bubble-barnacle interaction. Slide where barnacles settled was not vertically faced camera but with a tilt angle of 45^{o} to have a clear view of bubble-barnacle interaction. The bubble created impinged directly towards the barnacle.

6.3. Results

6.3.1. Results of ultrasonic cavitation

The spectrum of ultrasound signal was analyzed using LABVIEW 2009 and is shown in Figure 6.4. In the spectrum, not only the driving frequency of 27 kHz, sub-harmonics and ultra-harmonics were detected as well. The presence of sub-harmonics and ultra-harmonics suggests that at the acoustic pressure of 50 kPa, ultrasonic cavitation has occurred (Avvaru and Pandit 2009; Frohly et al. 2000).

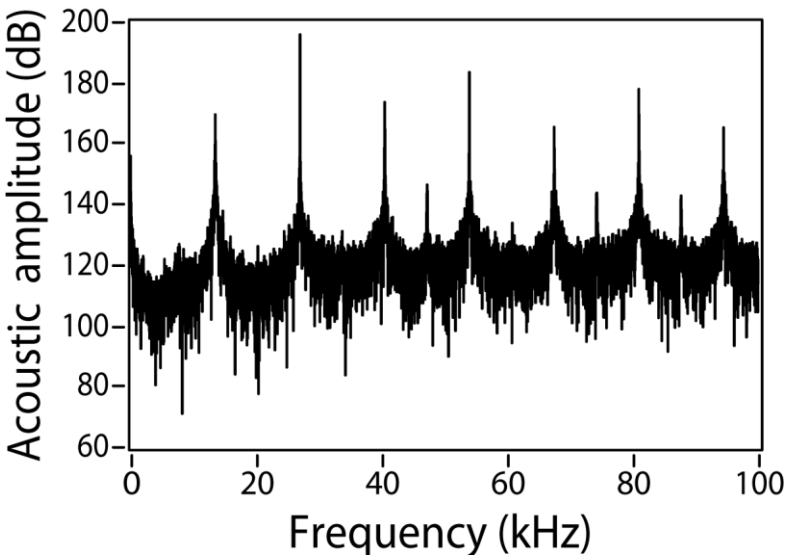

Figure 6.4. The power spectrum density analysis of ultrasound signal. The driving frequency was 27 kHz and the acoustic pressure was 50 kPa.

As the newly metamorphosed (day 0) barnacles were very small (0.38±0.06 μm base plate diameter), they were not clearly captured by the camera, and the interaction process between bubble-barnacle could only be deduced from post-treatment condition of the animals. The condition of the barnacles before and after ultrasound exposure is given in Figure 6.5. At this stage, the shells of barnacles are relatively fragile which can be damaged by the ultrasonic cavitation induced liquid jet. As it is shown, part of the barnacle shells were damaged after 30 s exposure (Figure 6.5A); most of the shells were damaged after 60 s exposure (Figure 6.5B), and the shells were completely removed after 150 s exposure (Figure 6.5C). The pressure for inducing such damage was not directly measured and was larger than the value of 50 kPa as indicated by the hydrophone.

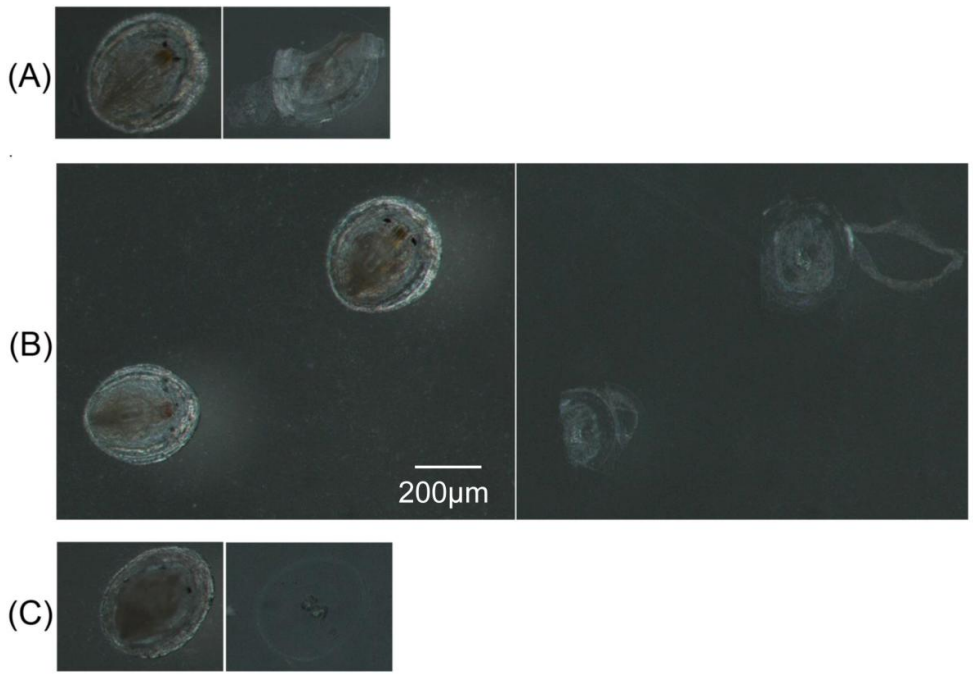

Figure 6.5. Effect of ultrasound cavitation on day 0 barnacles. (A) is the image comparison after 30 s' exposure; (B) is the image comparison after 60 s' exposure; (C) is the image comparison after 150 s' exposure. The scale bar applies for all barnacles.

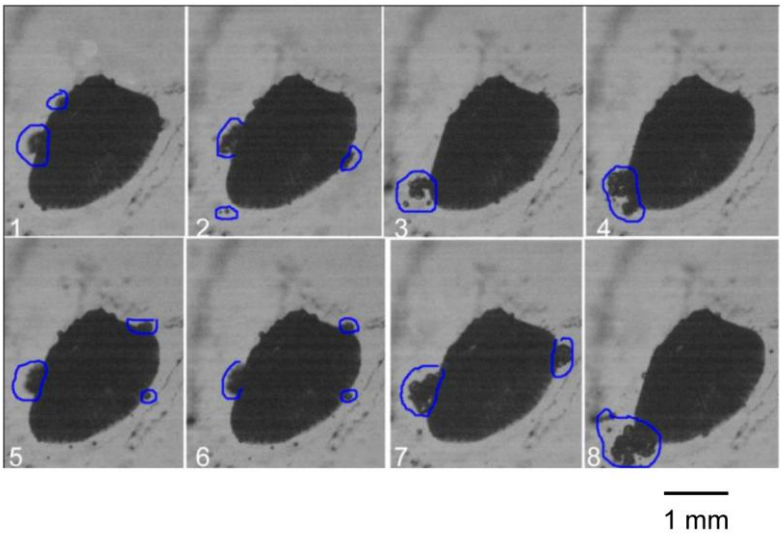

Figure 6.6. Ultrasonic cavitation bubbles impingement on 10-day old barnacles. Bubble clusters were marked with blue circles and were observed impacting barnacle randomly. The frame rate was set at 20000 frames/s. The barnacle was measured with the length of 2.73 mm.

The images of bubble-barnacle interaction on 10-day old barnacles are shown in Figure 6.6. It was observed that cavitation bubbles were generated in the form of clouds and impinged on the barnacles in a rather random or unpredicted manner with an associated high speed. However, at the same acoustic intensity imposed on newly metamorphosed barnacles, these micro bubbles did not appear to cause any immediate visible damage. However, the barnacles were found dead the next day with no observation of the usual "catching feed" behavior, which refers to barnacle beating their feathery appendages rhythmically to draw in plankton and detritus.

6.3.2. Results of spark generated bubbles

6.3.2.1. Relation between bubble size and voltage

A positive correlation was observed between the input voltage and bubble size. With higher voltage, the generated bubbles were larger; but this relationship was not linear (Figure 6.7). Strictly, any size of (non-equilibrium) bubble may be chosen as long as the impact due to the bubble collapse is sufficient to destroy/dislodge the barnacles. A smaller size bubble, however, enables easier visualization of the impact process which may be blocked by the larger bubble. However, excessively smaller bubbles give rise to a much lower impact intensity which may not be of sufficient strength to have any effect on the barnacles. Therefore, a suitable sized bubble had to be chosen for the analysis. After some preliminary tests, an effective voltage of 36V was selected, which generated a (maximum) bubble radius of 1.8 ± 0.2mm.

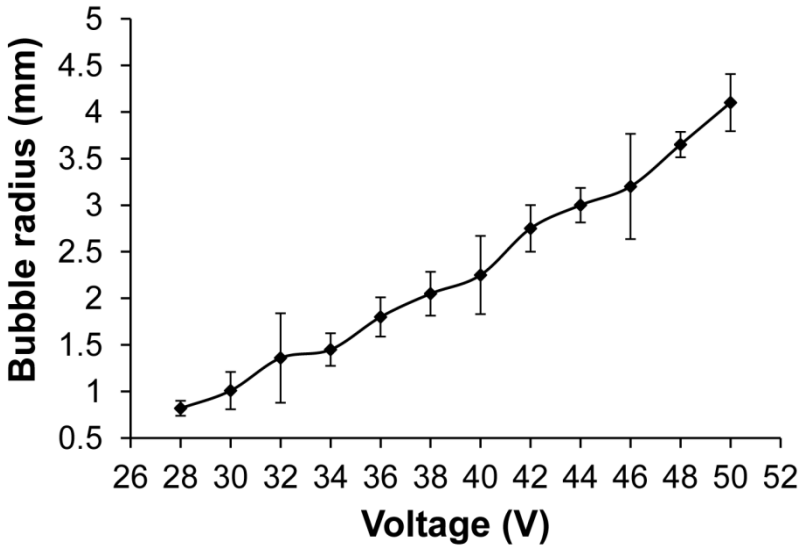

Figure 6.7. The relationship between free-field maximum bubble radius and voltage. Six repeats for each voltage were conducted and the error bars are standard errors.

6.3.2.2. Bubble dynamics in the free field

In all experiments, the time was set to 0 at the moment when the spark was firstly generated. In the first frames after spark generation, the bubble radius could only be recorded with some uncertainty, as compared to those clearly depicted after several frames later. A typical bubble radius in the free field as a function time is shown in Figure 6.8. The bubble rebounded (or re-expanded) a second time after reaching its minimum size. The first expansion and collapse phase was slightly non-symmetric and the collapse phase was found faster than the expansion phase. The bubble would lose most of its energy during the first expansion and collapse phase, and this was evident from the subsequent much smaller maximum bubble size (Figure 6.8).

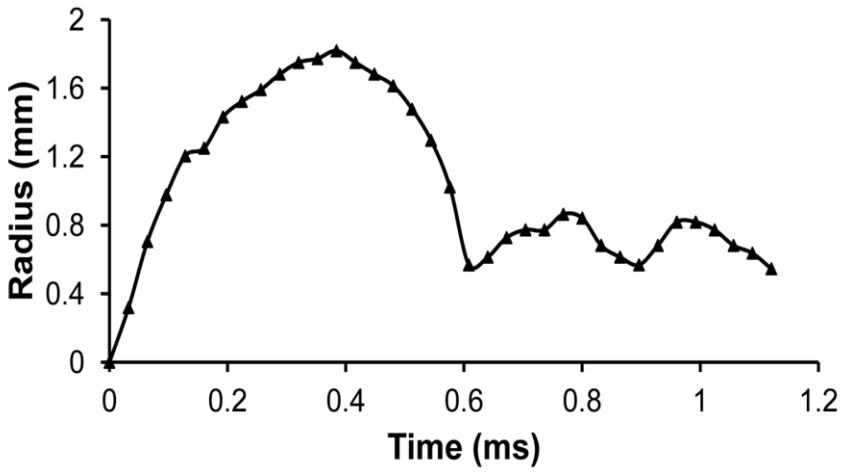

Figure 6.8. Radius (R)–time (t) plot for a typical bubble in a free field. The maximum bubble radius is 1.8 mm.

6.3.2.3. Bubble dynamic behavior near a rigid boundary

In free field, the bubble oscillates, accompanied with energy dissipation. However, when the bubble is generated close to a hard boundary, a very different behavior is produced. As the bubble collapses near a boundary, there is a formation of liquid jet within the bubble. For such a phenomenon to occur, the distance between bubble formation point and the boundary (H) must be comparable to the maximum bubble radius Rm. A dimensionless distance $H'=H/R_m$ was used to define the distance. During the collapse phase, a phenomenon not observed in the free field appears: a liquid jet originated from the far side of the bubble surface picks up speed and traverses across the main bubble body. This jet then makes impact on the side of bubble surface nearest to the wall. At the same time the bubble as a whole moves towards the plate.

The collapse process of a single spark-generated bubble near a boundary is shown in Figure 6.9. The camera was filmed at 31000 FPS. The maximum bubble radius R_m was 1.9 mm and H' was 1.26. The bubble expanded almost spherically in the first

stage and reached the maximum radius of 1.9 mm at the time of 0.45 ms (Frame 15). As the bubble collapsed, it moved towards the boundary as a result of translational motion induced in the final stage of the collapse. At this point, a liquid jet originating from the far side of the bubble surface penetrated the lower surface of the bubble that was nearest to the surface and collided with the boundary (Frame 28-31). The jet then turned outwards in a radial flow (Frame 40).

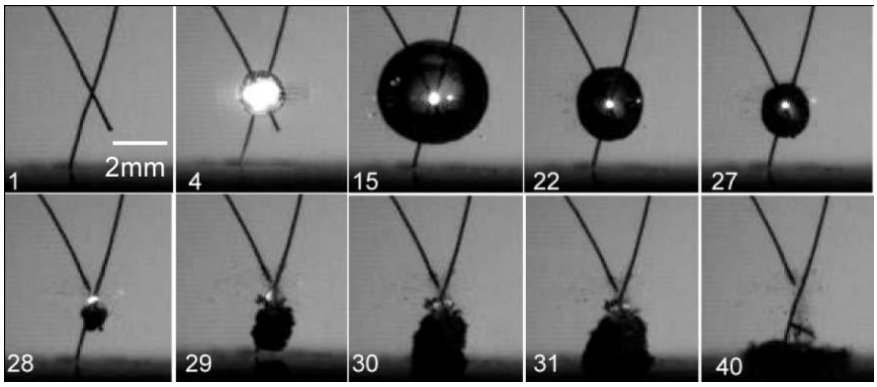

Figure 6.9. Experimental result of the collapse phase of a spark generated bubble jetting towards the glass slide at the bottom. The bubble was initiated about 4.94 mm away from the slide. Frames were numbered in chronological order. The camera was set at 31000 FPS. The bubble was initialized at frame 1 corresponding to the time of 0ms.The maximum bubble radius was obtained at t =0.45 ms (Frame 15). The collapsing bubble induced a jet towards the bottom wall.

6.3.2.4. The interaction of bubble-barnacle with various H'

In this section, by varying H', the bubble-barnacle interaction was explored using 10-day old barnacles (2.3±0.13 mm in length). The dimensionless H' is defined as the ratio of the distance between bubble formation point and the top of barnacle (H) to the maximum bubble radius Rm. The controlled H' for the series studies was set at: 2.00±0.11, 1.25±0.08, 1.00±0.03, 0.75±0.067 and 0.50±0.02, and the interaction process were recorded with the camera operating at 37500 FPS. In each experiment, a fresh barnacle was used. In the following, representative results at the above mentioned five different H' were provided.

(1). Bubble-barnacle interaction at H'=2

The interaction process of bubble-barnacle is shown in Figure 6.10. The bubble reached its maximum radius of 1.8 mm at Frame 12 (0.293 ms). Subsequently, the jet was formed and impinged on the top of barnacle at Frame 46 (1.2 ms). However, due to the relatively long distance of bubble initial point and barnacle, the jet velocity was reduced significantly when the impact occurred. As such, there appeared no observable difference on the barnacles as they were still alive the next day after the impingement.

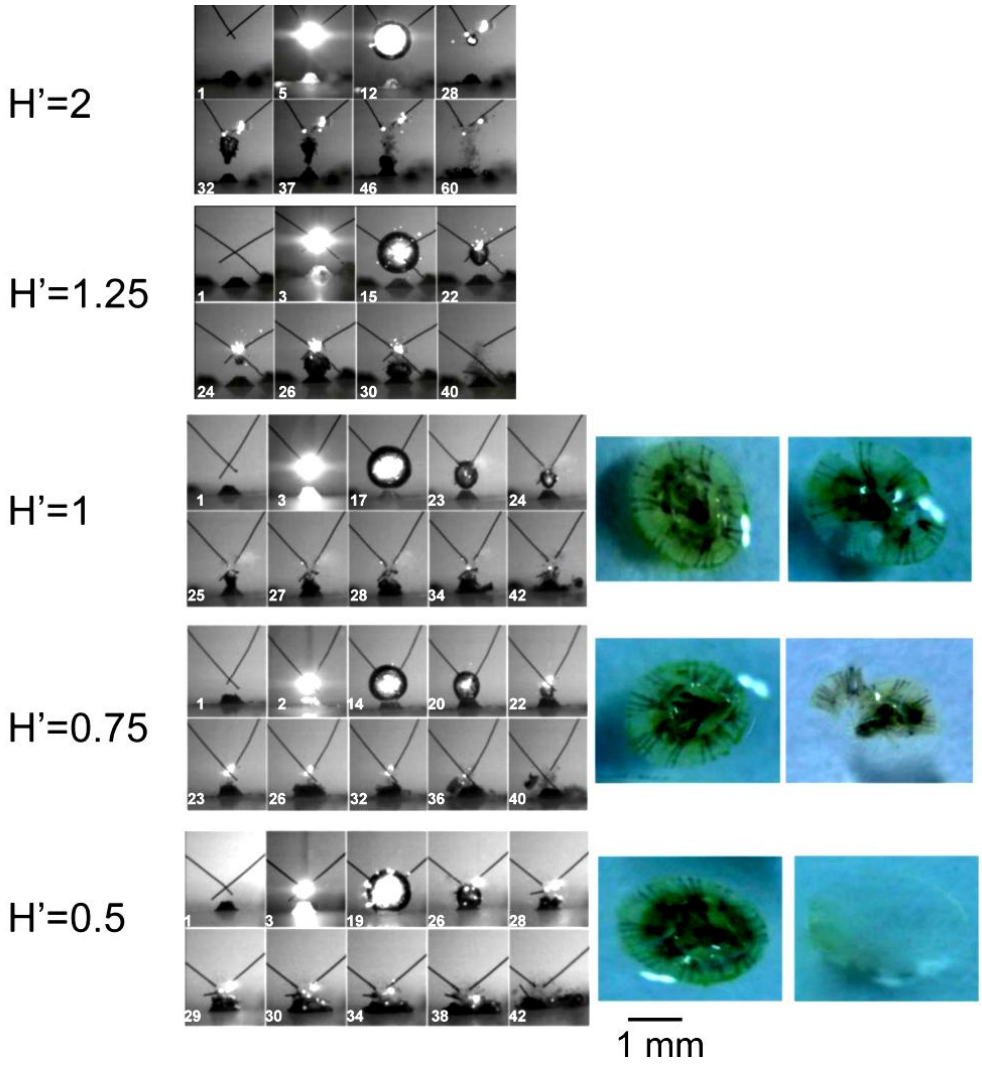

Figure 6.10. The collapse phases of spark generated bubbles impinged on 10-day old barnacles with various H'. The frame rate was set at 37500 FPS. The bubbles were controlled with maximum radius of 1.8 mm approximately. The bubble was initialized at Frame 1 corresponding to the time of 0 ms, and the frames were numbered in chronological order for each case. Barnacle images were compared before and after the experiment with the spark generated bubble.

(2). Bubble-barnacle interaction at H'=1.25

The dimensionless distance H' was adjusted to 1.25±0.08 and the experiments were conducted on different barnacles. The bubble reached its maximum size at Frame 15 (0.373 ms) and impact on the barnacle occurred at Frame 26 (0.67 ms). The impact velocity on the barnacle was increased; however, the impact still generated no

apparent effect on the barnacle, which remained intact and was observed alive on the next day.

(3). Bubble-barnacle interaction at H'=1

When the experiments were conducted on the barnacles with H'=1, the phenomenon observed changed drastically. The bubble reached its maximum size at Frame 17 (0.43 ms) with the radius of 1.8 mm, and the bubble just about made contact with the top of barnacle. The liquid jet impinged on the barnacle at Frame 25 (0.64 ms) and the impact was observed to be more violent. Parts of the barnacle shell were observed to break off as depicted at Frame 42.

(4). Bubble-barnacle interaction at H'=0.75 and H'=0.5

When the distance was adjusted to H'=0.75, the maximum bubble size was reached at Frame 14 (0.35 ms). The bubble touched the top of barnacle and appeared to be flattened at the bottom section (Frame 14). As the bubble was not spherically symmetric, the radius was measured horizontally with the radius of 1.76 mm. The bubble then collapsed and the jet impinged on the barnacle at Frame 22. The impact of liquid jet was found to be very violent as numerous parts of the barnacle shell were found to have broken off from the barnacle (Frame 36 and 40).

When the distance was further decreased to H'=0.5, similar phenomenon as at H'=0.75 was found. Bubble reached its maximum radius at Frame 19 (0.48 ms) and impinged on the barnacle at Frame 29. The liquid jet impact was so much stronger such that practically all the barnacle shell was removed after the impingement.

6.3.2.5. Impact pressure estimation

The jet impact velocity and high-pressure pulse resulting from the jet impact can be estimated from images of high speed photography (Tomita and Shima 1986). According to the images of high speed photography, the distance that the front part of the liquid jet travelled and the time taken can be precisely measured. Therefore, the averaged velocity can be calculated. Since the direct measurement of impact velocity was technically difficult, for the present study, we used the averaged velocity as equivalent to the impact velocity.

An example to estimate impact velocity is given in Figure 6.11 for H'=2. The distance between the front part of the liquid jet and the top of barnacle was measured at 0.27 mm, and the time taken for the two sequential images was 5.3×10^{-2} ms, therefore, the averaged velocity was 5.1 m/s, which was used to estimate the impact velocity. A similar impact velocity at H'=2 was also described in Lew et al. (2007). In the same manner, the impact velocity at H'=1.25 and H'=1 were estimated at 9.25, and 12.4 m/s, respectively. For the dimensionless distances of 0.75 and 0.5, the maximum bubble size was found to be already in contact with barnacle, and hence the distance used to estimate the impact velocity could not be determined with any reasonable level of accuracy. It was however evident that when H' decreases from 2 to 1, the velocity rises monotonically.

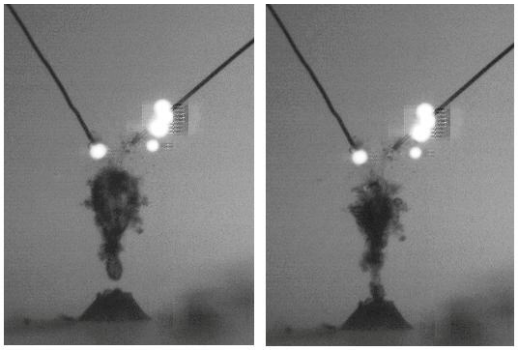

Figure 6.11. Impact velocity estimation at H'=2. The distance between front part of liquid jet and top of barnacle is measured at 2.7 mm, and the time taken to travel this distance is 5.3×10^{-2}ms.

The impact pressure due to liquid jet is similar to the water-hammer pressure induced by an impacting liquid jet which can be readily expressed as described in Tomita and Shima (1986) as:

$$P_{jet}= \rho cv \qquad (1)$$

where ρ is the density of water, c is the velocity of sound in water, and v is the liquid jet impact velocity.

Based on the velocities estimated, the impact pressures at H' of 2.00 ± 0.11, 1.25 ± 0.08, 1.00 ± 0.03 were next estimated at 7.64 ± 0.67, 13.9 ± 1.18 and 18.6 ± 2.04 MPa, respectively.

From the results shown in Figure 6.10, with the bubble size of R_m=1.8mm, H'=1 could be reckoned as the threshold distance for substantial barnacle damage. The impact pressure of 18.6 MPa at H'=1 can be considered as the threshold pressure to damage or removal of the 10 day old barnacles.

Another close-up detail and perhaps a better view of bubble-barnacle interaction is shown in Figure 6.12 with the experimental setup of Figure 6.3. The camera was operated at 8400 FPS and the experiments were conducted on the 10-day old barnacles. The dimensionless height H' was measured with values of 1.25±0.17, 0.68 ±0.087 and 0.5 ±0.039, representing nominally, far, medium and close distances. The interaction between liquid jets and barnacles is clearly seen. For the far distance (H'=1.25), the impact was not quite so strong and the barnacle remained intact after the impingement (Figure 6.12A). When H' was reduced to 0.68, the jet impact became very intense and the barnacle shells were partially removed (Figure 6.12B). When H' was further adjusted to 0.5, the impact pressure was so strong that the whole barnacle shell was removed (Figure 6.12C). The results are consistent with the images shown in Figure 6.10. For the 10-day old barnacle, although the shells can be removed, the barnacle basal plate was still attached on the surfaces.

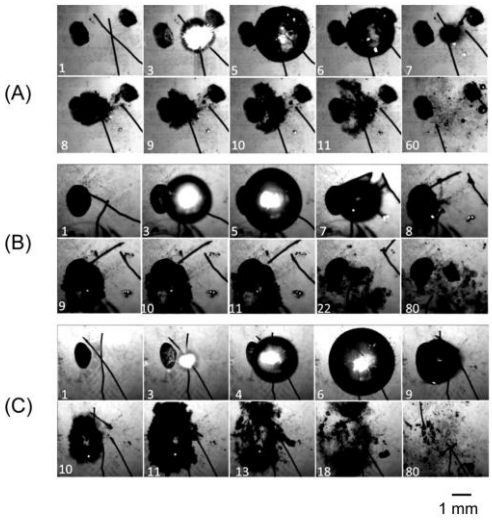

Figure 6.12. Interaction of bubble-barnacle with H' of 1.25, 0.68 and 0.5. (A) are the image sequences with H' at 1.25; (B) are the image sequences with H' at 0.68 and (C) are the image sequences with H' at 0.5, respectively. The bubbles were initialized at Frame 1 corresponding to time of 0, and the frames are numbered in chronological order.

6.3.2.6. Age comparison

To study barnacle age on the removal efficiency, barnacles with ages of 0, 10, and 20 days were used. These barnacles had base plate size of 0.38±0.06, 2.30±0.13, and 3.10±0.27 mm in length, respectively. In keeping to an H' value of 0.5, bubbles with maximum radius of 1.00 ± 0.06, 1.8±0.2, and 2.8±0.3 mm were applied, respectively. The camera was set at 8400 FPS. With the same H' of 0.5, the impact generated by the liquid jet successfully removed all the attached barnacles (Figure 6.13). However, the barnacle cement was still attached on the surfaces after removal of the 10 and 20 day old barnacles (Figure 6.13B and C)). For the day 0 barnacle, the whole barnacle can be completely removed (Figure6.13A, Frame 10).

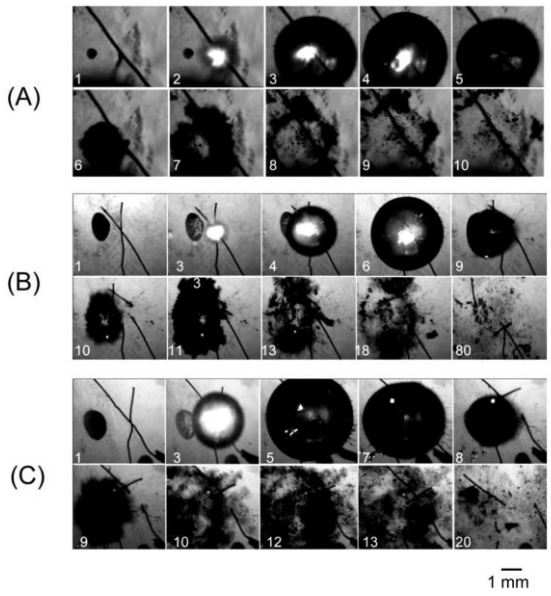

Figure 6.13. Bubble-barnacle interaction comparison among different age barnacles. For (A), the images were magnified 2 times for the visibility of the day 0 barnacles; (B) are the images of bubble interaction with 10-day old barnacles; (C) are the images of bubble interaction with 20-day old barnacles. The bubbles were initialized at Frame 1 corresponding to time of 0, and the frames are numbered in chronological order.

6.4. Discussion

The effect of cavitation bubbles on juvenile barnacles was investigated and the mechanism of the cavitation impacts was described in detail. The injury induced by ultrasonic cavitation bubbles on juvenile barnacles was verified by the visible presence of bubble clusters impinging on the barnacle shells, as recorded by the high speed camera. Broken shells and mortality of the juvenile barnacles were detected after ultrasound exposure, and these results were consistent with previously reported barnacle cyprid and naupliar mortality (Guo et al. 2011a; Guo et al. 2011b; Seth et al. 2010). While ultrasonic cavitation may generate forces by liquid jet, micro-streaming and shock waves may also induce biological damage. However, it is generally understood that cavitation damage is predominantly caused by impulsive pressure produced from collapsing bubbles (Bremond et al. 2006; Liu et al. 2009; Palanker et al. 2003). This is because ultrasonic cavitation induced bubbles collapse near a solid wall, whilst the microjets pass across the cavity, and penetrated into the lower surface and impinged on the boundary (Lew et al. 2007; Bai et al. 2008). The high speed jets impinged on the hard boundary with high pressure. The cavitation produced liquid jet impinged on the surface have been used to detach bacteria and biofilms (Mason et al. 2003; Parini et al. 2005).

In practice, ultrasonic cavitation bubbles were often observed in "clouds" in which bubble/bubble interaction and bubble deformation effects occur at the same time (Wójs et al. 2006); see also Figure 6.6. Just exactly how the liquid jets impinge and damage the barnacles remains unknown. Therefore, to have a better understanding of cavitation bubble interaction with barnacle, the single spark-generated bubble was introduced. When a bubble is generated close to a substrate, i.e., a small H' ($H'=H/R_m$), the liquid jet produced will impact the rigid boundary. The jet impact pressure is greatly affected by H' (Lew et al. 2007; Tomita and Shima 1986). The

smaller the H' is, the larger the impact generates. The impact pressure, which was also discussed earlier, can be quantified as water hammer pressure, and is positively correlated with the jet velocity. There is a threshold distance that caused the 10-day old barnacle to sustain some injuries (see Figure 6.10). With essentially the same bubble size, the liquid jet generated no apparent damage on the barnacle shell with H'>1. When H'≤1, the liquid jet damaged the barnacle shell and it completely removed the attached barnacles when H'≤ 0.5.

The liquid jet impact is considered as a dominant factor in cavitation damage, although the shear force is also generated by the radial flow accompanied by the jet impact the surface. The jet behavior has been studied by many investigators (Badarinath et al. 2011; Tomita and Shima 1986). The liquid jet impact has been shown to be capable of removing bacteria and biofilms (Mason et al. 2003; Parini et al. 2005). There is also an example of the use of cavitating jets in the biological world. Marine animals such as the Mantis shrimp are known to fracture their prey's shell using cavitation generated jet impact with a brief, yet powerful strike of their raptorial appendages (Patek and Caldwell et al. 2005). However, no reports have shown how the jet interacts with the targeted organisms. In our study, the interaction of bubble-barnacle was explicitly investigated and the water hammer pressure was estimated. The pressures at H'=2, H'=1.25 and H'=1 were estimated at 7.64, 13.9 and 18.6 MPa, respectively. However, only the pressure exceeded 18.6 MPa showed ability to damage the shell of the attached 10-day old barnacles. Adult barnacles use calcium carbonate to form their exoskeletons, and the hardness and elastic modulus values of the shell fall within a range of approximately 2-3 and 50-70 GPa, respectively (Pérez et al. 2008; Swift 2012).

The value of 18.6 MPa is much lower than the strength of adult barnacle shell, however, it can damage the shell of 10-day old juvenile barnacles, which was only partially calcified and relative fragile. The microjet formed during cavitation bubble collapse is affected by the property of the surface against which it is collapsing. "Softer" surfaces lead to less violent collapse and less erosivity (Kalumuck et al. 1995). This may provide a possible mechanism for cavitating jets to remove marine fouling without damaging the softer paint. Also, the hardness of modulus values of the polymer coatings were investigated to be within the range of approximately 0.3-0.6 and 3-7 GPa, respectively (Gu et al. 2004). And the hardness of plasma modified polycarbonate and PDMS/polycarbonate system fall within a range of approximately 0.2-0.6 GPa (Breake et al. 2002). These values were far beyond the 16.8 MPa value that could damage the shells of 10-day barnacles; therefore, the damage of the jet to the antifouling coating may not be a problem. Also, to remove barnacles younger than 10-days old, much less impact will be required and the danger to the coating will be significantly reduced.

Barnacles of different ages interact with bubbles differently. For day 0 barnacles, with the same H'=0.5, bubble of relatively smaller dimension was sufficient to completely remove the attached barnacles. On the other hand, much more energy was required to dislodge the older barnacles. Whist the shell of the older barnacle can be removed with higher input energy in the form of a larger single bubble, it was observed that the barnacle cement was still attached on the surface, thereby indicating that the forces generated by bubble cavitation are insufficient to cause delamination. Beyond aesthetics, the presence of this residual cement serves as a settlement pheromone, resulting in further gregarious settlement of more barnacles (Clare and

Matsumura et al. 2000). Thus, for effective application, “bubble-cleaning” would be best applied to fouling at an early stage.

6.5. Conclusion for chapter 6

The interaction of cavitation bubbles and barnacles was investigated using high speed photography. Ultrasonic cavitation induced liquid jet was shown to damage the barnacle shell and remove the newly attached barnacles. Using spark generated bubbles, the interaction between bubbles and barnacle was observed in detail. Bubbles generated close to a barnacle form a liquid jet that impinges on the attached barnacle. The impact intensity was dependent on the dimensionless parameter H’: the smaller the value of H’, the stronger the impact intensity generated. In general, the barnacle is more easily and completely removed at a younger stage. In older barnacles, the liquid jet impact could only remove the barnacle shells, leaving behind the base plate cement on the surface. This study indicates that ultrasound cavitation would be optimal only if it is applied to early stages of fouling, before the formation of hard calcareous structures.

Chapter 7. Conclusions

Barnacles are considered as the most problematic marine biofouling organisms because of their sizes and gregarious colonization of solid surfaces, which generates serious impact on the marine industries, in particular onz the shipping industries. In this thesis, we conducted a systematic study of ultrasound on barnacle cyprids and juvenile barnacles. We studied high and low amplitude ultrasound on cyprid settlement inhibition and investigated the possible mechanism. We probed the effects of ultrasound on the secretion of cyprid footprints and juvenile barnacle's adhesion strength. Finally, we explored cavitation bubbles on the damage or removal of juvenile barnacles and recorded the interaction between cavitation bubbles and barnacles using high speed photography. The thesis revealed that ultrasound showed great potential as an effective strategy on the barnacle induced marine biofouling prevention.

Firstly, the effect of ultrasound on cyprids settlement and mortality was studied with frequencies of 23, 63 and 102 kHz and with various ultrasound amplitudes. The cyprid settlement was reduced after ultrasound exposure and enhanced inhibition was achieved with increased ultrasound treatment. Among the three frequencies, both the highest efficacy against settlement and the highest mortality was observed at 23 kHz.

A cyprid behavioral assay based on microscopic observations of surface exploration, demonstrated significant differences between ultrasound-treated and control cyprids. Ultrasound treated cyprids showed an altered exploration behavior: step duration was increased, while step length, walking pace, and the fraction of cyprids exploring the surface were significantly reduced with respect to control cyprids. The change in

cyprids' exploration behavior following exposure to ultrasound mimics the trend observed for cyprids exploring a less favored surface, whereby the cyprids move more slowly, presumably performing a more detailed assessment of the substrate. The reduced settlement and increased mortality correlated with altered surface exploration behavior, which suggests cyprids may have suffered physical or physiological impact due to ultrasound exposure.

Next, we explored the possible inhibitory mechanism using the acoustic emission spectrum method. The results showed that with the same ultrasonic amplitude, more cyprid settlement reduction was achieved in FSW than in PDFSW. Also, the cavitation intensity, quantified using nonlinear energy was stronger in FSW condition. The correlation of enhanced settlement inhibition with stronger cavitation suggests that ultrasonic cavitation is the mechanism for cyprid settlement inhibition and increased mortality. The cavitation induced force might lead to physical or even physiological damage to the cyprids which subsequently reduce the ability to settle.

It is hypothesized that the altered cyprid exploration behavior may be attributed to ultrasonic cavitation induced damage to the cyprid antennules. In a future study, it will be interesting to probe ultrasound-induced damage to the cyprid's organism, possibly by SEM, focusing on the antennules terminations, which are used to generate temporary anchoring points while exploring the solid surface.

High intensity ultrasound showed ability on barnacle cyprid settlement prevention. However, it may endanger other marine organisms, although with proper design the effects can be greatly minimized. Therefore, the possibility of using low intensity ultrasound on cyprid settlement control was further explored. The experiments were conducted at a pressure of 5 kPa, which was below the cavitation threshold, to study the possible inhibitory effect. The results revealed that low intensity ultrasound with

longer exposure was also able to inhibit settlement, and generated no injuries to cyprids. The strongest inhibition of settlement was observed at 23 kHz in both conditions, when acoustic pressure was set at 5 kPa, and when substratum amplitude was controlled at 10.05 nm. This result reveals that the inhibitory effect may not only be related to amplitude but also to ultrasound frequency. Furthermore, the application of ultrasound treatment in an intermittent mode of "5 min on and 20 min off" at 20-25 kHz and at low intensity of 5 kPa achieved the same effect as with the continuous application of 23 kHz. The reason why low frequency, low amplitude ultrasound inhibited settlement remains unclear. It is possible that the acoustic wave may have interacted with the dynamic behavior of cyprids in a phenomenon known as resonance, resulting in detachment of the cyprids attached by temporary adhesive laid down during exploration. However, it is highly speculative, and further exploration is needed. In the future study, a dynamic model could be proposed and the hypothesis of resonant vibration might be verified by obtaining parameters, such as cyprid's material property and mass.

Then the effects of ultrasound on cyprid footprints and juvenile barnacle's adhesion strength were explored using AFM and Nano-tensile tester, respectively. After cyprids exposed to 23 kHz at 20 kPa for 5 mins, cyprid footprints deposited on the NH_2 terminated substrates were scanned using AFM and compared to that without ultrasound treatment. The results showed that ultrasound significantly changed the morphology of footprints and reduced the footprint protein secretion. The adhesion strength of the newly settled (day 0) barnacles metamorphosed from ultrasound treated cyprids was lower than control barnacles.

However, no difference in adhesion strength was observed in the 4-8 day old juvenile barnacles. The evidence from this study suggests that ultrasound treatment results in a

reduction of cyprid footprint secretion and affects the subsequent recruitment of barnacles onto a substrate by reducing the ability of larval and early settlement stages of barnacles from firmly adhering to the substrate. Therefore, ultrasound may offer a means to enhance the performance of fouling release substrates by reducing the ability of early settlement stages of barnacles from firmly adhering to the substrate.

As ultrasound demonstrated the ability to reduce the newly metamorphosed barnacle' adhesion strength, it is surmised that the mechanical property of the footprints may also be affected. Therefore, in the future study, exploration of the cyprid temporary adhesive protein using contact mode AFM in the situ condition may provide more information with regarding to the mechanism of ultrasound induced settlement inhibition.

Other than the effect of ultrasound on barnacle cyprids, the ability of ultrasound on the removal or damage of juvenile barnacles was studied using high speed photography. Ultrasonic cavitation generated liquid jet damaged newly metamorphosed (day 0) barnacles and impaired the 10-day old barnacles. The mechanism was further explored using the spark generated bubble and the interaction process was recorded using high speed camera. The liquid jet generated by the bubble collapse was directed towards barnacles with various impact intensities. The jet impact intensity is largely related to the dimensionless distance H'. With lower value of H', higher speed liquid jet was produced; consequently larger impact pressure was generated. And the threshold of impact pressure that damaged the 10-day old barnacle was estimated by water hammer pressure. Also, barnacles were found to be more easily and completely removed at younger ages. For the aged barnacles, liquid jet impact could only remove the barnacle shells, leaving the cement to remain on the surface, which might attract other barnacle larvae to settle. However, the shells and

cement of newly metamorphosed barnacles could be totally removed with much lower intensity. Therefore, it is strongly recommended to remove barnacle fouling at earlier stages.

Based on our study, it is found that ultrasound might be a promising strategy on the barnacle induced marine fouling prevention. It processes several benefits over chemical-based or biocide strategies. Biocide-based antifouling coatings function through the gradual release of molecules from the coating's surface, however, ultrasound exposure does not generate a cumulative effect. In addition, ultrasound can be applied in a highly controlled manner, as opposed to biocides that are released continuously based on the chemistry of the coating. For example, ultrasound could be implemented in a regimented pulsed fashion, or could be turned on while in port and turned off once a ship has reached cruising speed, thus potentially saving power and other resources. Moreover, ultrasound may be conveniently applied to surfaces with low liquid shear forces, where fouling release coatings limited effectiveness. Last but not least, as the results revealed that ultrasound can reduce the adhesion strength of newly metamorphosed barnacles, the combination of FRCs and ultrasound strategies may provide a more efficient antifouling strategy. Undoubtedly, a thorough assessment of the effect of ultrasound on the marine environment would be prudent before its widespread application. With an optimized engineering design, its implementation will ideally prevent the barnacle fouling, while limiting the impact of ultrasound to the marine environment.

Bibliography

Ahn CY, Joung SH, Jeon JW, Kim HS, Yoon BD, Oh HM. 2003. Selective control of cyanobacteria by surfactin-containing culture broth of *bacillus subtilis* c1. Biotechnology Letters 25:1137-1142.

Aldred N. 2007. The adhesion and adhesives of barnacle cyprids (*Balanus amphitrite*; *Semibalanus balanoides*) and mussels (*Mytilus edulis*). PhD thesis, Newcastle University.

Aldred N, Clare AS. 2008. The adhesive strategies of cyprids and development of barnacle-resistant marine coatings. Biofouling 24:351-363.

Aldred N, Ista LK, Callow ME, Callow JA, Lopez GP, Clare AS. 2006. Mussel (mytilus edulis) byssus deposition in response to variations in surface wettability. Journal of the Royal Society Interface 3:37-43.

Aldred N, Li G, Gao Y, Clare AS, Jiang S. 2010a. Modulation of barnacle (balanus amphitrite darwin) cyprid settlement behavior by sulfobetaine and carboxybetaine methacrylate polymer coatings. Biofouling 26:673-683.

Aldred N, Phang IY, Conlan SL, Clare AS, Vancso GJ. 2008. The effects of a serine protease, alcalase, on the adhesives of barnacle cyprids (*balanus amphitrite*). Biofouling 24:97-107.

Aldred N, Scardino A, Cavaco A, de Nys R, Clare AS. 2010b. Attachment strength is a key factor in the selection of surfaces by barnacle cyprids (*balanus amphitrite*) during settlement. Biofouling 26:287-299.

Almeida E. 2007. Marine paints: The particular case of antifouling paints. Progess in Organic Coatings 59:2-20.

Apfel RE. 1997. Sonic effervescence: A tutorial on acoustic cavitation. Journal of Acoustical Society of America 101:1227-1237.

Ashokkumar M, Hodnett M, Zeqiri B, Grieser F, Price GJ. 2007. Acoustic emission spectra from 515 kHz cavitation in aqueous solutions containing surface-active solutes. Journal of American Chemical Society 129:2250-2258.

Atchley AA, Frizell LA, Apfel RE, Holland CK, Madanshetty S, Roy RA. 1988. Thresholds for cavitation produced in water by pulsed ultrasound. Ultrasonics 26:280-285.

Avvaru B, Pandit AB. 2009. Oscillating bubble concentration and its size distribution using acoustic emission spectra. Ultrasonics Sonochemistry 16:105-115.

Badarinath K, Pillai K, Klaseboer E, Ohl SW, Khoo BC. 2011. Collapsing bubble induced pumping in a viscous fluid. Sensors and Actuators A: Physical 169:151-163.

Barbe K; Pintelon R; Schoukens J. 2010. Welch method revisited: nonparametric power spectrum estimation via circular overlap. IEEE Transactions on Signal Processing. 58:553-565.

Bartlett MS. 1948. Smoothing periodograms from the time series with continuous spectrum. Nature 161: 686-687.

Bai L, Baker DR, Rivers M. 2008. Experimental study of bubble growth in stromboli basalt melts at 1 atm. Earth and Planetary Science Letters 267:533-547.

Bayoudh S, Ponsonnet L, Ouada HB, Bakhrouf A, Othmane A. 2005. Bacterial detachment from hydrophilic and hydrophobic surfaces using a microjet impingement. Colloids and Surfaces A: Physicochemical and Engineering Aspects 266:160-167.

Beake BD, Leggett GJ, Alexander.2002. Characterisation of the mechanical propterties of plama-polymerised coatings by nanoindentation and nanotribology. Journal of materials science.37:4919-4927.

Berglin M, Larsson A, Jonsson PR, Gatenholm P. 2001. The adhesion of the barnacle, *balanus improvisus*, to poly(dimethylsiloxane) fouling-release coatings and poly(methyl methacrylate) panels: The effect of barnacle size on strength and failure mode. Journal of Adhesion Science and Technology 15:1485-1502.

Berntsson KM, Andeasson H, Jonsson PR, Larsson L, Ring K, Petronis S, Gatenholm P. 2000. Reduction of barnacle recruitment on micro-textured surfaces: Analysis of effective topographic characteristics and evaluation of skin friction. Biofouling 16:245-261.

Berntssona KM, Jonssona PR, Lejhalla M, Gatenholmb P. 2000. Analysis of behavioral rejection of micro-textured surfaces and implications for recruitment by the *barnacle balanus improvisus*. Journal of Experimental Marine Biology and Ecology 251:59-83.

Bi X, Huang S, Hartono D, Yang KL. 2007. Liquid crystal based optical sensors for simultaneous detection of multiple glycine oligomers with micromolar concentrations. Sensors and Actuators B 127:406-413.

Billinghurst Z, Clare AS, Fileman T, Mcevoy J, Radman J, Depledge MH. 1998. Inhibition of barnacle settlement by the environmental oestrogen 4-nonylphenol and the natural oestrogen. Marine Pollution Bulletin 36:833-839.

Bott TR. 2000. Biofouling control with ultrasound. Heat Transfer Engineering 21:43-49.

BradyJr RF. 2001. A fracture mechanical analysis of fouling release from nontoxic antifouling coatings. Progress in Organic Coatings 43:188-192.

Branscomb ES, Rittschof D. 1984. A investigation of low frequency sound waves as a means of inhibiting barnacle settlement. Journal of Experimental Marine Biology and Ecology 19:145-154.

Bremond N, Arora M, Ohl CD, Lohse D. 2006. Controlled multibubble surface cavitation. Physical Review Letters 96:224501-224504.

Brondum J, Egebo M, Agerskov C, Busk H. 1998. Online pork carcass grading with the auto-form ultrasound system. Journal of Animal Science 76:1589-1868.

Brooks S, Waldock M. 2009. The use of copper as a biocide in marine antifouling paints. In: Hellio, c., yebra, d. (eds.), advances in marine antifouling coatings and technologies. Woodhead Publishing Limited, Cambridge.

Cai M, Wang S, Zheng Y, Liang H. 2009. Effects of ultrasound on ultrafiltration of *radix astragalus* extract and cleaning of fouled membrane. Separation Science and Technology 68:351-356.

Callow JA, Callow ME. 2011. Trends in the development of environmentally friendly fouling-resistant marine coatings. Nature Communications 2:1-10.

Callow ME, Callow JA. 2002. Marine bifouling: A sticky problem. Biologist 49:1-5.

Carl C, Poole AJ, Sexton BA, Glenn FL, Vucko MJ, Williams MR, Whalan S, de Nys R. 2012. Enhancing the settlement and attachment strength of pediveligers of mytilus galloprovincialis by changing surface wettabilty and microtopography. Biofouling 28:175-186.

Carman ML, Estes TG, Feinberg AW, Schumacher JF, Wilkerson W, Wilson LH, Callow ME, Callow JA, Brennan AB. 2006. Engineered antifouling microtopographies-correlating wettabililty with cell attachement. Biofouling 22:11-21.

Chambers LD, Stokes KR, Walsh FC, Wood RJK. 2006. Modern approaches to marine antifouling coatings. Surface and Coatings Technology 201:3642-3652.

Chaw KC, Birch WR. 2009. Quantifying the exploratory behavior of amphibalanus amphitrite cyprids. Biofouling 25:611-619.

Chaw KC, Dickinson GH, Ang K, Deng J, Birch WR. 2011. Surface exploration of Amphibalanus amphitrite cyprids on microtextured surfaces. Biofouling 27:413-422.

Chesworth JC, Donkin ME, Brown MT. 2004. The interactive effects of the antifouling herbicides irgarol 1051 and diuron on the seagrass zostera marina (L.). Aquatic Toxicology:296-305.

Choi CH, Scardino AJ, Dylejko PG, Fletcher LE, Juniper R. 2013. The effect of vibration frequency and amplitude on biofouling deterrence. Biofouling 29:195-202

Clare AS, Freet RK, McClary MJ. 1994. On the antennular secretion of the cyprid of Balanus amphitrite amphitrite, and its role as a settlement pheromone. Journal of the Marine Biology of the Association of United Kingdom 74:243-250.

Clare AS, Matsumura K. 2000. Nature and perception of barnacle settlement pheromones. Biofouling 15:57-71.

Clare AS, Rittschof D, Gerhart DJ, Maki JS. 1992. Molecular apporaches to non-toxic antifouling. International society of invertebrayte reproduction and development. 22:67-76.

Crisp DJ. 1955. The behaviour of barnacle cyprids in relation to water movement over a surface. Journal of Experimentyal Biolog 32: 569 – 590.

Crisp DJ, Meadows P. 1962. The chemical basis of gregariousness in cirripedes. Proceedings of the Royal Society B 156:500-520.

Crisp DJ, Wlaker G, Young GA, Yule AB. 1985. Adhesion and substrate choice in mussels and barnacles. Journal of Colloid and Interface Science 104:40-50.

Laurent D, Chantal C, Michel L. 2010. Biofouling protection for marine environmental sensors. Ocean Science 6:503-510.

Dicker S, Mleczko M, Schmitz G, Wrenn SP. 2010. Determination of microbubble cavitation threshold pressure as function of shell chemistry. Bubble Science, Engineering and Technology 2:55-64.

Dobretsov S, Dahms HU, Qian PY. 2006. Inhibition of biofouling by marine microorganisms and their metabolites. Biofouling 22:43-54.

Dobretsov S, Teplitski M, Bayer M, Gunasekera S, Proksch P, Paul VJ. 2011. Inhibition of marine biofouling by bacterial quorum sensing inhibitors. Biofouling 27:893-905.

Dolez PI, Love BJ. 2002. Acid cleaning solutions for barnacle-covered surfaces. International Journal of Adhesion and Adhesives 22:297-301.

Donskoy DM, Ludyanskiy M, Wright DA. 1996. Effects of sound and ultrasound on zebra mussels. Journal of the Acoustical Society of America 99:2577-2603.

Dreanno C, Kirby RR, Clare AS. 2006. Smelly feet are not always a bad thing: The relationship between cyprid footprint protein and the barnacle settlement pheromone. Biology Letters 2:423-425.

Engler CR, Robinson CW. 1981. Effects of organism type and growth conditions on cell disruption by impingement. Biotechnology Letters 3:83-88.

Fischer E, Castelli V, Rodgers S, Bleile H. 1981. Marine biodeterioration: An interdiciplinary study. Naval Institute Press.

Frohly J, Labouret S, Bruneel C, Looten BII, Torguet R. 2000. Ultrasonic cavitation monitoring by acoustic noise power measurement. Journal of the Acoustical Society of America 108:2012-2020.

Fusetani N. 2004. Biofouling and antifouling. Natural Products Reports 21:94-104.

Ghidaoui MS, Zhao M, Mclnnis DA, Axworthy DH. 2005. A review of water hammer theory and practice. Applied Mechanics Reviews 58:49-76.

Giordano R, Leuzzi U, Wanderlingh F. 1976. Effects of ultrasound on unicellular algae. Journal of the Acoustical Society of America 60:275-278.

Groves S, Price D, Hindon S. 2009. Blue & Green Marine Limited, Ultra-sonic device. US patent 12,484,559.

Gu X, Nguyen T, Sung LP, Vanlandingham MR, Fasolka MJ, Martin JW. 2004. Multiscale physical characterization of an outdoor-exposed polymeric coating system. Journal of Coatings Technology and Research. 6:67-79.

Gu JD. 2003. Microbiological deterioration and degradation of synthetic polymeric materials: Recent research advances. International Biodeterioration and Biodegradation 52:69-91.

Guo S, Lee HP, Teo SLM, Khoo BC. 2012. Inhibition of barnacle cyprid settlement using low frequency and intensity ultrasound. Biofouling 28:131-141.

Guo S, Lee HP, Khoo BC. 2011a. Inhibitory effect of ultrasound on barnacle (*amphibalanus amphitrite*) cyprid settlement. Journal of Experimental Marine Biology and Ecology 409:253-258.

Guo SF, Lee HP, Chaw KC, Miklas J, Teo SLM, Dickinson GH, Birch WR, Khoo BC. 2011b. Effect of ultrasound on cyprids and juvenile barnacles. Biofouling 27:185-192.

Hao H, Wu M, Chen Y, Tang J, Wu Q. 2004. Cavitation mechanism in cyanobacterial growth inhibition by ultrasonic exposure. Colloids Surfaces A 5:151-156.

Hartono D, Bi X, Yang KL, Yung LYL. 2008. An air-supported liquid crystal system for real-time and label-free characterization of phospholipases and their inhibitors. Advanced Functional Materials 18:2938-2945.

Hellio C, Yebra D. 2009. Advances in marine antifouling coatings and technologies. Cambridge, UK: Woodhead Publishing Ltd. pp:94-104 .

Hoagland KD, Rosowski JR, Gretz MR, Roemer SC. 1993. Diatom extracellular polymeric substances: Function, fine structure, chemistry and physiology. Journal of Phycology 29:537-566.

Hodson SL, Burke CM, Bissett AP. 2000. Biofouling of fish-cage netting: The efficacy of a silicone coating and the effect of netting colour. Aquaculture 2000:277-290.

Holland C, O'Brien W, Tarantal A, Crum L, Ferrer F. 2000. Bioeffects in tissues with gas bodies. Nonthermal mechanical bioeffects. Journal of Ultrasound in Medicine 19:97-108.

Huggett M, Williamson J, de Nys R, Kjelleberg S, Steinberg P. 2006. Larval settlement of the common australian sea urchin <i>heliocidaris erythrogramma in response to bacteria from the surface of coralline algae. Oecologia 149:604-619.

Ishibashi K, Shimada K, Kawato T, Kaji S, Maeno M. 2010. Inhibitory effects of low-energy pulsed ultrasonic stimulation on cell surface protein antigen c through heat shock proteins groel and dnak in *streptococcus mutans*. Applied and Environmental Microbiology 3:751-756.

Jiang S, Cao Z. 2010. Ultralow-fouling, functionalizable, and hydrolyzable zwitterionic materials and their derivatives for biological applications. Advanced Materials 22:920-932.

Jokinen H, Ollila J, Aumala O. 2000. On windowing effects in estimating averaged periodograms of noisy signals. Measurement 28: 197-207.

Joyce E, Phull SS, Lorimer JP, Mason TJ. 2003. The development and evaluation of ultrasound for the treatment of bacterial suspensions. A study of frequency, power and sonication time on cultured bacillus species. Ultrasonics Sonochemistry 10:315-318.

Kalumuck KM, Chahine GL, Duraiswami R. 1995. Analysis of the Response of a Deformable Structure to Underwater Explosion Bubble Loading Using a Fully Coupled Fluid-Structure Interaction Procedure. 66th Shock and Vibration Symposium 2:277-286.

Kanegsberg B, Kanegsberg E. 2011. Handbook for critical cleaning. CRC press, second edition. pp:255.

Kavanagh CJ, Schultz MP, Swain GW, Stein J, Truby K, Wood CD. 2001. Variation in adhesion strength of balanus eburneus, crassostrea virginica and hydroides dianthus to fouling-release coatings. Biofouling 17:155-167.

Kay SM, Marple SL. 1981. Spectrum analysis-A moden pespective. Proceedings of the IEEE. 69:716-723.

Kem W, Soti F, Rittschof D. 2003. Inhibition of barnacle larval settlement and crustacean toxicity of some hoplonemertine pyridyl alkaloids. Biomolecular Engineering 20:355-361.

Kinsler LE, Frey AR, Coppens AB, Sanders JV. 1982. Fundamentals of acoustics. 3rd ed. New York (USA):John Wiley and Sons. pp. 124-128.

Kitamura H, Takahashi K, Kanamaru D. 1995. Effect of ultrasound waves on the lavarl settlement of the barnacle, *balanus amphitrite* in the laboratory. Marine Fouling 12:9-13.

Koehl MR. 2007. Mini review: Hydrodynamics of larval settlement into fouling communities. Biofouling 23:357-368.

Kratochvíl B, Morntein V. 2006. Monitoring the effects of cavitation ultrasound on *Artemia* salina larvae. Scripta Medica 79:3-8.

Lagsir NO, Gros AM, Boistier E, Blum LJ, Bonneau M. 2000. The development of an ultrasonic apparatus for the noninvasive and repeatable removal of fouling in food processing equipment. Letters in Applied Microbiology 30:47-52.

Lambert S, Thomas K, Davy A. 2006. Assessment of the risk posed by the antifouling booster biocides irgarol 1051 and diuron to freshwater macrophytes. Chemosphere 63:734-743.

Larsson AI, Mattsson-Thorngren L, Granhag LM, Berglin M. 2010. Fouling-release of barnacles from a boat hull with comparison to laboratory data of attachment strength. Journal of Experimental Marine Biology and Ecology 392:107-114.

Law AM. 1983. Statistical Analysis of Simulation Output Data. Operations Research. 31: 983-1029.

Lew KSF, Klaseboer E, Khoo BC. 2007. A collapsing bubble-induced micropump: An experimental study. Sensors and Actuators A: Physical 133:161-172.

Liang Z, Zhou G, Lin S, Zhang Y, Yang H. 2006. Study of low-frequency ultrasonic cavitation fields based on spectral analysis technique. Ultrasonics 44:115-120.

Liang H, Nan J, He WJ, Li GB. 2009. Algae removal by ultrasonic irradiation-coagulation. Desalination 239:191-197.

Liu X, He J, Lu J, Ni X. 2009. Effect of liquid viscosity on a liquid jet produced by the collapse of a laser-induced bubble near a rigid boundary. Japanese Journal of Applied Physics 48:016504.

Llyichev VI, Koretz LV, Melnikov NP. 1989. Spectral characteristics of acoustic caviation. Ultrasonics 27: 357-361.

Ma B, Chen Y, Hao H, Wu M, Wang B, Lv H, Zhang G. 2005. Influence of ultrasonicfield on microcystinsproduced by bloom-formingalgae. Colloids and Surfaces B: Biointerfaces 41:197-201.

Marechal JP, Hellio C, Sebire M, Clare AS. 2004. Settlement behavior of marine invertebrate larvae measured by ethovision 3.0. Biofouling 20:211-217.

Marhaeni B, Radjasa O, Bengen D, Kaswadji D. 2009. Screening of bacterial symbionts of seagrass enhalus sp. Against biofilm-forming bacteria. Journal of Coastal Development 13:126-132.

Maruzzo D, Conlan S, Aldred N, Clare AS, Høeg JT. 2011. Video observation of surface exploration in cyprids of *balanus amphitrite*: The movements of antennular sensory setae. Biofouling 27:225-239.

Mason TJ, Joyce E, Phull SS, Lorimer JP. 2003. Potential uses of ultrasound in the biological decontamination of water. Ultrasonics Sonochemistry 10:319-323.

Mason TJ, Lorimer JP. 2002. Applied sonochemistry: The uses of power ultrasound in chemistry and processing. Wiley-VCH.

Mason TJ, Paniwnyk L, Lorimer JP. 1996. The uses of ultrasound in food technology. Ultrasonics Sonochemistry 3:253-260.

Matsumura K, Nagano M, Kato-Yoshinaga Y, Yamazaki M, Clare AS, Fusetani N. 1998. Immunological studies on the settlement-inducing protein complex (sipc) of the barnacle balanus amphitrite and its possible involvement in larva-larva interactions. Proceedings of the Royal Society B:Biological Sciences 265:1825-1830.

Matsuura K, Hirotsune M, Nunokawa Y, Sotoh M, Honda K. 2003. Acceleration of cell growth and ester formation by ultrasonic wave irradiation. Journal of Fermentation and Bioengineering 77:36-40.

Mitragotri S. 2005. Healing sound: The use of ultrasound in drug delivery and other therapeutic applications. Nature Reviews Drug Discovery 4:255-260.

Moholkar VS, Sable SP, Pandit AB. 2000. Mapping the cavitation intensity in an ultrasonic bath using the acoustic emission. AIChE Journal 46:684-694.

Molino PJ, Campbell E, Wetherbee R. 2009. Development of the initial diatom microfouling layer on antifouling and fouling-release surfaces in temperate and tropical australia. Biofouling 25:685-694.

Monsen T, Lovgren E, Widerstrom M, Wallinder L. 2009. In vitro effect of ultrasound on bacteria and suggested protocol for sonication and diagnosis of prosthetic infections. Journal of Clinical Microbiology 47:2496-2501.

Mori E, Yamaguchi Y, Nishikawa A. 1969. The anti-fouling effect of ultrasonic waves on hulls. Mitsubishi heavy industries. Technical Review 6:1-9.

Mott IEC, Stickler DJ, Coakley WT, Bott TR. 1998. The removal of bacterial biofilm from water-filled tubes using axially propagated ultrasound. Journal of Applied Microbiology 84:509-514.

Naik RR, Brott LL, Rodriguez F, Agarwal G, Kirkpatrick SM, Stone MO. 2003. Bio-inspired approaches and biologically derived materials for coatings. Progress in Organic Coatings 47:249-255.

Newby BZ, Chaudhury MK, Brown HR. 1995. Macroscopic evidence of the effct of interfacial slippage on adhesion. Science 269:1407-1409.

Nishida A, Ohkawa K, Ueda I, Yamamoto H. 2003. Green mussel perna viridis l.: Attachment behavior and preparation of antifouling surfaces. Biomolecular Engineering:381-387.

Nott JA, Foster BA. 1969. On the structure of the antennular attachment organ of the cypris larva of *balanus balanoides*. Philosopical Transactions of the Royal Society B: Biological Science 56:115-134.

Nyborg WL. 1982. Ultrasonic microstreaming and related phenomena. British Journal of Cancer 5:156-160.

Ohl SW, Klaseboer E, Khoo BC. 2009. The dynamics of a non-equilibrium bubble near bio-materials. Physics in Medicine and Biology 54:6313-6336.

Omae I. 2003. Organotin antifouling paints and their alternatives. Applied Organometallic Chemistry 17:81-105.

Palanker D, Vankov A, Miller J, Friedman M, Strauss M. 2003. Prevention of tissue damage by water jet during cavitation. Journal of Applied Physics 94:2654-2661.

Pérez HA, Cusack M, Zhu W. 2008. Assessment of crystallographic influence on material properties of calcite brachiopods. Mineralogical Magazine 72:563-568.

Petosić A, Ivancević B, Svilar D. 2009. Measuring derived acoustic power of an ultrasound surgical device in the linear and nonlinear operating modes. Ultrasonic 49:522-531.

Patek SN, Caldwell RL. 2005. Extreme impact and cavitation forces of a biological hammer: Strike forces of the peacock mantis shrimp odontodactylus scyllarus. Journal of Experimental Biology 208:3655-3664.

Phang IY, Aldred N, Clare AS, Vancso GJ. 2007. Effective marine antifouling coatings. Nanos 1:35-39.

Phang IY, Aldred N, Clare AS, Callow JA, Vancso GJ. 2006. An in situ study of the nanomechanical properties of barnacle (balanus amphitrite) cyprid cement using atomic force microscopy (afm). Biofouling 22:245-250.

Phang IY, Chaw KC, Choo SS, Kang RK, Lee SS, Birch WR, Teo SLM, Vancso GJ. 2009. Marine biofouling field tests, settlement assay and footprint micromorphology of cyprid larvae of balanus amphitrite on model surfaces. Biofouling 25:139-147.

Pitombo FB. 2004. Phylogenetic analysis of the balanidae (*cirripedia, balanomorpha*). Zoologica Scripta 33:261-276.

Pitt WG, Ross SA. 2003. Ultrasound increases the rate of bacterial cell growth. Biotechnology Progress 19:1038-1044.

Qian PY, Rittschof D, Sreedhar B. 2000. Macrofouling in unidirectional flow: Miniature pipes as experimental models for studying the interaction of flow and surface characteristics on the attachment of barnacle, bryozoan and polychaete larvae. Marine Ecology Progress Series 207:109-121.

Qian PY, Xu Y, Fusetani N. 2010. Natural products as antifouling compounds: Recent progress and future perspectives. Biofouling 26:223-234.

Ralston E, Swain G.2009. Bioinspiration--the solution for biofouling control? Bioinsp. Biomim. 4:1-9.

Rediske AM, Roeder BL, Nelson JL, Robison RL, Schaalje GB, Robison RA, Pitt WG. 2000. Pulsed ultrasound enhances the killing of *escherichia coli* biofilms by aminoglycoside antibiotics in vivo. Antimicrob Agents Chemother 44:771-772.

Rittschof D. 2000. Natural product antifoulants: One perspective on the challenges related to coatings development. Biofouling 15:119-127.

Rittschof D, Forward RB, Jr, Cannon G, Welch JM, McClary MM, Jr, Holm ER, Clare AS, Conova S, McKelvey LM, Bryan P, Van Dover CL. 1998. Cues and context: larval responses to physical and chemical cues. Biofouling 12:31-44

Rittschof D, Branscomb ES, Costlow JD. 1984. Settlement and behavior in relation to flow and surface in larval barnacles, balanus amphitrite darwin. Journal of Experimental Marine Biology and Ecology 82:131-146.

Rittschof D, Lai CH, Kok LM, Teo SLM. 2003. Pharmaceuticals as antifoulants: Concept and principles. Biofouling 19:207-212.

Roberts D, Rittschof D, Holm E, Schmidt AR. 1997. Factors influencing intitial larval settlement: temporal, spatial and surface molecular components. Journal of Experimental Marine Biology and Ecology 150:203-221.

Ruan J, Wang Y, Crum L, Mitchell S. 2010. Ultrasound generated mechanical induction of mesenchymal stem cells. Ultrasonics Symposium (IUS):1763-1766.

Rudolf S, Paul K, Zhou B. 1997. A settlement inhibition assay with cyprid larvae of the barnacle baianus amphitrite. Bulletin of Environmental Contamination and Toxicology 35:1867-1874.

Salerno MB, Logan BE, Velegol D. 2004. Importance of molecular details in predicting bacteruak adhesion to hydrophobic surfaces. Langmuir 20:10625-10629.

Scardino AJ, Guenther J, de Nys R. 2008. Attachment point theory revisited: The fouling response to a microtextured matrix. Biofouling 24:45-53.

Scardino AJ, de Nys R. 2011. Mini review: Biomimetic models and bioinspired surfaces for fouling control. Biofouling 27:73-86.

Scheider R. 1997. Bacterial adhesion to solid substrata coated with conditioning films derived from chemical fractions of natural waters. Journal of Adhesion Science and Technology 11:979-994.

Scherba G, Weigel RM, O'Brien WD. 1991. Quantitative assessment of the germicidal efficacy of ultrasonic energy. Applied and Environmental Microbiology 57:2079-2084.

Schultz M. 2007. Effects of coating roughness and biofouling on ship resistance and powering. Biofouling 23:331-341.

Schumacher J, Aldred N, Callow ME, Finlay J, Callow JA, Clare AS, Brennan A. 2007. Speciesspecific engineered antifouling topographies: Correlations between the settlement of algal zoospores and barnacle cyprids. Biofouling 23:307-317.

Seth N, Chakravarty P, Khandeparker L, Anil AC, Pandit AB. 2010. Quantification of the energy required for the destruction of balanus amphitrite larva by ultrasonic treatment. Journal of the Marine Biological Association of the United Kingdom 90:1475-1482.

Shigihara T, Kobayashi M. 2002. Method for preventing deterioration of submarine structure and ultrasonic vibration unit used for the method. Journal of the Acoustical Society of America 111:1513-1513.

Shrestha A, Fong SW, Khoo BC, Kishen A. 2009. Delivery of antibacterial nanoparticles into dentinal tubules using high-intensity focused ultrasound. Journal of Endodontics 35:1028-1033.

Slabbekoorn H, Bouton N, Opzeeland LV, Coers A, Cate C, Popper AN. 2010. A noisy spring: The impact of globally rising underwater sound levels on fish. Trends in Ecology and Evolution 25:419-427.

Smith ME, Kane AS, Popper AN. 2004. Noise-induced stress response and hearing loss in goldfish. Journal of Experimental Biology 207:427-435.

Soltani Z, Volz KR, Hansmann DR. 2008. Effect of modulated ultrasound parameters on ultrasound-induced thrombolysis. Physics in Medicine and Biology 53:6837-6847.

Standing JD, Hooper IR, Costlow JD.1983. Inhibition and induction of barnacle settlement by natural products present in octocorals. Journal of Chemical Ecology 10 : 823-834.

Suslink K, Nyborg W. 1988. Ultrasound: Its chemical, physical, and biological effects. Journal of the Acoustical Society of America 87:919-920.

Suzuki H, Konno K. 1970. Basic studies on the antifouling by ultrasonic waves for ship's bottom fouling organisms. Journal of the Tokyo University of Fisheries 56:31-48.

Swain GW, Nelson WG, Preedeekanit S. 1998. The influence of biofouling adhesion and biotic disturbance on the development of fouling communities on non-toxic surfaces. Biofouling 10:187-197.

Swift NB. 2012. Biomineral structure and strength of barnacle exoskeletons. Colgate Academic Review 8:121-134.

Tegtmeyer K, Rittschof D. 1989. Synthetic peptide analogs to barnacle settlement pheromone. Peptides 9:1403-1406.

Thomas KV, McHugh M, Hilton M, Waldock M. 2003. Increased persistence of antifouling paint biocides when associated with paint particles. Environmental Pollution 123:153-161.

Thouvenin M, Peron JJ, Langlois V, Guerin P, Langlois JY, Vallee-Rehel K. 2002. Formulation and antifouling activity of marine paints: A study by a statistically based experiments plan Progress in Organic Coatings 44:85-92.

Tomita Y, Shima A. 1986. Mechanisms of impulsive pressure generation and damage pit formation by bubble collapse. Journal of Fluid Mechanics 169:535-564.

Tribou M, Swain G. 2010. The use of proactive in-water grooming to improve the performance of ship hull antifouling coatings. Biofouling 26:47-56.

Ubeyli ED, Isik H, Guler I. 2003. Application of FFT and arma spectral analysis to arterial doppler signals. Mathematical and computational applications. 8: 311-318.

Voulvoulis N, Scrimshaw MD, Lester JN. 1999. Alternative antifouling biocides. Applied Organometallic Chemistry 13:135-143.

Walker G. 1971. The histology, biochemistry and ultrastructure of the cement apparatus of three adult sessile barnacles, *elminius modestus, balanus balanoides* and *balanus haemri*. Marine Biology 7:239-248.

Walker G, Yule AB. 1984. Temporary adhesion of barnacle cyprids: the existence of an antennular disc secretion. Journal of the Marine Biology Association of United Kingdom. 64:679-686.

Walker G. 1987. Marine organisms and their adhesion. In synthetic adhesives and sealants (ed. W. C. Wake). Chichester, UK: Wiley. pp:112-135.

Welch PD. 1967. The use of fast fourier transform for the estimation of power spectra: A method based on time averaging over short, modified periodograms. IEEE Trans. Audio Electroacoust 15:70-73.

Wendt DE, Kowalke GL, Kim J, Singer IL. 2006. Factors that influence elastomeric coating performance: The effect of coating thickness on basal plate morphology, growth and critical removal stress of the barnacle balanus amphitrite. Biofouling 22:1-9.

Whomersley P, Picken GB. 2003. Long-term dynamics of fouling communities found on offshore installations in the north sea. Journal of the Marine Biological Association of the United Kingdom 83:897-901.

Wójs K, Gudra T, Redzicki R. 2006. Experimental research into the cavitation noise spectrum in water solutions of high molecular weight polymers. Ultrasonics 44:350-359.

Wysocki LE, Dittami JP, Ladich F. 2006. Ship noise and cortisol secretion in european freshwater fishes. Biological Conservation 128:501-508.

Yebra DM, Kiil S, Dam JK. 2004. Antifouling technology--past, present and future steps towards efficient and environmentally friendly antifouling coatings. Progress in Organic Coatings 50:75-104.

Yule AB, Crisp DJ. 1983. Adhesion of cypris larvae of the barnacle, *balanus balanoides*, to clean and arthropodintreated surfaces. Journal of the Marine Biological Association of the United Kingdom 63:261-271.

Yule AB, Walker G. 1985. Settlement of Balanus balanoides: the effect of cyprid antennular secretion. Journal of Marine Biology of the United Kingdom 65:707-712.

Zhang Z, Finlay J, Wang L, Gao Y, Callow JA, Callow ME. 2009. Polysulfobetaine-grafted surfaces as environmentally benign ultralow fouling marine coatings. Langmuir 25:13516-13521.

Zhou Y. 2011. High intensity focused ultrasound in clinical tumor ablation. World Journal of Clinical Oncology 2:8-27.

Publications

Journal publications related to the thesis

1. Guo SF, Lee HP, Chaw KC, Miklas J, Teo SLM, Dickinson GH, Birch WR, Khoo BC. 2011. Effect of ultrasound on cyprids and juvenile barnacles. Biofouling 27:185-192.

2. Guo S, Lee HP, Khoo BC. 2011. Inhibitory effect of ultrasound on barnacle (*Amphibalanus amphitrite*) cyprid settlement. Journal of Experimental Marine Biology and Ecology 409:253-258.

3. Guo S, Lee HP, Teo SLM, Khoo BC. 2012. Inhibition of barnacle cyprid settlement using low frequency and intensity ultrasound. Biofouling 28: 131-141.

4. Guo S, Khoo BC, Teo SLM, Zhong S, Lim CT, Lee HP. 2013. Effect of ultrasound on cyprid footprints and juvenile barnacle adhesion strength on a fouling release material. Biofouling (Resubmitted).

5. Guo S, Khoo BC, Teo SLM, Lee HP. 2013. The effects of cavitation bubbles on the removal of juvenile barnacles. Journal of Colloids and Surfaces B: Biointerfaces (Accept).

Conference presentation

Guo S, Lee HP, Teo SLM, Khoo BC. 2012. The effects of low intensity ultrasound on barnacle cyprids. In Proceeding of the 16th international congress on marine corrosion and fouling, Seattle, Washington, USA.